



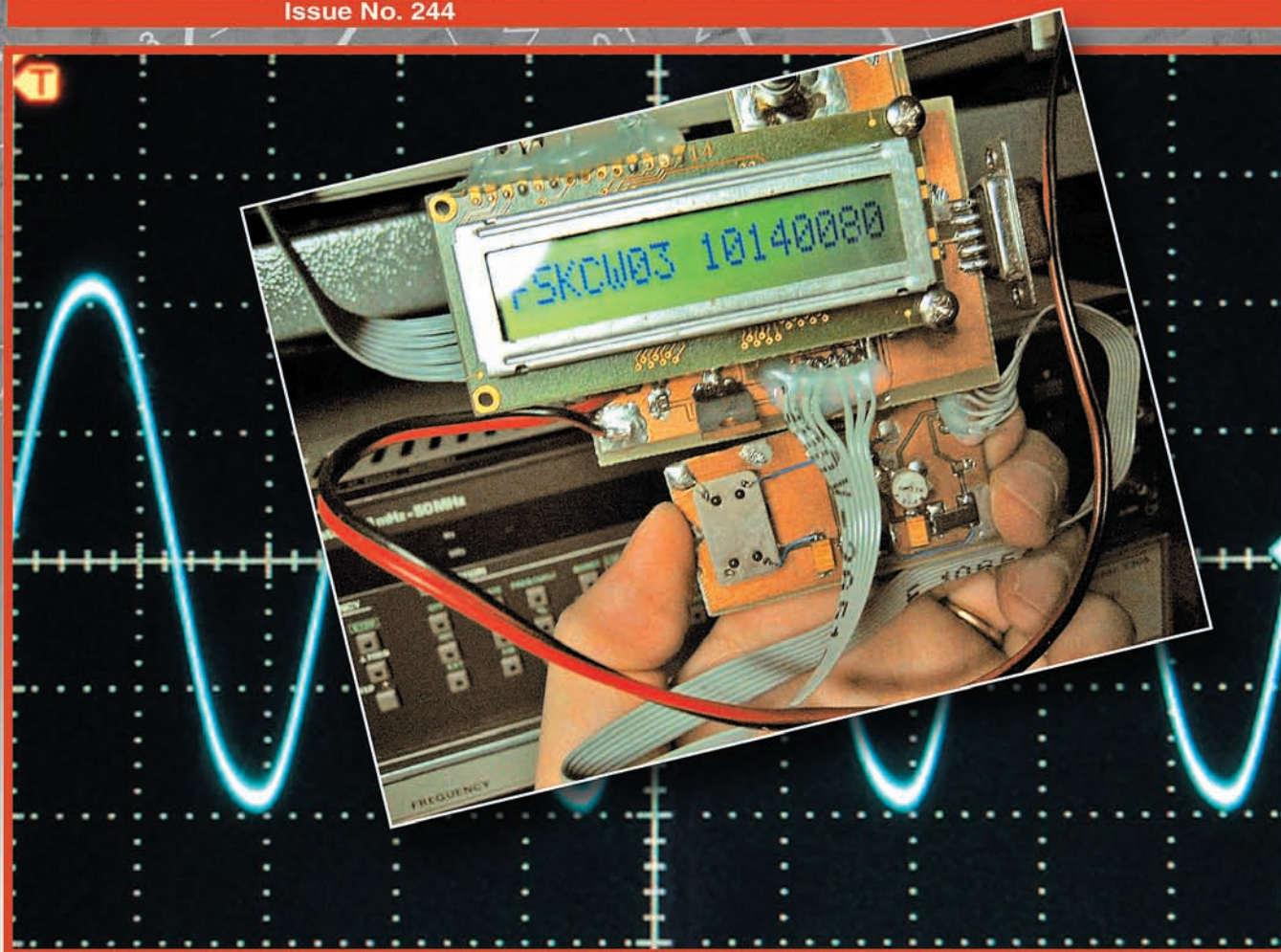
QEX

September/October 2007

\$5

A Forum for Communications Experimenters

Issue No. 244



IZ2EEQ uses a DDS module and a PIC control module to build a low power transmitter for use as a QRSS (very slow speed CW) beacon.

ARRL The national association for
AMATEUR RADIO

225 Main Street
Newington, CT USA 06111-1494

HL-1.5Kfx

HF/50MHz Linear Power Amplifier



Auto Band Set

This compact and lightweight 1kW desktop HF/50MHz linear power amplifier has a maximum input power of 1.75kW. Our solid-state broad-band power amp technology makes it the smallest and lightest self-contained amplifier in the industry.

Typical output power is 1kW PEP/SSB on HF and 650W on 6m band with the drive power of 85-90W. Bands set automatically with the **built-in band decoder**. You can forget about the band setting when the amplifier is connected to your modern radio through **supplied band data cables for ICOM CI-V, DC voltage (ICOM, Yaesu), and RS-232C (Kenwood)**. Manual band setting selectable as well.

All these data cables are included with the amplifier.

Features

- Lightest and most compact 1kW HF amplifier in the industry.
- The amplifier's decoder changes bands automatically with most ICOM, Kenwood, Yaesu.
- The amp utilizes an advanced 16 bit MPU (microprocessor) to run the various high speed protection circuits such as overdrive, high antenna SWR, DC overvoltage, band miss-set etc.
- Built in power supply.
- AC (200/220/235/240V) and (100/110/115/120V) selectable.
- Equipped with a control cable connection socket, for the HC-1.5KAT, auto antenna tuner by Tokyo Hy-Power Labs.
- Two antenna ports selectable from front panel.
- Great for desktop or DXpedition!

Specifications

Frequency:
1.8 ~ 28MHz all amateur bands including WARC bands and 50MHz

Mode:
SSB, CW, RTTY

RF Drive:
85W typ. (100W max.)

Output Power:
HF 1kW PEP max.
50MHz 650W PEP max.

Matching Transceivers for Auto Band Decoder:
Most modern ICOM, Yaesu, Kenwood

Drain Voltage:
53V (when no RF drive)

Drain Current:
40A max.

Input Impedance:
50 OHM (unbalanced)

Output Impedance:
50 OHM (unbalanced)

Final Transistor:
SD2933 x 4 (MOS FET by ST micro)

Circuit:
Class AB parallel push-pull

Cooling Method:
Forced Air Cooling

MPU:
PIC 18F452 x 2

Multi-Meter:
Output Power - Pf 1Kw
Drain Voltage - Vd 60V
Drain Current - Id 50A

Input/Output Connectors:
UHF SO-239

AC Power:
AC 240V default (200/220/235)
- 10 A max.
AC 120V (100/110/115)
- 20 A max.

AC Consumption:
1.9kVA max. when TX

Dimension:
10.7 x 5.6 x 14.3 inches (Wx-HxD)/272 x 142 x 363 mm

Weight:
Approx. 20kgs. or 45.5lbs.

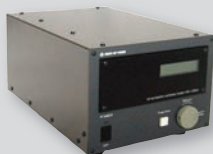
Accessories Included:
AC Power Cord
Band Decoder Cables included for Kenwood, ICOM and Yaesu
Spare Fuses and Plugs
User Manual

Optional Items:
Auto Antenna Tuner (HC-1.5KAT)
External Cooling Fan (HXT-1.5KF for high duty cycle RTTY)

More Fine Products from TOKYO HY-POWER



HL-1.2Kfx
HF amp
750W out



HC-1.5KAT
HF 1.5KW
Auto Tuner



HL-350Vdx
VHF 330W
Amplifier

Watch for Our
NEWEST and MOST
POWERFUL full legal
Limit. HL-2.5Kfx
available early Fall!

*All of these devices have been authorized as required by the rules of the FCC.

QEX

QEX (ISSN: 0886-8093) is published bimonthly in January, March, May, July, September, and November by the American Radio Relay League, 225 Main Street, Newington, CT 06111-1494. Periodicals postage paid at Hartford, CT and at additional mailing offices.

POSTMASTER: Send address changes to: QEX, 225 Main St, Newington, CT 06111-1494 Issue No 244

Harold Kramer, WJ1B
Publisher

Larry Wolfgang, WR1B
Editor

Lori Weinberg, KB1EIB
Assistant Editor

L. B. Cebik, W4RNL
Zack Lau, W1VT
Ray Mack, W5IFS
Contributing Editors

Production Department

Steve Ford, WB8IMY
Publications Manager

Michelle Bloom, WB1ENT
Production Supervisor

Sue Fagan, KB1OKW
Graphic Design Supervisor

Devon Neal, KB1NSR
Technical Illustrator

Joe Shea
Production Assistant

Advertising Information Contact:

Janet L. Rocco, W1JLR
Business Services
860-594-0203 direct
800-243-7768 ARRL
860-594-4285 fax

Circulation Department

Cathy Stepina, QEX Circulation

Offices

225 Main St, Newington, CT 06111-1494 USA
Telephone: 860-594-0200
Fax: 860-594-0259 (24 hour direct line)
e-mail: qex@arrl.org

Subscription rate for 6 issues:

In the US: ARRL Member \$24,
nonmember \$36;

US by First Class Mail:
ARRL member \$37, nonmember \$49;

Elsewhere by Surface Mail (4-8 week delivery):
ARRL member \$31, nonmember \$43;

Canada by Airmail: ARRL member \$40,
nonmember \$52;

Elsewhere by Airmail: ARRL member \$59,
nonmember \$71.

Members are asked to include their membership control number or a label from their QST when applying.

In order to ensure prompt delivery, we ask that you periodically check the address information on your mailing label. If you find any inaccuracies, please contact the Circulation Department immediately. Thank you for your assistance.

Copyright ©2007 by the American Radio Relay League Inc. For permission to quote or reprint material from QEX or any ARRL publication, send a written request including the issue date (or book title), article, page numbers and a description of where you intend to use the reprinted material. Send the request to the office of the Publications Manager (permission@arrl.org).



About the Cover

Matteo Campanella, IZ2EEQ, uses a DDS module and a PIC control module to build a QRP beacon transmitter for QRSS operation. An Analog Devices AD9851 DDS IC, a PIC 16F84AP controller and an LCD form the basis for this project.



Features

- 3 Octave for Circle Diagrams**
By Maynard A. Wright, W6PAP
- 11 An Unusual Vector Network Analyzer**
By Dr George R. Steber, WB9LVI
- 24 A DDS Based QRSS (and CW) Beacon**
By Matteo Campanella, IZ2EEQ
- 29 Very High Q Microwave Cavities and Filters**
By Paolo Antoniazzi, IW2ACD, and Marco Arecco, IK2WAQ
- 37 A Differential Leveling Microphone**
By J. R. Laughlin, KE5KSC
- 44 Turbo Delphi Explorer: Develop Amateur Radio Projects for Windows with a Free Compiler**
By Steve Gradijan, WB5KIA
- 48 Using Gain-Probability Data to Compare Antenna Performances**
By Fred Glenn, K9SO

Columns

- 51 Antenna Options**
By L. B. Cebik, W4RNL
- 57 Letters**
- 59 Upcoming Conferences**
- 61 Next Issue**

Sep/Oct 2007 QEX Advertising Index

American Radio Relay League: 61, 62,
63, 64
Array Solutions: 23, Cov III
Atomic Time: 36
Communications Specialists, Inc: 50
Down East Microwave Inc: 36
Elkins Marine Training International: 56

Kenwood Communications: Cov IV
National RF, Inc: 60
Nemal Electronics International, Inc: 60
Teri Software: 60
Tokyo Hy-Power Labs, Inc: Cov II
Tucson Amateur Packet Radio: 61



The American Radio Relay League, Inc. is a noncommercial association of radio amateurs, organized for the promotion of interest in Amateur Radio communication and experimentation, for the establishment of networks to provide communications in the event of disasters or other emergencies, for the advancement of the radio art and of the public welfare, for the representation of the radio amateur in legislative matters, and for the maintenance of fraternalism and a high standard of conduct.

ARRL is an incorporated association without capital stock chartered under the laws of the state of Connecticut, and is an exempt organization under Section 501(c)(3) of the Internal Revenue Code of 1986. Its affairs are governed by a Board of Directors, whose voting members are elected every three years by the general membership. The officers are elected or appointed by the Directors. The League is noncommercial, and no one who could gain financially from the shaping of its affairs is eligible for membership on its Board.

"Of, by, and for the radio amateur," ARRL numbers within its ranks the vast majority of active amateurs in the nation and has a proud history of achievement as the standard-bearer in amateur affairs.

A *bona fide* interest in Amateur Radio is the only essential qualification of membership; an Amateur Radio license is not a prerequisite, although full voting membership is granted only to licensed amateurs in the US.

Membership inquiries and general correspondence should be addressed to the administrative headquarters:

ARRL, 225 Main Street, Newington, CT 06111 USA.

Telephone: 860-594-0200

FAX: 860-594-0259 (24-hour direct line)

Officers

President: JOEL HARRISON, W5ZN

528 Miller Rd, Judsonia, AR 72081

Chief Executive Officer: DAVID SUMNER, K1ZZ

The purpose of QEX is to:

- 1) provide a medium for the exchange of ideas and information among Amateur Radio experimenters,
- 2) document advanced technical work in the Amateur Radio field, and
- 3) support efforts to advance the state of the Amateur Radio art.

All correspondence concerning QEX should be addressed to the American Radio Relay League, 225 Main Street, Newington, CT 06111 USA. Envelopes containing manuscripts and letters for publication in QEX should be marked Editor, QEX.

Both theoretical and practical technical articles are welcomed. Manuscripts should be submitted in word-processor format, if possible. We can redraw any figures as long as their content is clear. Photos should be glossy, color or black-and-white prints of at least the size they are to appear in QEX or high-resolution digital images (300 dots per inch or higher at the printed size). Further information for authors can be found on the Web at www.arrl.org/qex/ or by e-mail to qex@arrl.org.

Any opinions expressed in QEX are those of the authors, not necessarily those of the Editor or the League. While we strive to ensure all material is technically correct, authors are expected to defend their own assertions. Products mentioned are included for your information only; no endorsement is implied. Readers are cautioned to verify the availability of products before sending money to vendors.

A Change in Leadership

Many readers saw the notice that appeared on the ARRL Web site on July 16. (www.arrl.org/news/stories/2007/07/17/100/?nc=1) For those who did not, QEX has a new Editor.

Unfortunately, for personal reasons, Doug Smith was unable to continue as our Editor. ARRL Publications Manager, Steve Ford, WB8IMY, asked me to take over the reins. This was a step up from the role of Managing Editor, which I held since Bob (KU7G) Schetgen's untimely passing in December 2005. I was pleased to accept the new responsibilities.

Doug Smith became Editor with the Sep/Oct 1998 issue of QEX, when he took over for Rudy Severns, N6LF. Doug has served our readership well for 9 years, and we thank him for his dedication to this *Forum for Communications Experimenters*. On behalf of all our readers, and all of the ARRL Headquarters Staff, Thanks Doug.

Moving from Managing Editor to Editor is a big step. As I looked over the history of our "little" magazine, I saw a list of technical heavyweights that make me wonder if I am qualified for the position. I guess time will tell.

You may be wondering, "Who is Larry Wolfgang, and why should he be the Editor of QEX?" The announcement on the ARRL Web page contained a bit of information about me, and I won't repeat that here. I thought you might like to know a little bit more about me, though.

Since my Novice days, when I was in high school, I have enjoyed a wide variety of Amateur Radio activities. My first transmitter was a Knight T-60 kit transmitter, and I built a variety of station accessories and antennas in those early years. I continue to enjoy building both commercial kits and published projects. (I built a Heath HW-5400 for a QST Product Review, as well as an Elecraft K2/100.) I enjoy CW, SSB, FM repeaters and occasionally some digital modes such as PSK-31. I enjoy diving into a DX pileup sometimes, and like operating as a "casual contester." So I've dabbled in a wide array of Amateur Radio activities, but there are certainly many areas I have not yet tried. Part of the allure of Amateur Radio for me is that there always seems to be something new to learn about, and try.

So, what are my plans for QEX? Well, as the old saying goes, "A new broom sweeps clean," and I want to take this opportunity to make some refinements to QEX that I hope you will like. I don't expect you will notice any radical changes (at least not right away), but I do have a few ideas. I am also very interested in your input. Let me know what you like about the magazine, and please share any ideas you have for improvements.

While reading the editorial in issue number 1, December 1981, I realized that Paul Rinaldo, W4RI, established some lofty goals for this newsletter. I became aware that much of what Paul had to say could still define what I hope QEX is today, and what it can become.

"It is our intent to achieve a balance in the editorial content. In one respect, we want to feature about as much original research and development as we do practical construction articles. In another, we want to keep some sort of a balance between digital electronics (computers, etc.) and the analog world of receivers and transmitters. Within the digital domain, it makes sense to include some software as well as hardware. But that doesn't mean that *each issue* will

reflect that balance. Also, we may concentrate more than a fair share of space on a topic when it's hot and rolling. It seems reasonable to push the newer technology as much as possible, even at the expense of overlooking some more mature topics."

"If you are interested in an article, we're sure that the author would like to hear from you [and so would we]. The whole idea is to get a dialog going between experimenters."

In the past few years, it seems to me that many QEX articles have been "polished" final projects or detailed theoretical discussions. Those are good articles, but I wonder how many readers have been working on projects that others would like to learn about, but they are reluctant to write about their work and send it to us. Perhaps there are readers who don't believe their efforts would "measure up" to the standards of other articles they have read in QEX. I would like to encourage you to describe the details of your efforts to the best of your ability and send it in for possible publication. Part of my job as Editor will be to help smooth out some of the rough spots and help present your article in the best way possible.

I would like to see some articles that go back to that original charter of publishing ongoing experiments. If you have been working on a project, but are stumped by some particular problem, other QEX readers might have a solution. This is the idea of a forum for communications experimenters. It is a place to exchange information about ongoing work, where many people have an opportunity to add to the progress of the project.

If you have ideas that you think would improve QEX, please share them with me. I can't promise that we will make every change you suggest, but if it seems to make editorial and financial sense, we might be able to give it a try. For example, I received a suggestion that we add a column for readers to send brief descriptions of projects they have been working on, without going into a lot of construction or operational details. I believe we already have such a space in QEX. It is called Letters, and I encourage readers to send such notes for that column. ("Hi, I just found a new transistor, a Superduper 525, that I have used to build a low-noise RF preamplifier for a receiver project...") If we receive enough such notes, we may eventually decide to assign a new column name for that section. Let's see what happens.

As it would be with any publication, another goal for QEX is to increase circulation. I believe if more hams knew about the kinds of technical articles we publish in QEX, they would want to read every issue. We will continue to look for new ways to call attention to QEX, but one of the best sales tools is word of mouth advertising. If you read an article you particularly liked, tell a friend who doesn't receive the magazine. Help spread the word about the technical material we are publishing.

Of course, without you, our readers, we really can't do anything with the magazine. We need you to write articles about things that interest you. We need you to share ideas with other readers. We need you to respond to requests for help when you read about something about which you have particular experience and expertise.

I am looking forward to working with all of you to make QEX an even better publication than it already is. Thank you for your help and support.

— 73, Larry Wolfgang, WR1B



Octave for Circle Diagrams

The author shows us again that Octave is a powerful analysis tool, with mathematical and graphing capabilities that can serve a wide array of applications.

Maynard A. Wright, W6PAP

In “Understanding SWR by Example,” Darrin Walraven, K5DVW, provides an excellent overview of SWR and debunks some myths that have been floating around for decades.¹ Darrin makes good use of the Smith Chart in the sidebar “Adding Reactance to the Picture.” Even without reactive terminations to consider, the Smith Chart is a very useful tool when analyzing transmission lines and other situations involving transformations of complex impedances.

Software tools such as *winSMITH 2.0* can aid us in using the Smith Chart.² Using a software defined chart allows us to experiment with various networks, terminations, and lengths and types of transmission lines without using up a lot of expensive paper Smith Charts, and without wearing our pencil erasers down to a nub.

We’ve used the tool GNU *Octave* for transmission line calculations and for calculations that require graphical output.^{3,4,5} Can we use *Octave* to generate our own Smith Charts? We could certainly generate the circles and arcs using *Octave*, but the labeling would be difficult using the basic graphical capabilities of *Octave*, and the whole project would probably be a bit tedious. There may be an alternative, though: the circle diagram.

Circle Diagrams on Rectangular Coordinates

The circle diagram is described by B. Whitfield Griffith, Jr, N5SU, in *Radio-Electronic Transmission Fundamentals*.⁶ The circle diagram is useful for calculations and design work involving lumped components as well as transmission lines. The Smith Chart, in fact, evolved from a rectangular chart designed for transmission line calculations. Figure I.2 of Phillip H. Smith’s

¹Notes appear on page 8.

Electronic Applications of the Smith Chart, is very similar to the chart shown in Figure 25-3 of Griffith.⁷ (Also see Note 6.) [These figures are reproduced in the sidebar for the convenience of our readers, by permission of the publisher. —Ed.] The two charts differ in that Smith’s chart is normalized and includes arcs representing distance (in wavelengths) and Griffith’s circle diagrams are not normalized and don’t include the distance arcs.

There are several differences between each of the rectangular charts and the Smith Chart.

Table 1

Octave Code for Unit Radius Circle Centered on Origin

```
angl = linspace(0, 2 * pi, 100);
x = cos(angl);
y = sin(angl);
plot(x,y)
axis('equal');
pause;
```

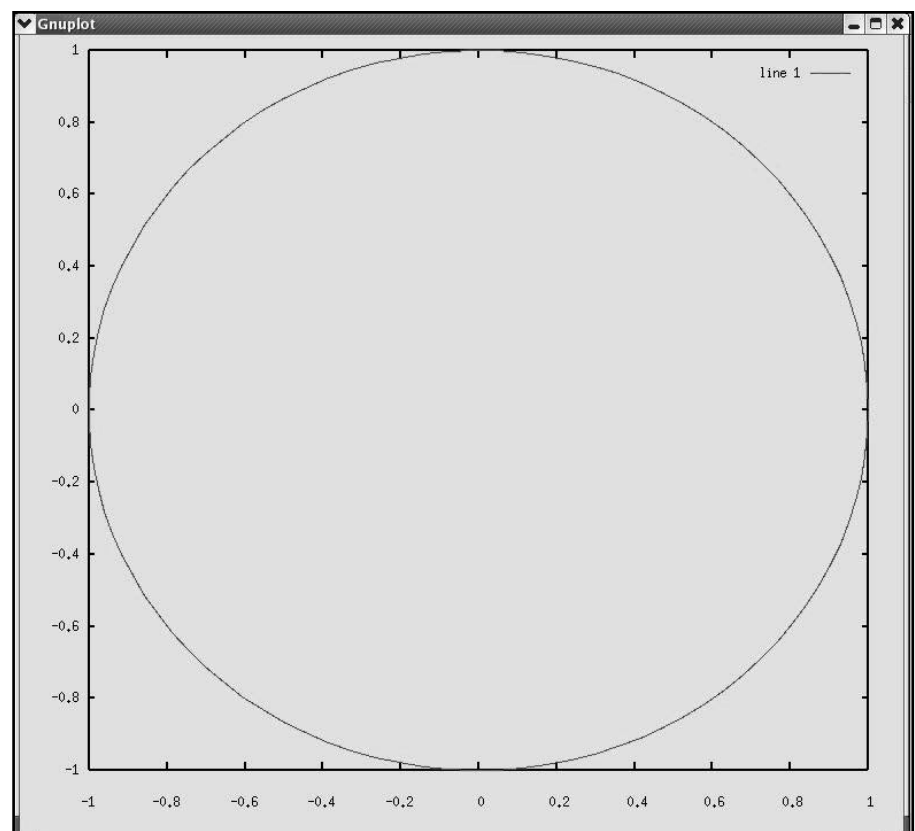


Figure 1 — Circle centered on origin.

6930 Enright Dr
Citrus Heights, CA 95621
m-wright@eskimo.com

The one that is immediately apparent is that the Smith Chart can accommodate all possible values of resistance and reactance while the rectangular chart can represent only a limited range of resistances and reactances. There is, though, as we will see shortly, an important difference that probably won't be apparent to the casual viewer of these charts.

We'll look at this matter by using *Octave* to generate some circle diagrams. Not only will we gain an understanding of the relationships between the various charts that might be used for transmission line calculations, but we'll end up with some software that may be useful for solving problems and

for studying some of the theory in which Griffith uses circle diagrams.

When we are restricted to paper charts, having to prepare different scales for each problem would be a pain. Worse, we might have to backtrack and redo the scales for a particular problem if we changed impedance ratios or other parameters during a design session. This makes a normalized chart very handy as it can be used to solve problems dealing with wide ranges of impedances. If, though, we use *Octave* to generate an SWR circle diagram, we can automate the choice of scale for the x and y axes. The plotting features of *GNUPlot* that *Octave* accesses

will then take care of the rectangular grid and the labels.⁸ We will simply write a circle onto the plot and scale it properly. We can therefore conveniently deal with actual impedance values and avoid the mathematics required to normalize inputs and denormalize results.

How do we draw a circle using *Octave*? The most convenient method, for our purposes, requires a set of parametric equations for the abscissa (x) and ordinate (y) values of each point around the circle.⁹ The parameter for our equations will be the angle (angl in the equations below and in the code in the tables) of a line between the center of the circle and a

Circle Diagrams and the Original Smith Chart

This article has made several references to drawings from *Radio-Electronic Transmission Fundamentals*, by B. Whitfield Griffith, Jr as well as a drawing from *Electronic Applications of the Smith Chart*, by Phillip H. Smith. (See Notes 6 and 7.)

For the convenience of our readers, we obtained permission from the current publisher, SciTech Publishing, Inc, Raleigh, NC to reproduce the referenced drawings with the article.

IMPED. ALONG TRANS. LINE VS. STANDING WAVE RATIO (r) AND DISTANCE (D), IN WAVELENGTHS, TO ADJACENT CURRENT (OR VOLTAGE) MIN. OR MAX. POINT.

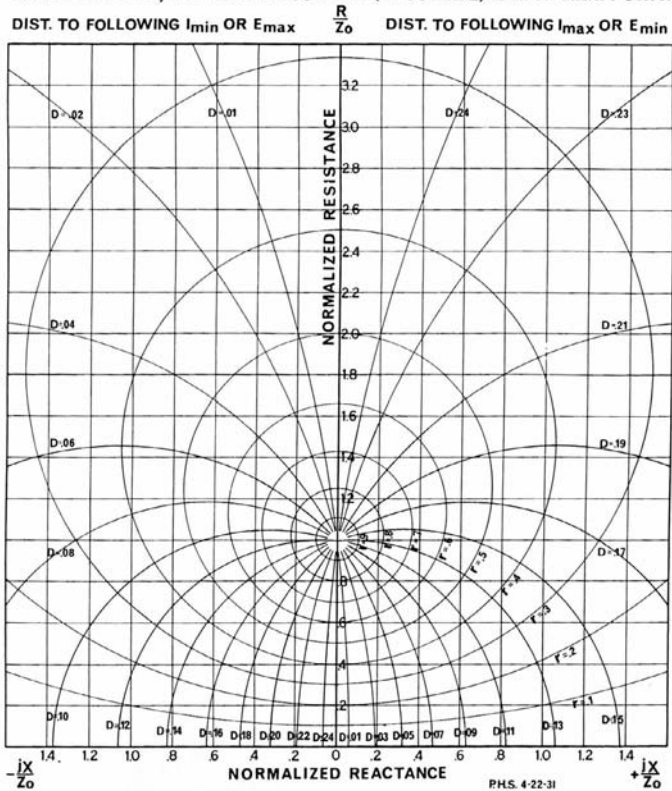


Figure 1.2 — The original rectangular transmission line chart. From *Electronic Applications of the Smith Chart*, by Phillip H. Smith, McGraw-Hill, 1969. Second edition reissued by Noble Publishing (now SciTech Publishing), 2000. Reproduced by permission from SciTech Publishing, Inc, Raleigh, NC.

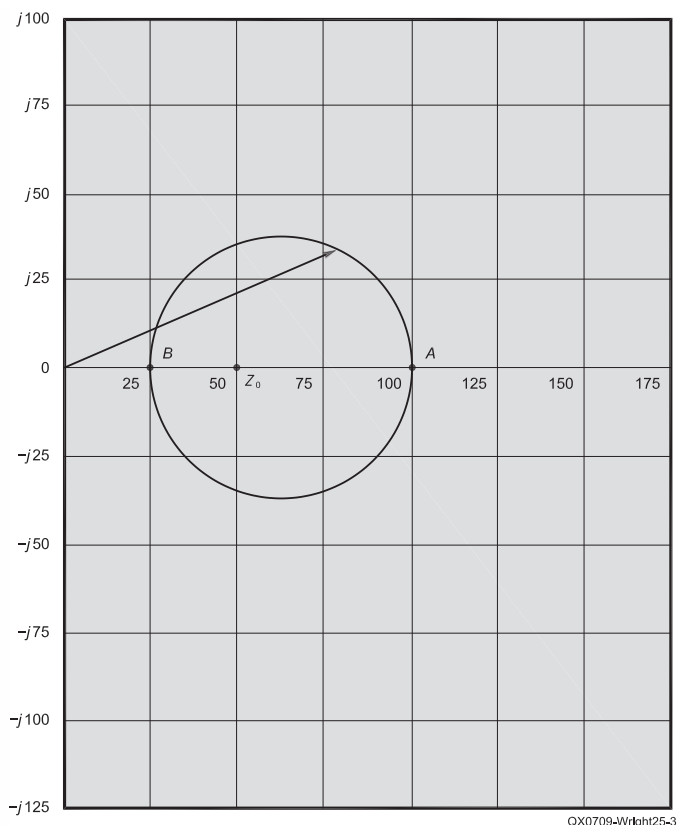


Figure 25-3 — An impedance locus of constant SWR. From *Radio-Electronic Transmission Fundamentals*, by B. Whitfield Griffith, Jr, McGraw-Hill, 1962. Reissued by Noble Publishing (now SciTech Publishing), 2000. Reproduced by permission from SciTech Publishing, Inc, Raleigh, NC.

point on the circumference. By sweeping the parameter through 2π radians, we can draw all the points needed to represent a complete circle.¹⁰ The two equations we need are:

$$x = \cos(\text{angl})$$

$$y = \sin(\text{angl})$$

A unit radius circle centered on the origin can be plotted using the *Octave* code from Table 1.¹¹ If we run this code in *Octave*, we get the circle shown in Figure 1. We need, though, to be able to scale and shift the circle if it is to represent anything meaningful. If we know the characteristic impedance of a transmission line, Z_0 , and the SWR on the line, the circle representing all possible complex

impedances along the line will pass through the two points $\text{SWR} \times Z_0 + j0$ and $Z_0 / \text{SWR} + j0$. The radius of the circle will then be:
 $\text{radius} = ((\text{SWR} \times Z_0) - (Z_0 / \text{SWR})) / 2$
 $\text{radius} = Z_0 \times (\text{SWR} - 1 / \text{SWR}) / 2$

If we multiply the two expressions for x and y in Table 1 by the radius, we will get a circle of the proper radius that is still centered on the origin.

To move the circle to its proper location, we need to find its center and then translate it to the right along the x axis by that value. The center is just one radius to the left of the maximum value of the circle, the value of the circle as it makes its "right hand" crossing

of the x axis:

$$\text{center} = Z_0 \times \text{SWR} - \text{radius}$$

We can then plot a circle of the proper radius that is centered at the right point by using the following parametric equations:

$$x = \text{radius} \times \cos(\text{angl}) + \text{center}$$

$$y = \text{radius} \times \sin(\text{angl})$$

Plotting SWR Circles

As usual, the code that does the work we want to accomplish is buried in several lines of "housekeeping" code. Code to plot a circle diagram for a specific SWR and characteristic impedance is listed in Table 2. Executing the program, from the command line or from

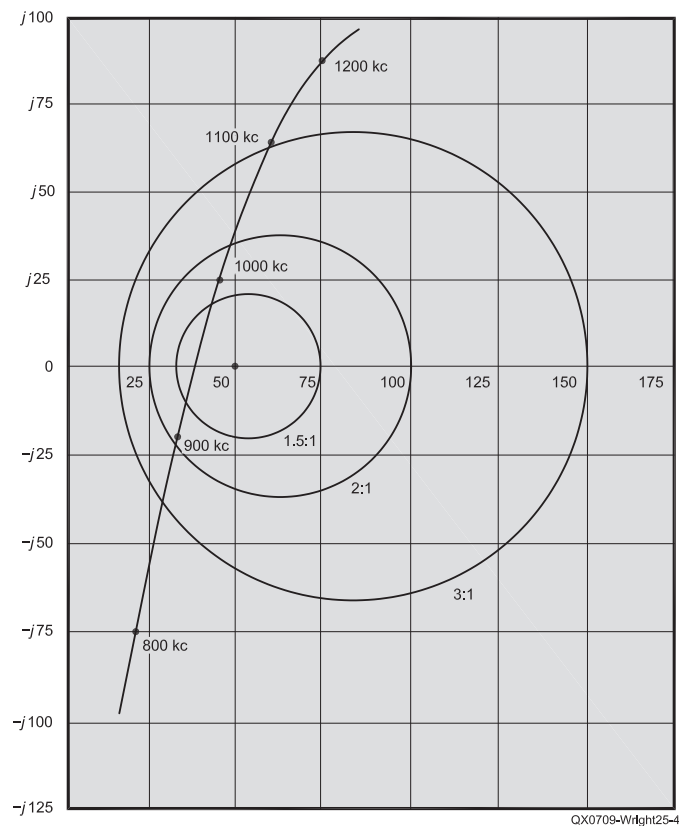


Figure 25-4 — A family of SWR circles. From *Radio-Electronic Transmission Fundamentals*, by B. Whitfield Griffith, Jr, McGraw-Hill, 1962. Reissued by Noble Publishing (now SciTech Publishing). Reproduced by permission from SciTech Publishing, Inc, Raleigh, NC.

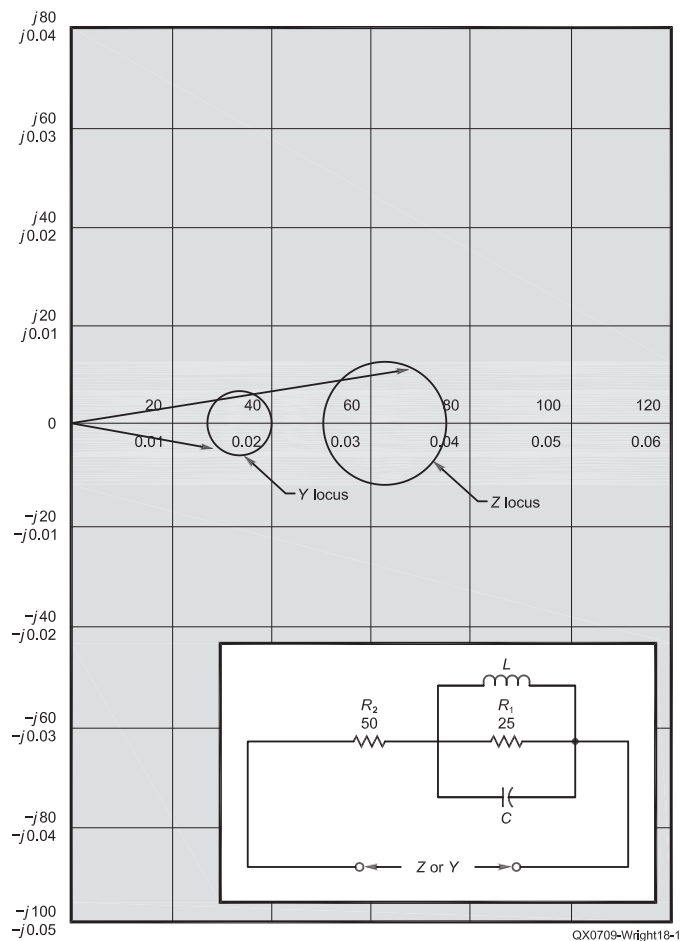


Figure 18-1 — Circle diagram for a network. From *Radio-Electronic Transmission Fundamentals*, by B. Whitfield Griffith, Jr, McGraw-Hill, 1962. Reissued by Noble Publishing (now SciTech Publishing), 2000. Reproduced by permission from SciTech Publishing, Inc, Raleigh, NC.

within *Octave*, will cause the program to prompt for SWR and Z_0 values. The program will plot an appropriate circle on rectangular coordinates that are automatically scaled for the problem at hand. A separate line, of zero length, plots a small cross at the center of the circle.

The output of the code in Table 2 for SWR = 2 and $Z_0 = 50$ is shown in Figure 2. Note that a line from the origin of the plot (point 0, 0 at the left end of the x axis) to a particular point on the circle represents the impedance

vector associated with that point. Since we have truncated the left end of the figure in the axis statement in Table 2, there is no point 0, 0 in Figure 2. If we want to print out Figure 2 and use it for graphical calculations, we might want to extend the left end of the plot to $x = 0$ so that the point 0, 0 is included. We can do that by changing the left x boundary in the axis statement in Table 2 to zero:

```
axis([0, Z0 * (1.1 * SWR), -abs(1.1 * max(y)),
abs(1.1 * max(y))]);
```

The built in variables `xtics` and `ytics` set

the intervals between major tic marks along the x and y axes. The variables `mxtics` and `mytics` set the number of minor tic marks between major tic marks. I chose the values at which the tic mark labeling changes to suit my particular display and personal preference. You can fiddle with these values without changing the numerical accuracy of the output. Note that the small dashes that comprise the vertical and horizontal lines of the grid are arbitrary and don't represent meaningful divisions of the intervals defined by the horizontal and vertical axes on the edges of the graph. The real advantage of the circle diagram over an *Octave*-generated Smith Chart is that we can obtain pretty reasonable graphical accuracy by using the grid and the tic marks along the axes with a ruler. To obtain similar accuracy from a Smith Chart, we'd have to draw lots of circles and arcs as we see in commercial Smith Charts.

To make the *Octave* circle diagram really useful, we need to be able to accurately "sweep" through a particular angle from one position along the transmission line to another as we do when moving around the circumference of the Smith Chart. There is a problem here, however. Unlike the case with the Smith Chart, there is a nonlinear relationship in the circle diagram between the angle "swept" by a radius of a particular SWR circle and the distance that such an angle represents.¹² This can be seen in the arcs representing distance in Figure I.2 of Smith. See Note 7.

Can we deal with this without drawing a lot of arcs in *Octave*? If we complicate the drawing considerably, we would negate the reason we are doing this at all. Since the reflection coefficient is "properly" related to the distance along the line, we could relate the reflection coefficient back to the distance along the transmission line and use that relationship to show particular points in our diagram. Would this produce a useful chart, though? We'd still have to write the distance arcs onto the chart in addition to SWR circles to use it as a general purpose chart and it would be inferior to the Smith Chart in terms of convenience in moving impedances along a line.

This exercise gives us an idea about why the Smith Chart has almost universally replaced the various older rectangular transmission line charts. If we nonuniformly stretch a rubber sheet with a frowning face drawn on it, we might turn the frown into a smile. In like manner, Philip Smith applied a conformal transformation to the older chart and produced a chart that plots normalized impedances on which the relationship between a particular angle (or distance along the outer scales of the chart) and the distance along a transmission line remains linear for all SWR values. This changed the distance arcs of Smith's Figure I.2 to straight lines radiating from the center of the chart, and they are omitted from printed

Table 2

Octave Code for SWR Circle Diagram

```
printf("\n\n *** SWR CIRCLE DIAGRAM ***\n\n");

swr = input("\n\n ENTER SWR: ");
Z0 = input("\n\n ENTER Z0: ");

# Calculate an SWR circle for the specified SWR and Z0.

radius = Z0 * (swr - 1 / swr) / 2;
center = Z0 * swr - radius;
angl = linspace(0, 2 * pi, 100);
x = radius * cos(angl) + center;
y = radius * sin(angl);
y_center = 0;

# Set up plot parameters and plot SWR circle.

title "SWR CIRCLE";
xlabel "REAL Z";
ylabel "IMAG Z";
if ((Z0 * (1.1 * swr)) < 220)
    gset xtics 5;
    gset ytics 5;
elseif((Z0 * (1.1 * swr)) < 440)
    gset xtics 10;
    gset ytics 10;
elseif((Z0 * (1.1 * swr)) < 660)
    gset xtics 20;
    gset ytics 20;
elseif((Z0 * (1.1 * swr)) < 880)
    gset xtics 50;
    gset ytics 50;
endif
gset mxtics 5;
gset mytics 5;
grid("on");
axis([(Z0 * 1.1 * swr) - 2.5 * radius, Z0 * (1.1 * swr), \
-abs(1.1 * max(y)), abs(1.1 * max(y))]);
plot(x, y, '-', center, y_center, '+');
pause;
```


Smith Charts to avoid unneeded clutter. See Note 7. The scales along the circumference of the Smith Chart provide all the information we need about distances along the line.

Plotting a Range of Impedances

Since we can produce circle diagrams in *Octave* with relative ease, can we make any use of them if we're not going to build or replace the Smith Chart? For one thing, the code we have in Table 2 can be used to calculate the range of impedances we will see at various points along a transmission line. We can use a plot from this code to see, for example, what sort of impedances a tuner will have to match for particular mismatches between lines of various lengths and an antenna.

Another use for a chart of this type is to obtain a clear view of how the SWR of a particular antenna or transmission line varies with frequency. Griffith gives an example, aimed at a broadcast antenna, in the text on pages 216 and 217 and in Figure 25-4 of the text listed in Note 6.

Let's try 40 meters instead of the AM broadcast band example that Griffith used. We'll assume that we have a dipole in the attic that is too close to the air conditioning ducts and other metallic objects. We don't have any choice about the location of the antenna, though, so we'll measure the impedance at the coax where it enters the shack and use the techniques of "*Octave* for Transmission Lines" to refer the measurements back to the antenna to see just how our dipole performs on 40 meters. See Note 3. We get the results listed in Table 3.

From an examination of Table 3, we can see that we have a pretty close match at 7150 kHz, but how are we doing at the other frequencies? We can plot the results from Table 3 over a graph of several SWR circles to get an idea of how far from 7150 kHz we can wander without stressing our ability to handle mismatches. The code in Table 4 draws SWR circles for values of 1.5, 2, and 3 and overlays them with a trace from Table 3. The output of the code is shown in Figure 3.

We could curve-fit the data from Table 3 to produce a smooth curve and plot that, but the plotted points connected by linear segments are sufficient to see where the SWR is going with frequency and the corners between segments are easy to visually relate to the values, particularly the frequencies, from Table 3. We can see by inspection of Figure 3 that we had better not go beyond the range between about 7070 kHz to 7200 kHz if we want to keep the SWR at the junction between the transmission line and the antenna to an SWR of 2.0 or less. Depending on whether we want to concentrate on CW or SSB, we might want to add or subtract some wire and try again. Alternatively, we might choose a type and length of line such that

the SWR doesn't cause us too much pain.

By changing the SWR values in the code and by replacing the matrix values for x_4 and y_4 with other impedance values, we can analyze the SWR trends of any set of measurements or calculations. We could also add user interface code to accept values from the keyboard as we did with the code in Table 2 if there is a need for repetitive calculations with different SWR values or matrices of impedance data.

These examples give us some tools that may be useful even though we've determined

that the Smith Chart is a better tool than the circle diagram for general impedance calculations. The main advantage of the circle diagram in *Octave* is that it can be written using only a few lines of code and we can customize it as we like to learn more about the theory of such graphical tools or to perform various tasks. In this article, for example, we used unnormalized impedances so that we don't have to multiply and divide as we do when using a normalized chart. We can, of course, with a few tweaks to the code, produce a normalized chart if we would like to do that.

Griffith uses the circle diagram for lumped circuit calculations as well as for SWR diagrams, and the *Octave* code for circles we've developed here can be applied to the solution of the design problems that Griffith describes. See Note 6.

If, for example, we look at Griffith's Figure 18-1, we see an inductor, a capacitor, and a 25 Ω resistor in parallel with a resistor of 50 Ω in series with the parallel combination. For extremely high frequencies, the reactance of the capacitor approaches zero and for low frequencies, approaching dc, the reactance of the inductor approaches zero. Either case

Table 3

Input Impedance of 40 Meter Attic Dipole		
Freq (kHz)	Real Z_{in} (Ω)	Imaginary Z_{in} (Ω)
7010	153	-71
7050	107	-35
7100	76	-15
7150	55	-3.5
7200	31	+17
7250	33	+53
7290	57	+93

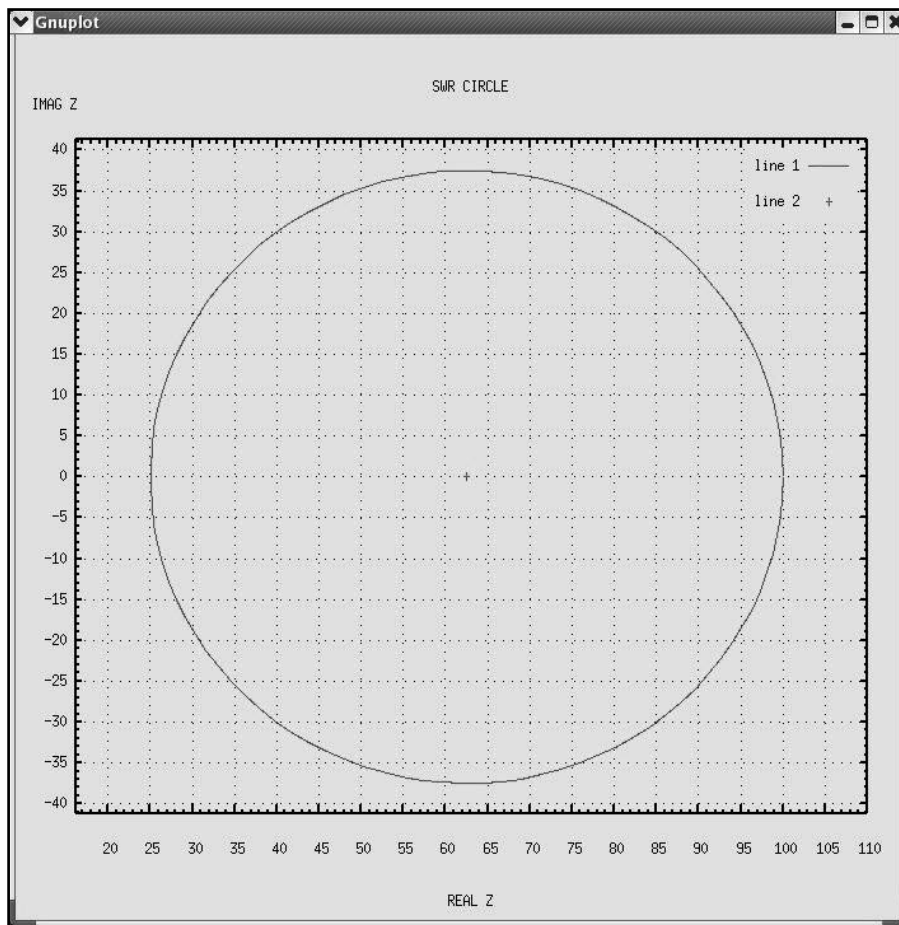


Figure 2 — Output of code in Table 2 for SWR = 2, $Z_0 = 50 \Omega$.

essentially shorts out the parallel combination and leaves only the series $50\ \Omega$ resistance. When L and C are in parallel resonance, they combine to produce a very high impedance, and the impedance of the network is essentially the series combination of the 50 and $25\ \Omega$ resistors. The impedance locus will therefore be a circle that crosses the resistance axis (x axis) at 50 and at $75\ \Omega$.

We can easily modify our SWR code to handle that situation, and the resulting code is shown in Table 5. We calculate the radius and the center of the circle as before, relating them to the minimum and maximum resistances of the network in Figure 18-1 of Griffith. For simplicity here, we'll calculate and plot only the impedance circle, leaving the admittance circle as an exercise for those interested in plotting it. Running the code produces the circle shown in Figure 4. See Note 10.

Using the same techniques, we can use *Octave* to plot any of the circle diagrams in Griffith to study them or to apply them to problems using component values other than those in Griffith's examples.

Software Updates

As is the case with commercial math software such as *Matlab* and *Mathcad*, the *Octave* development team is constantly working to improve the product. Some major changes are underway in the graphics functions in *Octave* that will improve compatibility between *Octave* and *Matlab* (see "NEWS" at www.octave.org for details). *Octave* is available in versions tagged as "STABLE" (currently 2.1.73), "TESTING," and "DEVELOPMENT" (both currently 2.9.12).

The code in this article has been developed and tested using stable versions of *Octave* (2.1.36 and 2.1.72). If you use a newer version (2.9.xx) and encounter a warning message about *gset*, or the code fails with a reference to *gset*, use a text or program editor to make a global change from *gset* to gnuplot_set (note the two underline characters before and after the two words, and the single underline between the words).

The 2.9.xx versions are preludes to the release of *Octave* 3. As is often the case

with software upgrades, it may be necessary to make some changes in older script files to take advantage of the new release when *Octave* 3 becomes available.

Notes

- ¹Darrin Walraven, K5DVW, "Understanding SWR by Example," *QST*, Nov 2006, pp 37-41.
- ²WinSMITH is described in the second edition of Phillip H. Smith's book, *Electronic Applications of the Smith Chart*. See Note 7.
- ³M. Wright, "Octave for Transmission Lines," *QEX*, Jan/Feb 2007, pp 3-11.
- ⁴M. Wright, "Octave for Signal Analysis," *QEX*, Jul/Aug 2005, pp 57-61.
- ⁵M. Wright, "Octave for System Modeling," *QEX*, Jul/Aug 2006, pp 13-18.
- ⁶B. Whitfield Griffith, Jr, *Radio-Electronic Transmission Fundamentals*, McGraw-Hill, 1962: reissued by Noble Publishing (now SciTech Publishing), available from your local ARRL dealer, or from the ARRL Bookstore, ARRL order item RETF. Telephone toll-free in the US 888-277-5289, or call 860-594-0355, fax 860-594-0303; www.arrl.org/shop; pubsales@arrl.org.
- ⁷Phillip H. Smith, *Electronic Applications of the Smith Chart*, McGraw-Hill, 1969: Second edition reissue by Noble Publishing (now

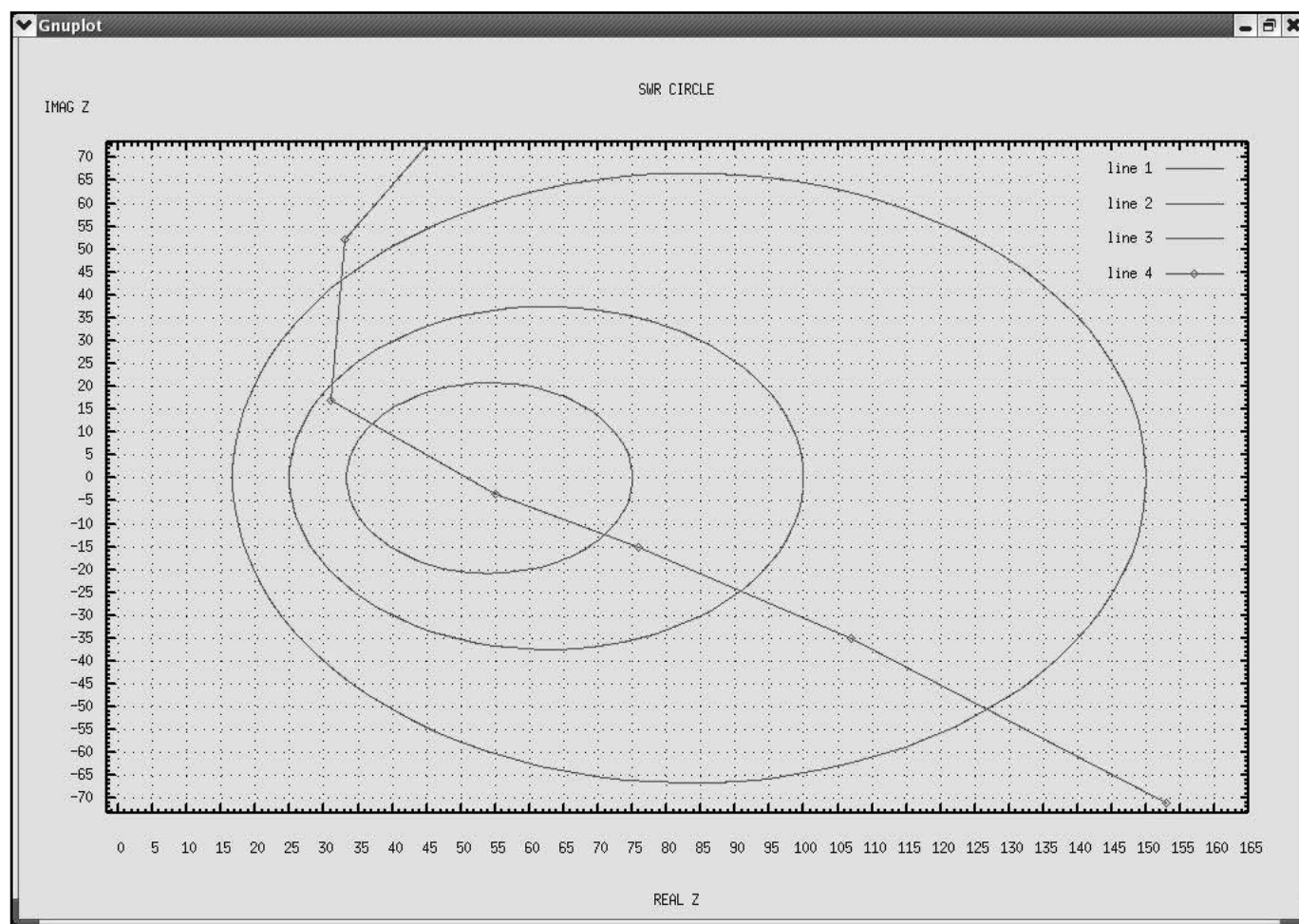


Figure 3 — SWR circle diagrams with antenna impedance trace.

Table 4**Octave Code for SWR Circle Diagram With Antenna Impedance Trace**

```
printf("\n\n *** SWR CIRCLE DIAGRAM ***\n\n");

# Calculate SWR circles for the specified SWRs and Zo.

Zo = 50;
swr1 = 1.5;
swr2 = 2.0;
swr3 = 3.0;
radius1 = Zo * (swr1 - 1 / swr1) / 2;
radius2 = Zo * (swr2 - 1 / swr2) / 2;
radius3 = Zo * (swr3 - 1 / swr3) / 2;
center1 = Zo * swr1 - radius1;
center2 = Zo * swr2 - radius2;
center3 = Zo * swr3 - radius3;
angl = linspace(0, 2 * pi, 100);
x1 = radius1 * cos(angl) + center1;
y1 = radius1 * sin(angl);
x2 = radius2 * cos(angl) + center2;
y2 = radius2 * sin(angl);
x3 = radius3 * cos(angl) + center3;
y3 = radius3 * sin(angl);

# Set up plot parameters and plot SWR circles.

title "SWR CIRCLE";
xlabel "REAL Z";
ylabel "IMAG Z";
if ((Zo * (1.1 * max(swr3))) < 220)
    gset xtics 5;
    gset ytics 5;
elseif((Zo * (1.1 * max(swr3))) < 440)
    gset xtics 10;
    gset ytics 10;
elseif((Zo * (1.1 * max(swr3))) < 660)
    gset xtics 20;
    gset ytics 20;
elseif((Zo * (1.1 * max(swr3))) < 880)
    gset xtics 50;
    gset ytics 50;
endif
gset mxtics 5;
gset mytics 5;
grid("on");
axis([(Zo * 1.1 * max(swr3)) - 2.5 * radius3, Zo * (1.1 * max(swr3)), \
-abs(1.1 * max(max(y3))), abs(1.1 * max(max(y3)))]);

# Set up matrix representing impedance trace and add to plot.

x4 = [153, 107, 76, 55, 31, 33, 57];
y4 = [-71, -35, -15, -3.5, 17, 52, 93];
plot(x1, y1, '-1', x2, y2, '-1', x3, y3, '-1', x4, y4, '-@1');
pause;
```

Table 5**Octave Code for Impedance Locus Circle Diagram**

```
printf("\n\n *** IMPEDANCE LOCUS CIRCLE DIAGRAM ***\n\n");

Rmax = input("\n\n ENTER MAXIMUM RESISTANCE: ");
Rmin = input("\n\n ENTER MINIMUM RESISTANCE: ");

# Calculate a circle for the two specified resistances.

radius = (Rmax - Rmin) / 2;
center = Rmax - radius;
angl = linspace(0, 2 * pi, 100);
x = radius * cos(angl) + center;
y = radius * sin(angl);
y_center = 0;

# Set up plot parameters and plot impedance locus circle.

title "IMPEDANCE LOCUS";
xlabel "REAL Z";
ylabel "IMAG Z";
if (Rmax < 220)
    gset xtics 5;
    gset ytics 5;
elseif(Rmax < 440)
    gset xtics 10;
    gset ytics 10;
elseif(Rmax < 660)
    gset xtics 20;
    gset ytics 20;
elseif(Rmax < 880)
    gset xtics 50;
    gset ytics 50;
endif
gset mxtics 5;
gset mytics 5;
grid("on");
axis([0, 1.1 * Rmax, -abs(1.1 * max(y)), abs(1.1 * max(y))]);
plot(x, y, '-', center, y_center, '+');
pause;
```

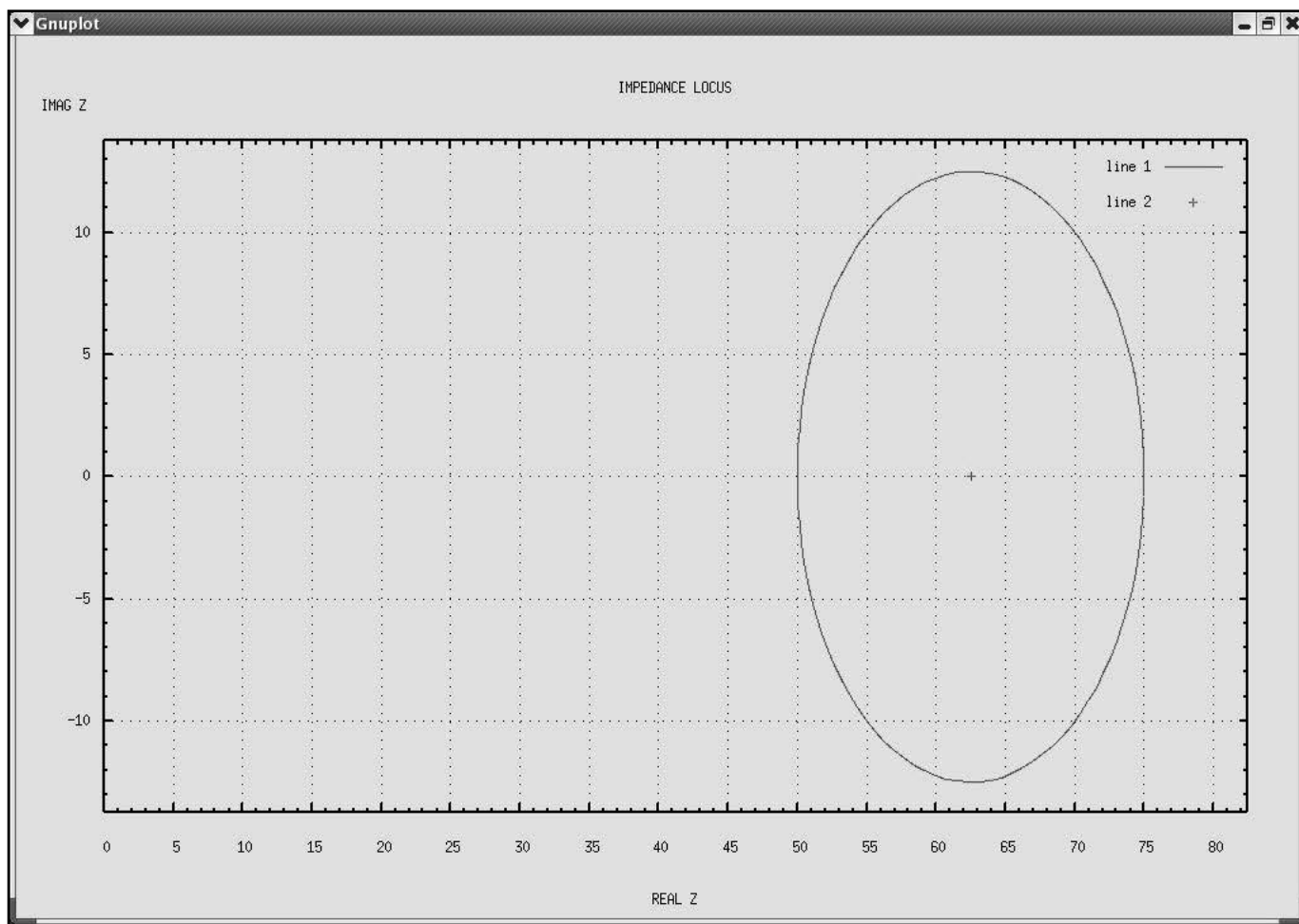


Figure 4 — Impedance locus circle diagram.

SciTech Publishing), available from your local ARRL dealer, or from the ARRL Bookstore, ARRL order no. 7261.

⁸John W. Eaton, "GNU Octave Manual," *Network Theory Limited*, 1997: This manual is also available via download from www.octave.org

⁹William L. Hart, *Analytic Geometry and Calculus*, D. C. Heath and Company, Boston, 1957, pp 151-153.

¹⁰Note that on both the Smith Chart and the circle diagram, a full rotation around the chart represents π radians, or one half wavelength. When drawing the diagram, though, the Octave software must consider the circle to be inscribed by a sweep through 2π radians to satisfy the trigonometric functions that are used to draw it. Be careful not to confuse the

two uses of angular measure.

¹¹For most versions of *GNUPlot* and for most computer displays, the plots produced by the code in this article will be initially shown as ellipses. It can be seen from the dimensions on the axes that the figures are really circles and they may be displayed as such by resizing the *GNUPlot* window with the cursor. I generally leave them full size to improve the resolution of the display even though they are not displayed as circles.

¹²The rectangular chart shown in Figure A on page 21.4 of *The ARRL Handbook*¹³ differs from Griffith's circle diagrams⁶ and Smith's rectangular transmission line chart⁷ in that Figure A plots reflection coefficients while Griffith and Smith plot impedances. In the

reflection coefficient plot, the angle swept out by a movement along a length of line is linearly proportional to the length of the line. That is not the case for a rectangular impedance chart, which is why Smith's rectangular chart includes distance arcs. (Note that the line on Figure A of *The Handbook* is plotted incorrectly. For a corrected version of the entire Smith Chart sidebar from *The Handbook*, see Note 3, pp 6-7.)

¹³Mark Wilson, K1RO, Ed, *The ARRL Handbook for Radio Communications*, 2007 Edition, The American Radio Relay League, Inc, 2006, pp 21.4-21.5. *The ARRL Handbook* is available from your local ARRL dealer, or from the ARRL Bookstore, ARRL order no. 9760.



An Unusual Vector Network Analyzer

Here are the details behind this remarkable VNA, comprised of only a PC, digital scope and signal generator.

Dr George R. Steber, WB9LVI

Building a vector network analyzer (VNA) often conjures up an image of a complex system involving exotic integrated circuit chips, PLLs, mixers, frequency synthesizers, meticulous construction techniques and custom microprocessor-based code for control. This project is a very different approach to constructing a VNA. It is based on employing commonly used equipment and writing high level PC software to capture, process and present the data.

Using this approach, virtually all of the

hardware construction is eliminated except for some simple fixtures needed for measurement. Photo 1 shows two of the main items used in this project: a signal generator and digital oscilloscope. To illustrate the fixtures involved, Photo 2 shows a simple setup used for measuring a 60 MHz low pass filter.

My system is completely automatic and capable of covering the frequency range from dc to 200 MHz. It provides a reasonable magnitude span and true 360° phase information without the need to tweak the frequency. It has been used for transmission measurements involving coaxial cables, delay lines, crystals, transformers, amplifiers and filters. It can also be used for reflection measurements of antennas, crystals, filters, circuit compo-

nents and other devices. Examples of these measurements are presented later on in the article. One of the top features of the system is that the primary equipment can go back to its original use when the VNA measurements are finished.

This article describes the details behind this unusual vector network analyzer. I don't expect that anyone will actually build a system exactly like this one, so this is not a construction article per se. It is more like reference material in case you decide to investigate the possibility of your own version. This is because, in all likelihood, you will have different equipment and consequently different interfacing requirements, resulting in different software. Even if you do not build an analyzer,

9957 N. River Road
Mequon, WI 53092
steber@execpc.com



Photo 1 — Here are the signal generator and oscilloscope I used in the VNA project.

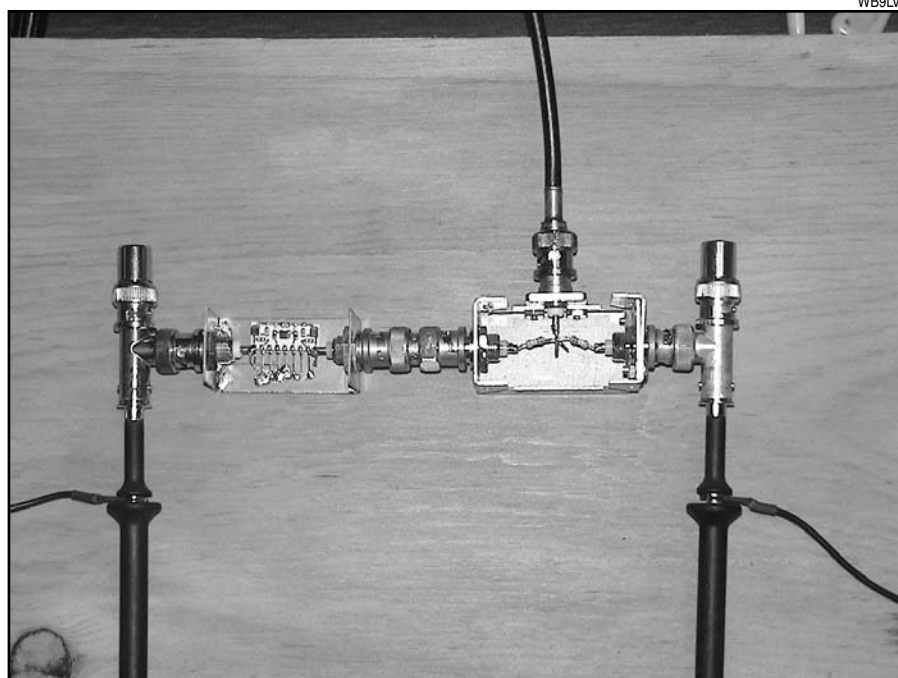


Photo 2 — My homebrew test fixture, showing the power splitter, scope probes and termination resistors, with a 60 MHz low pass filter being tested.

however, hopefully you will learn about a different approach to VNA construction and operation.

My system uses a *sampler* front end in contrast to the more classic *mixer* version. If you are new to VNAs there is a good article by Agilent about VNA basics available on the Internet.¹ It has a good discussion on mixer versus sampler front ends.

If you decide to pursue your own project, you will need a PC, a two channel digital oscilloscope with communications capabilities and a signal generator, also with communications capabilities, that covers the frequency range of interest. There are more details about the requirements for these items later in the article. You also should have some programming experience in a high level computer language such as Visual Basic, C++, QuickBasic or something similar. I have converted to Visual Basic from C++, so all of the annotations in this article will be in Visual Basic. In addition, a knowledge of serial RS232, USB or GPIB interfacing will be helpful, although this information can generally be picked up from the Internet on an ad hoc basis.

By way of history, this project was started as a result of another project (now on hold) to build a 1 GHz equivalent time digitizer — not to be confused with 1 giga sample / second (GS/s) — that would interface to a PC sound card. Problems arose obtaining parts and additional difficulties arose working with and soldering surface mount devices. One day, perusing the project in my home lab, I glanced over at my 1 GS/s Tektronix 200 MHz TDS 360 digital scope and the idea light bulb went on. Was there a way to use the high speed digitizer in this scope to capture RF data and transport it to my PC? The answer was a resounding *yes* and this project was born. Read on for more of the details on how this was done.

I will start this commentary by reviewing the equipment requirements. Pay close attention to the control and communications options of the equipment, as they are crucial to getting the system to work. Next, we'll focus on the theory behind the capturing and calculation process. After that, I will introduce the venerable vector voltmeter, and show how it relates to this project. Then I'll discuss various transmission and reflection measuring arrangements. After that, I'll discuss gain and compensation techniques implemented in software. Finally, I will give numerous examples of transmission and reflection measurements typical of those encountered by the ham experimenter. To get started, let's look at the requirements for the digital scope.

Digital Oscilloscope Requirements

This project requires a very high speed

two channel digitizer. My Tektronix scope satisfies that requirement. I obtained it for a project several years ago, and it has a communications adapter installed. This adapter was free with the scope purchase but I had not thought about or used it until this project arose. It comprises a VGA video output port, printer port, GPIB port and an RS232 serial port. The RS232 and GPIB ports allow complete control over the scope including initialization, capture, averaging, sampling and data transfer, to mention just a few. Many digital scopes today also have a USB port.

It is incredibly easy to control the scope in software like Visual Basic. Commands are sent over the RS232 or GPIB ports as simple ASCII text, terminated by a line feed or carriage return. Most commands can also have options such as "AQUIRE:STATE RUN" which tells the scope to perform a capture and save the data in scope memory. More information about programming is discussed later on.

In my experience, the GPIB bus is the fastest method of data transfer, followed by USB and RS232. However, if you use the GPIB bus you will need a controller. These can be found on internet auction sites. There are plug-in cards and external stand-alone devices. Not wanting to open my PC case to install a card, I opted for a surplus stand-alone IOtech Micro488EX controller that I found for \$50. It uses an RS232 serial port to talk to the PC, and has a GPIB bus for the instruments. It is very easy to use, and the operating manual is on the internet. Its major drawback is that it can only communicate at a maximum of 19,200 baud on the RS232 serial line. This presents a bottleneck when downloading many points of data from the scope. For example if the scope transfers 2000 points (both channels of a single capture), it takes about 1 second to transfer all the points at this rate using a binary transfer.

As noted above, direct control of the scope can also be achieved using RS232 but in my case the scope is also limited to a maximum rate of 19,200 baud, so there is no benefit. There are, however, plug-in GPIB cards and USB to GPIB controllers available that work at greatly improved speeds. These usually cost quite a bit more, but offer improved performance. I'll leave it to the reader to investigate these devices. In any case be aware that large amounts of data must be transferred to the PC when doing a frequency scan, so opt for the fastest data rate possible.

Most digital scopes have only 8 bits of resolution, particularly at the higher sampling rates. An article on the National Semiconductor Web site, describes the signal to noise ratio (SNR) limit often used for A/D converters.² This limit is given by Equation 1, where N is the number of bits.

$$\text{SNR Limit} = (6.02 \times N) \text{ dB} + 1.76 \text{ dB} \quad [\text{Eq 1}]$$

For the case of 8 bits this yields 49.9 dB. This may seem marginally adequate but measurements have shown that this is more than sufficient for many ham applications. Note that 1 bit is about 6 dB. Programming the scope vertical sensitivity can add an additional bit or more. For example doubling the gain of one channel (for a small signal) will increase the limit by 1 bit and provide an additional 6 dB between channels if necessary. This works because normally only the ratio of the two channels is needed for computation. More will be discussed on this subject later on.

Many scopes, like mine, offer waveform averaging. When this is employed 16 bits of data are returned. Although not privy to the internal working of my scope, I believe averaging works because of the slight noise on a signal. This causes a small variation of the amplitude, which causes a variation of the data, which can be averaged, yielding more bits. For example if you average two 8-bit bytes with numerical values of, say, 123 and 124, the result is 123.5, requiring more bits to represent the resulting number. I'm not convinced that averaging offers much benefit in this application when used with a good signal generator. It has been used with a noisy, unfiltered DDS signal generator, however, with good results.

It is important that the two channels of the scope sample synchronously. This will preserve phase data. Most scopes appear to do this but it is worthwhile to check this fact if buying a new scope. Scope sampling is usually classified as "single shot" or "equivalent time". Single shot often refers to transient signal capture while equivalent time sampling (ETS) requires a stationary signal but is usually capable of a much higher sampling rate. There are some low cost scopes on the market that offer ETS at 25 GS/s rates. It would be interesting to see one of those used in this application. My scope does not have ETS.

The relation of sampling rate to the bandwidth for most scopes is not at all obvious. It is usually *not* specified as the Nyquist limit of 2 samples per cycle. For my scope the sampling rate is 1 GS/s and the bandwidth is 200 MHz. I have seen 1 GS/s scopes that are rated at 100 MHz or less. The scope probes also are a limiting factor. So if you obtain a 200 MHz scope, don't use 100 MHz probes. Normally I use two 10 M Ω ($\times 10$) 200 MHz scope probes in a vector voltmeter arrangement with good results. Another possibility is to convert the scope inputs to 50 Ω using feed-through terminations. Then 50 Ω coaxial cable could be used for measurement. Note that this would work only in 50 Ω systems, while the scope probes work in almost any impedance environment.

Scope memory is another important fac-

¹Notes appear on page 23.

tor. This relates to the number of data points saved on a given capture. In my case this is 1000 points per input channel. Some scopes offer as few as 500 points at the high sample rates and 5000 or more points at slower rates. The number of points of data affects the magnitude and phase accuracy of the measurement, based on the algorithm used. More data points usually means less variation but also requires more download time to the PC. Typically, better than 0.1 dB resolution in magnitude and better than 0.1° in phase have been obtained using 1000 points.

Signal Generator Requirements

A good frequency synthesized sine wave signal generator (SG) is essential for high-quality results. I have experimented with three models. Each one has its quirks. The first one I used was a WaveTek Model 81 with GPIB, which I obtained some years ago as surplus. It is a fine SG that covers the frequency range of 10 mHz to 50 MHz. Unfortunately I found out that simply having a GPIB connector on the back does not guarantee good accuracy. The accuracy of the Model 81 is 0.1% and is good for only coarse measurements of antennas and filters.

Crystal measurements are touchier because of the uncertainty in frequency. It is very easy to program with ASCII text messages, though, and it was used for some time before I decided to opt for more accuracy. So the Model 81 went back on the shelf and a Marconi 2022C was obtained at an auction site. It covers the frequency range of 10 kHz to 1 GHz with excellent frequency stability and seven digit accuracy. It is completely GPIB controllable with ASCII text messages.

I discovered another quirk that appears to be common to many wide range signal generators. They have changeover frequencies where it takes longer for the generator to phase lock. Normally the 2022C will lock onto a new frequency in less than 200 ms after receiving a frequency command over the GPIB. When en-

countering a changeover frequency, however, it can take up to 1 s. Fortunately, there aren't many of these changeovers. My 2022C has a changeover frequency at 16.5 MHz. Knowing this, it's a simple matter to watch for it during a frequency scan and account for it by adding some delay time for it to settle down. The 2022C has become my favorite VNA signal generator and most of the data shown later on was obtained with it.

For the fun of it I experimented with a USB DDS signal generator obtained from Softmark for \$50 on an auction site.³ It works up to 50 MHz and produces a raw, unfiltered signal. I tapped across the 56 Ω resistor at the output of the DDS chip (AD9851) and achieved a good signal with nearly 50 Ω output impedance. The nice thing about this SG is that a Visual Basic program and runtime OCX are provided free, which can be incorporated into your program. Hence you can control the DDS over the USB port to change frequency and

provide frequency scans. By using waveform averaging with the scope, good results were obtained, about the same as the 2022C without averaging. So if you're looking for a low cost, albeit lower frequency SG, a USB DDS based on the AD9851 may be the ticket. I do recommend adding a low pass filter though, unless you're going to use the aliases. I haven't tried that here yet.

After playing around with the scope and signal generator, and verifying that both are controllable via GPIB (or whatever method is chosen), its time to get to work. The first step is to investigate a suitable data acquisition method and processing algorithm.

Capturing And Processing The Data

Numerous data acquisition techniques are available for the measurement of complex quantities like reflection coefficients or impedance. Among them are correlation, phase sensitive detection (lock-in amplifiers), and

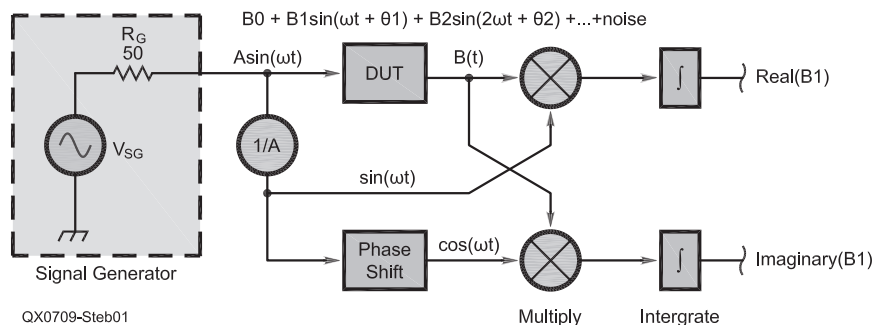


Figure 1 — This drawing illustrates the basic concept of sine correlation, showing the calculation of the real and imaginary components of the signal.

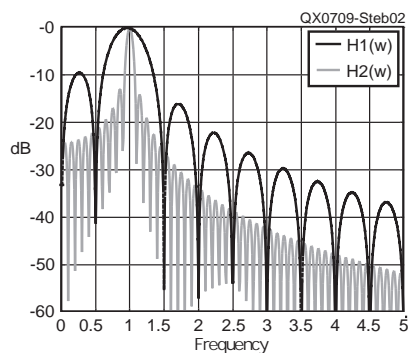


Figure 2 — This graph is the frequency response of the sine correlation filter for two different lengths, and a center frequency, ω_1 .

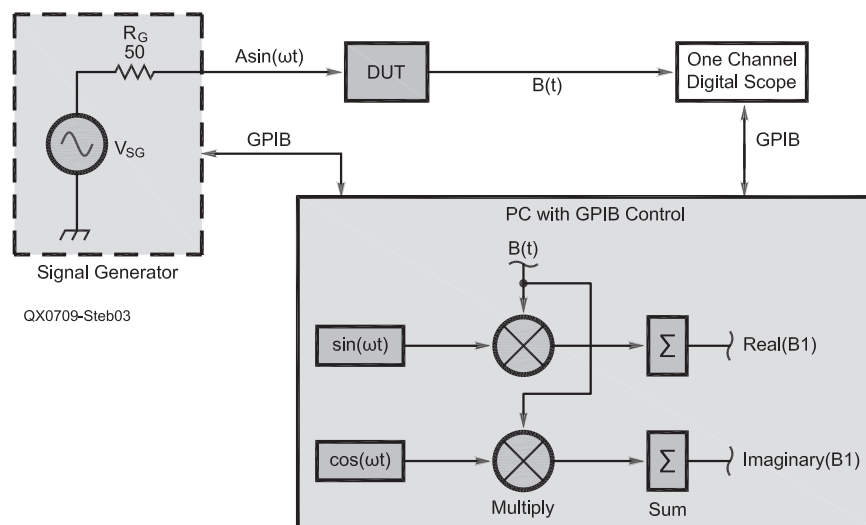


Figure 3 — This drawing shows sine correlation using a signal generator, a digital scope and a PC.

DFT techniques. The method used here is sine correlation. The correlation technique completely rejects harmonics and dc offsets. Furthermore, noise effects are significantly reduced by the selection of long integration times. Unlike some of the other techniques mentioned, this analysis method is appropriate for both linear and non-linear systems.

Figure 1 shows the basic concept employed here. The signal generator on the left generates a signal $A \sin(\omega t)$ which is applied to the “device under test” (DUT). The response output of the DUT is essentially a Fourier series with terms as shown in Equation 2.

$$\text{DUT response} = B_0 + B_1 \sin(\omega t + \theta_1) + B_2 \sin(2\omega t + \theta_2) + \dots + \text{noise} \quad [\text{Eq 2}]$$

The response typically has a dc offset, B_0 , and harmonic distortion components ($B_2, B_3, B_4 \dots$) and a noise component generated by the system. The part of the response signal that is required is the B_1 component, which is at the same frequency as the generator waveform. The spurious components of the response signal need to be rejected so that accurate measurements of the fundamental signal component, B_1 , can be made. Multiplication by reference waveforms and integration is used to filter out these unwanted signals. Those interested in more exotic experimentation with harmonics would use $\sin(n\omega t)$ for correlation where n is the harmonic of interest. It is only mentioned as an area of further study, possibly with DDS generators, and is not employed here.

The correlation process result is made up of two components, one of which is referred to as the *Real* (or *In Phase*) component. The other is the *Imaginary* (or *Quadrature*) component. By performing simple mathematical operations on these measured results, it is possible to obtain the magnitude and phase shift of the measured signal.

Considering the correlation process as a filter, its transfer function is given by Equation 3.

$$H(j\omega) = \frac{\omega_1 [1 - \exp(-j\omega T)]}{T(\omega^2 - \omega_1^2)} \quad [\text{Eq 3}]$$

where, $T = \frac{2\pi N}{\omega_1}$ N is the number of cycles, and ω_1 is the fixed center frequency of the filter. A nice derivation of this equation can be found in Solartron’s Frequency Response report.⁴ The center frequency, ω_1 , is shown offset from the origin only for illustration and plotting. The function $H(j\omega)$ is plotted in Figure 2 for $\omega_1 = 1$ and for two different integration times. As you can see, the averaging associated with the correlation acts as a bandpass filter, with center frequency, ω_1 , and with notches at the harmonics. As the averaging time, T , increases, the bandwidth of the filter becomes narrower. Thus, the corrupting influence of wide band noise is increasingly

filtered out as the correlation time is increased. Using averaging to reduce the noise is a particularly nice feature of this method, and should be kept in mind if considering other procedures that may not produce the simple filtering accuracy obtained here.

To take advantage of this method in our system the concept in Figure 1 is modified as shown in Figure 3. Only a signal generator and one channel of a digital scope are shown, both of which are GPIB controlled. In practice an *exact* frequency command is sent to the SG via the GPIB and then the output from the DUT is captured with the scope and transferred to the PC. Since we know the exact frequency “ ω ”, software functions $\sin(\omega t)$ and $\cos(\omega t)$ are used to multiply the input data. (These functions are, of course, sampled but shown on Figure 3 as continuous for clarity.) The outputs of the multipliers are summed over the 1000 points of data. The result is the same as before obtaining $\text{Real}(B_1)$ and $\text{Imag}(B_1)$. There are, obviously some differences to note and cautions to be observed.

First, it is important that the signal generator *actually* produce the frequency desired

so that the software is working with the correct frequency. For a good SG like the 2022C or the DDS mentioned earlier this is no problem.

The function in Equation 3 is only valid for an integral number of cycles. If a non-integral number of cycles is used, error will result in the form of leakage, as with most DFT methods. This can be ameliorated somewhat by using a window function on the data before correlation.

Finally, how do we account for the arbitrary phase difference between the signal generator and the software sine and cosine values in the program? The answer is that we don’t need to do that. In practice we will use two probes (A and B) and two channels of the scope in a vector voltmeter arrangement. The “A” probe will be the “reference” at the input of the DUT while the “B” probe will be the “test” at the output. In this case we will be dealing only with ratios of complex quantities and the arbitrary phase will cancel out. So now let’s see how we can use this method to make a vector voltmeter.

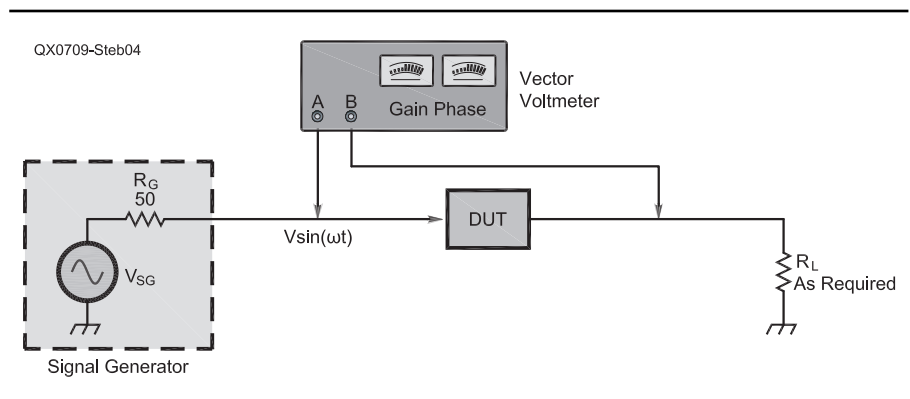


Figure 4 — Here is a typical set up for a vector voltmeter in the transmission measuring mode.

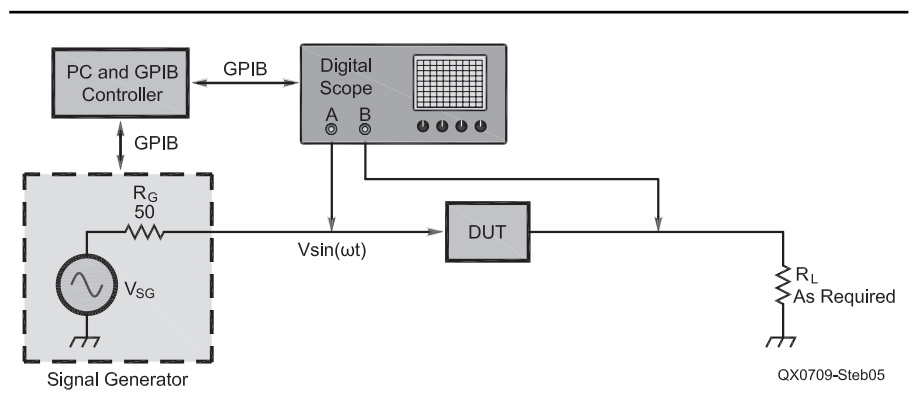


Figure 5 — This project describes a vector voltmeter using a digital scope, a signal generator and a PC.

Building a Vector Voltmeter and VNA

A vector voltmeter is a good place to start the discussion, as it puts in place most of the ideas needed for this type of VNA. A vector voltmeter is basically a sensitive two channel voltmeter. It allows you to make two simultaneous voltage measurements in a circuit and obtain ratio and phase difference measurements between the two channels. One of the earliest commercial units was the HP 8405A Vector Voltmeter (circa 1966). It used analog meters for both magnitude and phase display.

Interestingly enough it can still be found for sale on auction sites and appears to be in great demand. The specification sheet for the 8405A states that: "In addition to absolute voltage measurements, capabilities include insertion loss and computed group delay of bandpass filters and other transmission devices, gain and phase margin of amplifiers, complex impedance of mixers, antennas, matching the electrical lengths of cables, s-parameters of transistors, amplitude modulation index, RF distortion measurements and in-circuit

probing." So it seems to be quite a versatile instrument. It was capable of measuring gain or loss of up to 90 dB, $\pm 2\%$ full scale voltage accuracy and phase measurements with 0.1° resolution over a 360° phase range. My system will not perform nearly as well in gain span but it has acceptable accuracy and is even better in phase resolution while also covering a 360° phase range.

Figure 4 shows a typical analog vector voltmeter setup for a transmission measurement on a DUT like a filter, attenuator or

Table 1
Visual Basic Code Samples

```
`INITIALIZE THE GPIB CONTROLLER AND CLEAR GPIB
OutStr = "@@" + vbCr + vbLf: MSCComm1.Output = OutStr `clear Micro488
Call Tdelay(1.0) `wait for Micro488 to finish
OutStr = "clear" + Chr$(13): MSCComm1.Output = OutStr `clear all GPIB devices

`INITIALIZE THE MARCONI SG (GPIB ADR 04)
OutStr = "remote04" + Chr$(13): MSCComm1.Output = OutStr `remote the Marconi
AmpStr = Text9.Text `get SG ampl data for Marconi from txtbox
OutStr = "output04; LV" + AmpStr + "VL" + Chr$(10): MSCComm1.Output = OutStr
FreqStr = Format(Text2.Text, "00.000E+00") `get SG freq data from txtbox
FreqMarconiStr = Str(Val(FreqStr) * 0.000001)
OutStr = "output04; CF" + FreqMarconiStr + "MZ" + Chr$(10): MSCComm1.Output = OutStr

`INITIALIZE THE TEK SCOPE (GPIB ADR 14)
OutStr = "output14;acquire:stopafter sequence" + Chr$(10): MSCComm1.Output = OutStr
OutStr = "output14;data:source ch1,ch2" + Chr$(10): MSCComm1.Output = OutStr
OutStr = "output14;data:encdg rib" + Chr$(10): MSCComm1.Output = OutStr ` use binary
OutStr = "output14;data:width 1" + Chr$(10): MSCComm1.Output = OutStr
OutStr = "output14;data:start 1" + Chr$(10): MSCComm1.Output = OutStr
OutStr = "output14;data:stop 1000" + Chr$(10): MSCComm1.Output = OutStr ` 1000 pts

`SCOPE CAPTURE SUB
OutStr = "output14;*wai" + Chr$(10): MSCComm1.Output = OutStr `wait for scope rdy
OutStr = "output14;acquire:state run" + Chr$(10): MSCComm1.Output = OutStr

`SCOPE DATA TRANSFER SUB
OutStr = "output14;*wai" + Chr$(10): MSCComm1.Output = OutStr `wait for scope rdy
OutStr = "output14;curve?" + Chr$(10): MSCComm1.Output = OutStr `transfer data
OutStr = "enter14; EOI" + Chr$(10): MSCComm1.Output = OutStr `scope generates EOI
TekWFM = True `modify MSComm for TEK WF capture binary
Call cmdRead_Click `result in Tektemp variant

`SINE CORRELATION CH1
temp = Val(Comb1.Text) `get TEK Sampling Rate
c = 2 * pi * Val(FreqStr) / (temp)
TekCh1(0) = TekCh1(0) * 0.1 `smooth leading edge `slightly window the data
TekCh1(1) = TekCh1(1) * 0.5 `smooth leading edge
TekCh1(998) = TekCh1(998) * 0.5 `smooth trailing edge
TekCh1(999) = TekCh1(999) * 0.1 `smooth trailing edge
va.r = 0: va.i = 0
For k = 0 To 999 `do the correlation for va
    va.r = va.r + TekCh1(k) * Cos(c * k)
    va.i = va.i - TekCh1(k) * Sin(c * k)
Next k
```

amplifier. By convention, probe A is at the input of the DUT and probe B is at the output or load side. The complex ratio of the voltages V_B / V_A then carries the information about the gain and phase of the DUT.

Figure 5 shows a vector voltmeter setup using a digital scope, signal generator, GPIB controller and PC. Notice that the configuration is basically the same as the one in Figure 4 except that now the voltages are measured and captured in the scope. What has to happen next in order for the system to display the complex ratio V_B / V_A as in the analog setup?

The control sequence works like this. The PC, through the GPIB controller, causes the signal generator to be set to a specific frequency and amplitude. After allowing the SG and DUT to settle, the scope is commanded to capture the data on both channels A and B. Next, the captured data is transferred to the PC, again through the GPIB controller. In the PC we do a software simulation of a sine correlation on each channel as previously discussed. This calculates complex voltages V_A and V_B . In the final step, the ratio V_B / V_A is calculated and displayed. It may be shown as either a (Real, Imaginary) pair or as a (Magnitude, Phase) pair. It is actually much easier to do all of this than it sounds.

To get an idea of the software involved, Table 1 shows some Visual Basic code. The serial port MSCComm1 is used to communicate with the GPIB controller. Shown is code for initializing the GPIB controller, initializing and setting the SG parameters, initializing the scope, transferring the data to the PC and finally performing the sine correlation for the Channel 1 (A channel). Channel 2 (B channel) correlation is similar. A slight amount of windowing is also performed. Note that the result of the sine correlation is a real and imaginary number. Therefore, when calculating the ratio V_B / V_A , complex numbers must be used. Since Visual Basic does not have native complex variables this must be done by the programmer in software. There are many ways to do this and an internet search will turn up various ways of working with complex numbers in software.

By sweeping the frequency we can convert the vector voltmeter into a VNA. This is easily accomplished in software, and the results can be stored and presented in graphical form. In Visual Basic we use a FOR...NEXT loop to set the start frequency, perform the vector voltmeter calculations, increment the frequency and repeat until the total number of points is obtained. There are a few other niceties we can add in the software, like measuring plane compensation. More on this later. Now let's consider other test setups for measuring transmission and reflection parameters.

VNA Measurement Arrangements

There are other basic configurations of the

vector voltmeter for various measuring tasks like complex insertion loss or gain, complex reflection coefficient, complex impedance, two port network parameters and antenna impedance. Some of this material was adapted from the HP application notes (AN77-3) for the Model 8405A Vector Voltmeter.⁵ Photo 3 shows some of the test adapters and devices referred to in the remainder of the article.

Figure 6 shows an arrangement, without directional couplers, for complex measurements at frequencies to 100 MHz or more. It uses common insertion adapters like Ts and resistive power splitter. Notice from the figure that it comprises two resistors (matched 50 Ω resistors in this case) and should not be confused with a power divider, which has three resistors. Splitters are very expensive if bought from Agilent or Weinschel. To learn more about splitters visit the Weinschel Web site and look for a FAQ about the subject.⁶

It is easy to build your own splitter, in a small metal box with BNC connectors attached, for little cost. Use two noninductive resistors and very short leads. Photo 2 shows a homebrew splitter. Alternatively you could use two in-series resistor adapters like the Pomona 4391-50 (which is rated to 500 MHz.). Connect two of them to a T and that will make a splitter. My homebrew splitter is not as good as the one made with Pomona resistors but it is certainly less expensive. On a 200 MHz scan (with the DUT a short) the Pomona version shows a flatness of $-0.15 \text{ dB} \pm 0.1 \text{ dB}$ and a fairly smooth curve. My homebrew splitter shows $-0.35 \text{ dB} \pm 0.3 \text{ dB}$ and has several peaks and valleys. So it's not as easy as you might think to make a flat response resistive splitter. For the record, my homebrew splitter was used for most of the measurements in this article.

Notice that the function of the splitter is

to divide the signal into a reference and test channel. Reference channel A measures only the incident voltage, since it is terminated in 50 Ω . Test channel B measures the voltages at the input or output of the DUT.

If you prefer directional couplers, the circuit can be easily modified for their use. They would generally be preferred above 100 MHz. Experiments with a Mini-Circuits coupler, ZDC-20-3 (0.2-250 MHz) showed that it works well with this VNA. For now, however, we will concentrate on applications using the two resistor splitter.

Figure 6 shows that either S_{11} or S_{21} can be found (assuming matched loads) by connecting channel B to the appropriate T unit. Resistive terminations 1 and 6 are required, since it is assumed here that scope high impedance probes are used. In this case $\times 10$ probes should be used as they usually have smaller stray capacitance than $\times 1$ probes.

If you want to eliminate high-impedance probes for S_{21} measurements, you can employ coaxial feed-through insertion terminations at the scope and use coaxial cable to connect points A and B from the T units. In this case remove terminations 1 and 6, as the scope and feed-through terminations serve the same purpose. A similar method for S_{11} is described later in this article.

I will offer a word of caution if you use high-Z probes. They are extremely vulnerable to noise pickup. Do not rely on the small ground leads on the probes. Remove the probe clip and use the tip-to-BNC adapter that (hopefully) came with the probe. It fits over the probe tip and ground and provides a much better connection. See Photo 2 for an illustration. Also keep probe B away from any noise source including the probe A cable, as you will get noise induced into it. Using these methods can reduce the noise floor, which is

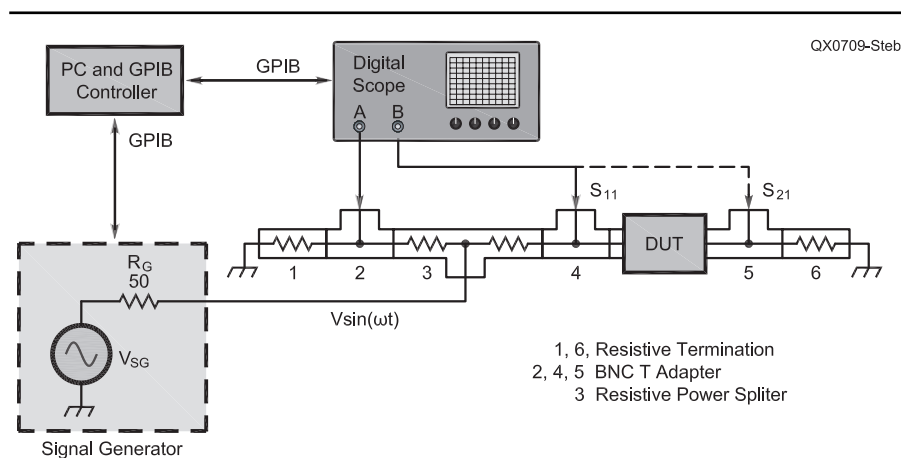


Figure 6 — This diagram shows complex parameter measurement without a directional coupler. Connect the B channel of the VNA to either the S_{11} or S_{21} measuring T.

important in VNA measurements. Of course the best performance will be obtained by foregoing the probes and using the 50 Ω terminations described above. Nonetheless, high-Z probes were used in most of my initial work and for most of the data presented here.

To calculate impedance using the setup of Figure 6, use Equation 4, where Z_0 is the splitter and termination resistance, usually 50 Ω.

$$Z_x = Z_0 \frac{\frac{V_B}{V_A}}{2 - \frac{V_B}{V_A}} \quad [\text{Eq 4}]$$

This works well for measurements of antennas, crystals, scans of coaxial cables and other reflective type measurements. It assumes that probe impedances are negligible compared to Z_0 .

Simplified arrangements for measurement of low impedances are shown in Figure 7. Figure 7A shows an arrangement, without a splitter, for use with high impedance probes. Not using a splitter avoids the 6 dB loss associated with it. This arrangement also works well for antennas, crystals and other devices. The unknown impedance Z_x is given by Equation 5.

$$Z_x = Z_0 \frac{\frac{V_B}{V_A}}{1 - \frac{V_B}{V_A}} \quad [\text{Eq 5}]$$

If you are using the low Z scope terminations, then use the arrangement shown in Figure 7B. The two grounded resistors, Z_0 , correspond to the scope terminations. For this case the unknown impedance Z_x is given by Equation 6.

$$Z_x = Z_0 \frac{\frac{V_B}{V_A}}{2(1 - \frac{V_B}{V_A})} \quad [\text{Eq 6}]$$

For measurement of high impedances, use the circuit in Figure 8. In this case, the unknown impedance Z_x is given by Equation 7.

$$Z_x = Z_0 \frac{1 - \frac{V_B}{V_A}}{\frac{V_B}{V_A}} \quad [\text{Eq 7}]$$

All of these equations for impedance require complex calculations, and can easily be implemented in the software. It should also be mentioned that the voltage on scope channel A should be as high as possible (without saturation) to use the full range of the A/D converter. This can be accomplished by setting the SG or the scope gain control as necessary. In my case the SG is set to maximum output (+13 dBm) and the scope channels are adjusted as needed

to get full range. Maximizing accuracy always requires using as much of the span as possible, particularly with 8 bit converters.

Gain and Compensation Methods

Since a PC is used here, it can be put to good use to adjust the scope B channel gain and to compensate the measurements. As mentioned earlier, the scope has 8 bits of resolution, which is adequate in many cases. For transmission measurements, however, we can use the following method to increase this to 11.3 bits (effective), which will increase the dynamic range from 49.9 dB to 69.9 dB. It is a sort of automatic gain control (AGC) in software. Basically what happens is that the magnitude of the complex ratio V_B / V_A is checked after each measurement. If it falls below some arbitrary level, say -40 dB, then we increase the B channel scope gain by a factor of 10 (about 20 dB). To maintain the correct ratio, V_B is multiplied by 0.10 in the software. As the gain is increased, noise becomes a problem. Thus, the above dynamic range is not always realizable since noise will often be the limiting factor. If the DUT is an amplifier, then a decrease in the B channel scope gain could be employed, in a similar manner, to increase the upper range above

0 dB. Similar techniques can be employed for reflection measurements.

Compensation is another story, and is done after the data has been captured. There are two compensations used, one for transmission and one for reflection. Consider the transmission compensation first.

In the transmission case we desire that the magnitude be unity and the phase be zero when a *short* replaces the unknown in the S_{21} test setup. One way to accomplish this is to first make a frequency scan with a *short* in place of the DUT and store the complex data in a calibration array or file. Then, on subsequent scans of an unknown, the DUT data is divided by the calibration data to account for the measuring fixture. This is pretty straightforward and works well.

The reflection case is a little more complicated. The method used here is the OSL (open, short, load) method described in Agilent Technologies *Impedance Measurement Handbook* of July, 2006.⁷ Here, three scans are made corresponding to an open circuit, short circuit and standard (load) impedance, usually a 50 Ω resistor. (To get better results at the higher end, sometimes a 200 Ω resistor is used for calibration.) Now, after a scan of an unknown, we know five things at a given frequency point:

- Z_0 = open circuit measurement
- Z_S = short circuit measurement
- Z_{SM} = standard value measurement
- Z_{STD} = true value of standard value measurement
- Z_{XM} = unknown DUT measurement.

These items can be used to correct the Z_{XM} data as shown in Equation 8.

$$Z_{DUT} = Z_{STD} \frac{(Z_0 - Z_{SM})(Z_{XM} - Z_S)}{(Z_{SM} - Z_S)(Z_0 - Z_{XM})} \quad [\text{Eq 8}]$$

This method can be used to compensate for different fixtures, connectors, and cable extensions. Of course a separate calibration file is needed for each case. Next, we will take a look at some practical examples of this VNA as used for transmission measurements. Reflection examples will follow that presentation.

Transmission Measurement Examples

Here are several examples of transmission type measurements, including a coaxial cable, delay line, crystal, RF transformer and seven pole filter. In the last case, a comparison is made with a commercial Rohde & Schwarz ZPV Vector Analyzer. The plots clearly show the benefits and limitations of this VNA.

Before we get to that, I should mention that my program does not have any fancy data plotting capabilities. It only includes a crude, real time display showing magnitude versus frequency to monitor the progress of the scan. Instead, for nicer looking results, the data is saved to a Microsoft Excel ".csv" file, and is processed by a freeware program called

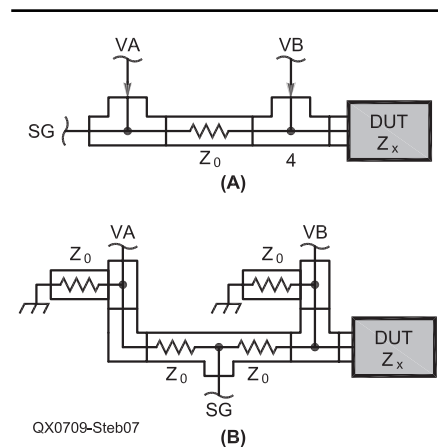


Figure 7 — Here is a simplified arrangement for making low impedance measurements. Part A shows the use of high impedance probes and Part B shows the same measurement using low impedance probes.

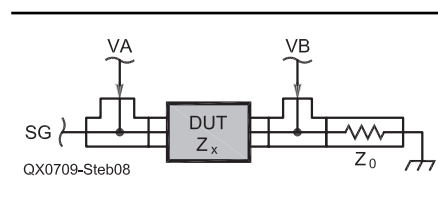


Figure 8 — This diagram shows a simplified arrangement for making high impedance measurements.

Zplots, written by Dan Maguire, AC6LA.⁸ It is necessary, however, to format the file to conform to one of those accepted by the program for other VNA systems. The figures shown here are obtained with this program based on data transferred from my program.

Before we get to the transmission line measurement, it is probably a good idea to insert known attenuators as the DUT, so a confirmation of the operation of the unit can be made. Figure 9 shows the frequency response plots for various values of attenuation obtained using some commercial Hameg in-line 50 Ω attenuators. Starting at the top are -10 dB, -30 dB, -40 dB, -50 dB, and -65 dB values. Several smaller attenuators were cascaded to achieve the larger attenuations, which probably accounts for the ripple. These are uncorrected plots.

Notice that the -50 dB and the -65 dB attenuator plots both increase with frequency, reducing the dynamic range at higher frequencies. It is not clear to me what is causing this increase. Possibilities include probe compensation, scope amplifiers, noise or something else in my setup. It is not caused by the attenuators or splitter, as they have been checked and are within 0.5 dB to beyond 200 MHz. My conjecture is that it may be due to the scope amplifiers rolling off with frequency. But since ratios are involved and the -10 dB plot doesn't suffer, there might be another explanation. In any case, there is over 60 dB of available range on the low end, decreasing with frequency thereafter.

By the way, care must be exercised in routing the probe cables and signal generator cable to the fixture. Errors will show up as hills and valleys for anything below -50 dB. This was discovered accidentally in my setup when the SG cable was inadvertently touching the B probe cable, causing extraneous peaks and notches in the response. Moving the cable away cleared up the problem. The 50 Ω cable setup mentioned earlier would probably not be as critical in this regard as the high-Z probes.

Now let's consider a transmission measurement on a plain, 50 Ω coaxial cable. An approximately 129 inches long, 50 Ω coaxial cable made of Belden RG58A/U #8259, with BNC connector on one end and UHF connector on the other was scanned in a 50 Ω arrangement. The cable, theoretically, has a velocity factor (VF) of 0.66. A transmission plot is shown in Figure 10. It's not clear what caused the tiny ripples (less than 0.1 dB) in amplitude. They may be related to the cascading of UHF-RCA-BNC adapters on the UHF connector end to adapt it to the BNC fixture.

The phase plot can be used to find the group delay from Equation 9.

$$t_D = -\frac{\Delta\phi}{360 \cdot \Delta f} \quad [\text{Eq 9}]$$

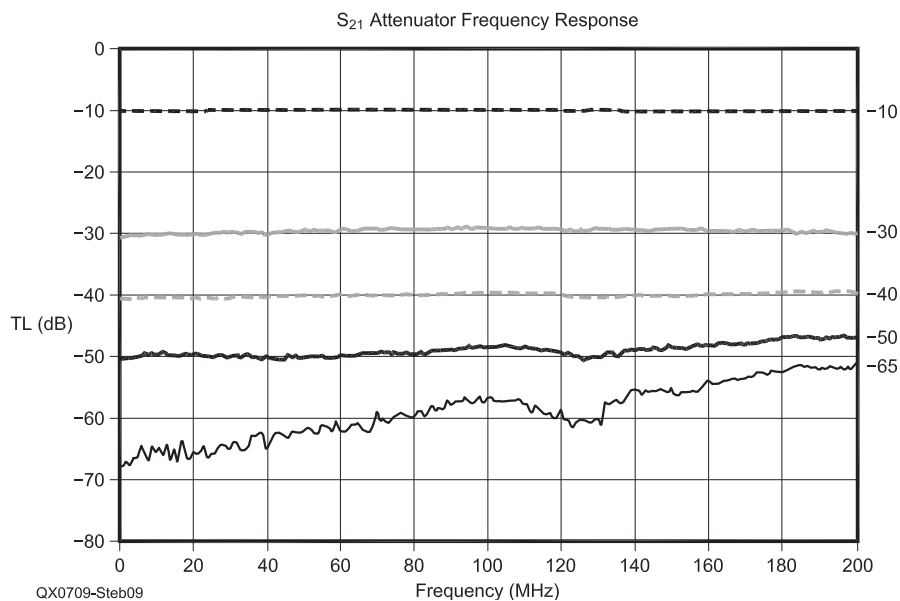


Figure 9 — This graph is an S_{21} plot of various commercial Hameg in-line 50 Ω attenuators and the noise floor. Starting at the top are -10 dB, -30 dB, -40 dB, -50 dB, and -65 dB attenuators.

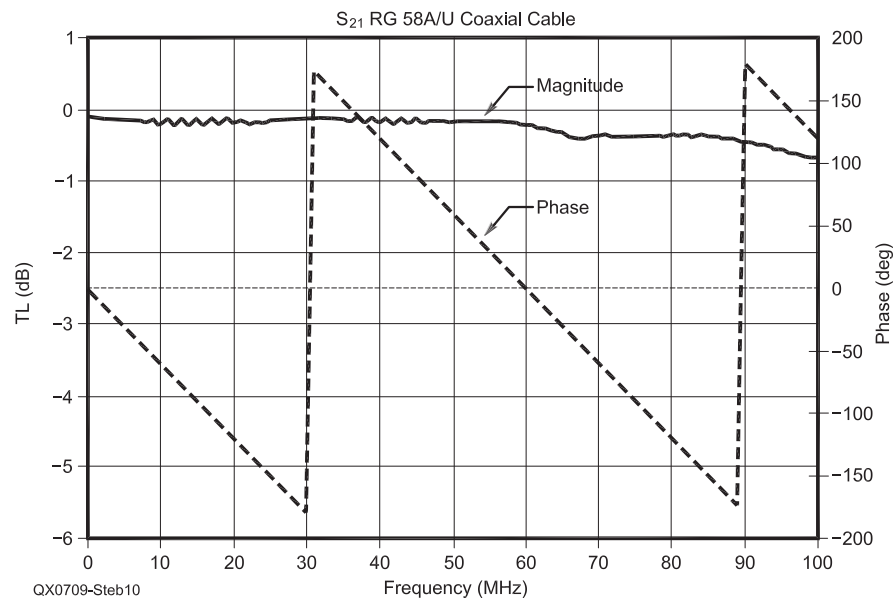


Figure 10 — Here is an S_{21} plot of a length of coaxial cable. Both magnitude and phase angle are shown.

Table 2
Measured and Theoretical Cable Loss versus Frequency

Frequency	Measured	Theoretical
1 MHz	0.11 dB	0.044 dB
10 MHz	0.21 dB	0.165 dB
100 MHz	0.67 dB	0.594 dB

where t_D = time delay, $\Delta\phi$ = change in phase, and Δf is the corresponding change in frequency. In this case, calculations from the plot indicate a value of $t_D = 16.639$ ns. To learn more about measuring cable delay with a VNA, see the informative Rohde and Schwarz presentation on this subject in Application Note 1EZ35_1E.⁹

Also for a coaxial line, Equation 10 is valid:

$$t_D = \frac{L}{VF \cdot c} \quad [\text{Eq 10}]$$

where L is the cable length, VF is the velocity factor and c is the speed of light (1.18×10^{10} in/s). Solving for L yields a theoretical length of 129.59 inches, which is close to my measured value. The electrical length (which is always longer than the physical length) would be L / VF , or 196.3 inches. Alternatively, one could find the VF for an unknown cable experimentally given L , c , and t_D .

The cable losses versus frequency are shown in Table 2, together with theoretical values for the losses. The theoretical values assume a matched load. Measured values are about 0.06 dB high. Since this is an old cable, these values aren't too bad. It should be noted that for cases like this, the "short" calibration is especially important.

Now let's look at a delay line. Some years ago several hams (myself included), who were interested in SSTV, investigated the possibility of adding color to SSTV through various schemes. This was about the time that the RCA Selectavision CED (Capacitance Electronic Disc) was departing the market and so we collected some of the surplus spare parts. One of the parts in my junk box is an RCA delay line from that product. To illustrate the use of the VNA under high and low impedance terminations, I decided to investigate the delay line's transfer characteristics. The input and output design impedances weren't known, so the delay line was just placed in the 50 Ω setup and measured. It showed severe ripples in the pass-band, indicating that it was not designed for 50 Ω terminations. The 50 Ω terminations (1 and 6 in Figure 6) were replaced with 1000 Ω terminations, and the device was scanned again.

Plots for both cases are shown in Figure 11. The top plot is for the 1 k Ω terminations and the lower for 50 Ω . The phase plot (in the passband) shows a relatively constant slope, which calculates to a delay of 346 ns. This is typical for color TV delay lines. The abrupt transition in the phase plot at 4.2 MHz is due to the fact that it is switching from -180° to $+180^\circ$. Only 200 data points were used for the plots, so it is somewhat coarse. In any case, it looks like my guess of 1000 Ω termination was not too far off the mark.

It is interesting to look at the transmission characteristics of a crystal. In this case an

18.432 MHz KDS crystal was investigated, as shown in Figure 12. Only a very small frequency band (18.340 to 18.640 MHz) was chosen to see the finer detail. A delta of 1.25 kHz was used, which resulted in 240 data points. The peak on the left is the fundamental and the accompanying phase

plot shows the extreme phase change through zero degrees at 18.432 MHz (the frequency marked on the case). It is an unusual crystal too, as there are several other peaks and phase changes later on after the fundamental frequency. For comparison purposes, the impedance of this same crystal was also measured

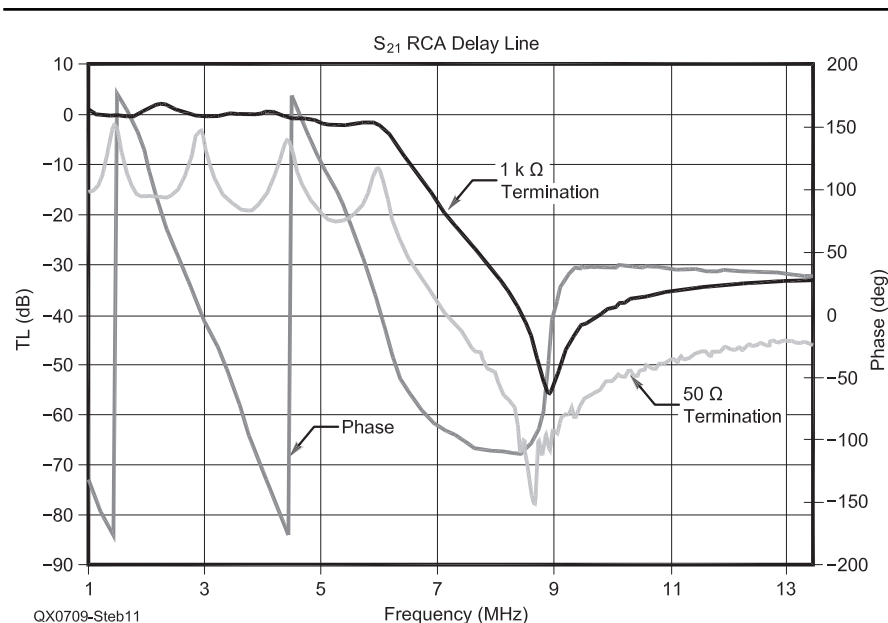


Figure 11 — This S_{21} plot is taken from an RCA delay line. The top line is for a 1 k Ω termination, and the lower one is for a 50 Ω termination. The phase plot shows an abrupt change around 4.2 MHz.

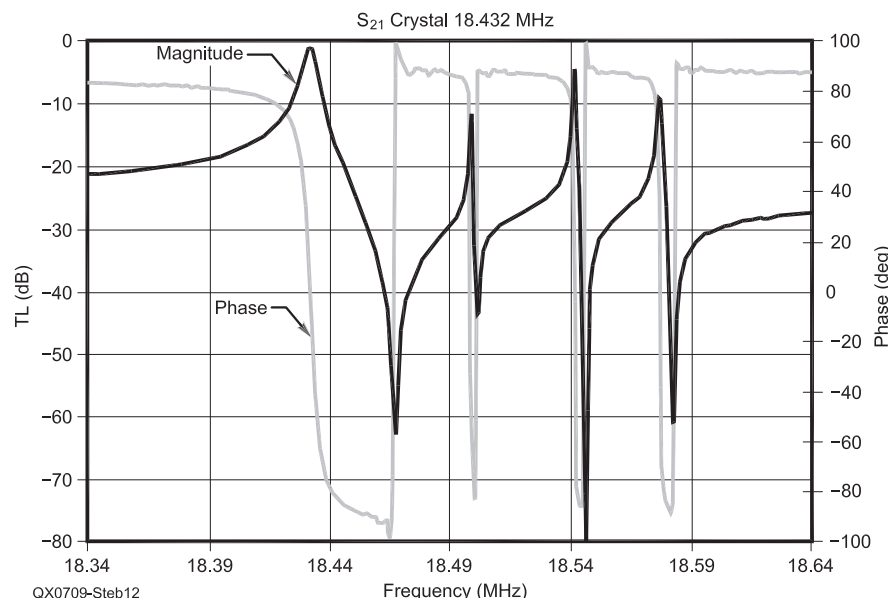


Figure 12 — Here is an S_{21} plot of an 18.432 MHz crystal. The first response peak on the left is the fundamental frequency. The phase plot shows an abrupt change around that frequency as well. Higher frequency response peaks and phase changes were also measured for this crystal.

and is shown in the next section.

There are some Mini-Circuits RF transformers in my junk box from an earlier project. One of the devices, a tiny transformer, Model T1-1 in a small six pin surface mount package was chosen for testing. According to the data sheet it is 50 Ω , with a ratio of 1:1, an insertion loss of 0.6 dB at 50 MHz and an insertion loss over the frequency range 0.3 to 200 MHz of 2 dB, referred to the mid-band loss of 0.6 dB. Figure 13 shows the magnitude and phase up to 100 MHz. Clearly, it is well within the specifications. On wide frequency scans such as this, a large increment can be used (2 MHz here) to get a fast scan. Only 50 points were used in this case. I am amazed at how well these little SMD transformers perform.

As a final transmission example, consider a seven pole 60 MHz low pass filter, known commercially as Coilcraft Part P7LP-606. It uses surface mount parts and is shown in Photo 2 at the beginning of the article. This filter exhibits a very steep roll-off and notches at 84 MHz and 130 MHz. An R&S ZPV analyzer was used to obtain the reference data, and these notches can be clearly seen on Figure 14 in the lower trace. My VNA is tracking the ZPV data okay up to about 100 MHz and shows the first notch. After that, the data becomes noisy and is no longer valid. This is due to the fact that the power splitter, scope and components used in the measuring fixture are showing their limitations at this low level. It is often difficult, at least for me, to make low level measurements (below -50 dB and above 100 MHz) without encountering stray effects. (For example, placing a metal cover over the filter, in this case, changes the plot considerably beyond 100 MHz.) To minimize these effects you should use judicious shielding, have a well designed splitter and use good fixture components. Having some knowledge of high frequency testing wouldn't hurt either.

On a side note, it is remarkable to me how well the ZPV and other commercial analyzers perform with very good accuracy at low levels of -90 dB to -100 dB. Given the problems encountered here in getting to only -60 dB, there is a renewed appreciation on my part for the specifications of those units. That's probably why they are in demand and also why they cost so much.

Reflection Measurement Examples

Covered here are examples of reflection type measurements including an RC circuit, coaxial cable, crystal and a 10 meter dipole antenna. In some cases the VNA data is compared to data from a commercial AIM4160 impedance analyzer, which has been found to be reliable and accurate. The plots clearly show the benefits and limitations of this VNA.

The program *Zplots* is used again to plot the data. It includes several other handy features like calculating equivalent circuits,

SWR and other items. It also has Smith charts and can compute the effects of adding or subtracting transmission lines.

It is always a good idea to test a new measuring device on something simple that can be easily checked. The first case chosen is a simple parallel RC circuit. In this

case a resistor of 100.3 Ω and capacitor of 527 pF, whose values were measured at an audio frequency of 1 kHz, were used. An impedance plot to 21 MHz together with an AIM reference curve is shown on Figure 15. There is very little discrepancy between the two. The bumpiness of the curve

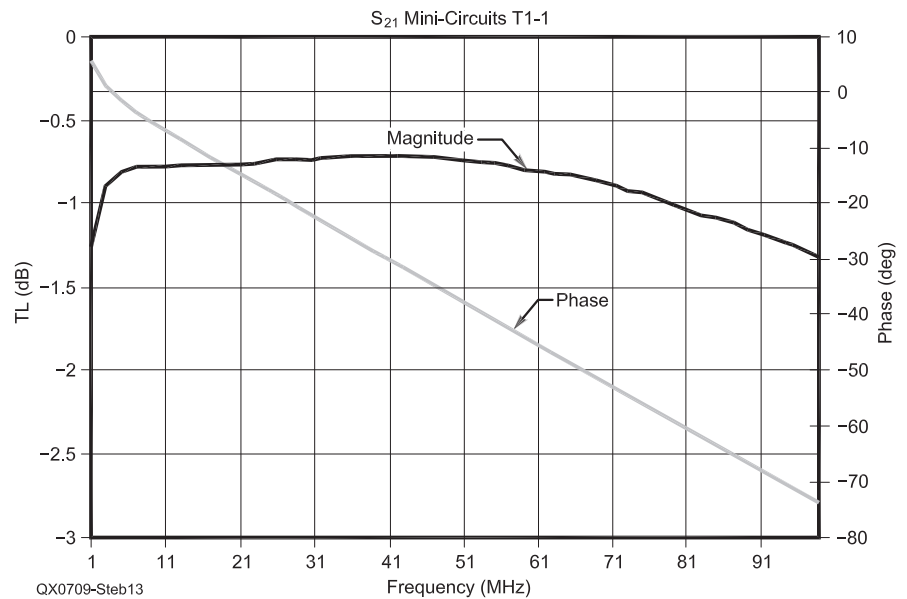


Figure 13 — Here is an S_{21} plot of a Mini-circuits T1-1 transformer. Both magnitude and phase are given.

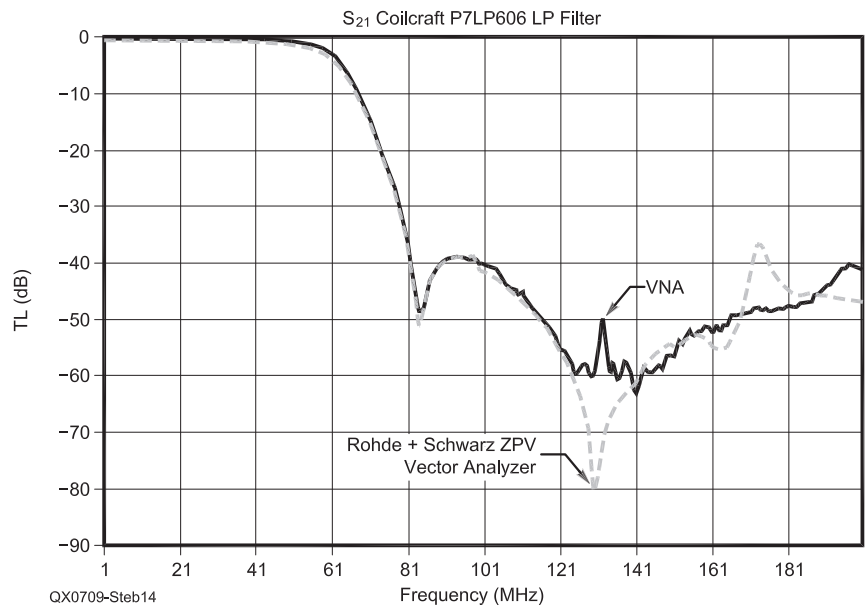


Figure 14 — An S_{21} plot of Coilcraft P7LP606 low pass filter is shown. The plot from the author's VNA is compared with a measurement from a Rohde & Schwarz ZPV vector analyzer.

is due to using only 42 data points. Comparison of the data at selected frequencies is given in Table 3.

An impedance measurement of a coaxial cable is next. A 21.5 foot long coaxial cable with a *short* at the far end is measured and shown in Figure 16 for a scan of 1 to 150 MHz. The characteristic peaks in the magnitude and phase shifts are clearly seen. Data falls pretty much on top of that of the AIM. There are 300 data points here (one every 0.5 MHz) so it takes a long time for my system to do the scan. This cable is used later on, in another example, as a feed line for a dipole antenna.

The magnitude of the impedance of the 18.432 MHz crystal, the same one measured in the transmission mode previously, is shown in Figure 17. The plot shows four high impedance peaks but the actual values of the peaks should not be considered very accurate since they are beyond the reasonable range of the VNA in low impedance mode. The dip in the curve around 18.4 MHz should be accurate, though, as it is well below 100 Ω. Table 4 gives data for two frequency points on opposite sides of 18.432 MHz. The data includes series resistance R_s , reactance X_s , and impedance Z .

There is a change in sign of the reactance, X_s , indicating a major phase change near 18.432 MHz. There are actually four major phase changes for this crystal, as seen previously on the transmission plot (Figure 12), corresponding to each of the peaks, but the fundamental one is at 18.432 MHz.

To conclude the measurements, a homebrew 10 meter (28 MHz) dipole wire antenna was scanned as shown in the lower plot of Figure 18. In this case a coax feeder of 21.5 feet of RG58 (this coax was measured as shown in Figure 16) was connected to a dipole consisting of two wires about 9 feet long attached at the far end in the typical dipole configuration. This was to be the first pass at the dipole, as I was expecting to trim the wires for an exact frequency later on. The scan shows a resonance at 25.7 MHz, which is a predictable lower frequency, since the wires are longer than the theoretical 8.2 feet. At this point, the following data was obtained. $SWR = 1.21:1$, $|Z| = 45.45 \Omega$, $\angle Z = 9.6^\circ$, $R_s = 44.82 \Omega$ and $X_s = 7.68 \Omega$. Note that R_s is less than the anticipated 75 Ω. Using the “subtract transmission line” feature of *Zplots* produced the upper curve, which theoretically is the plot of the dipole at the end of the coax. At the same frequency, it is found that R_s is now 68.3 Ω and $X_s = 0.75 \Omega$, which is closer to expected for a dipole near resonance. Now all that is left to do is to trim the wires for the desired frequency.

This completes the examples, but there are many more applications for the VNA and lots of them can be found in the references cited throughout the article.

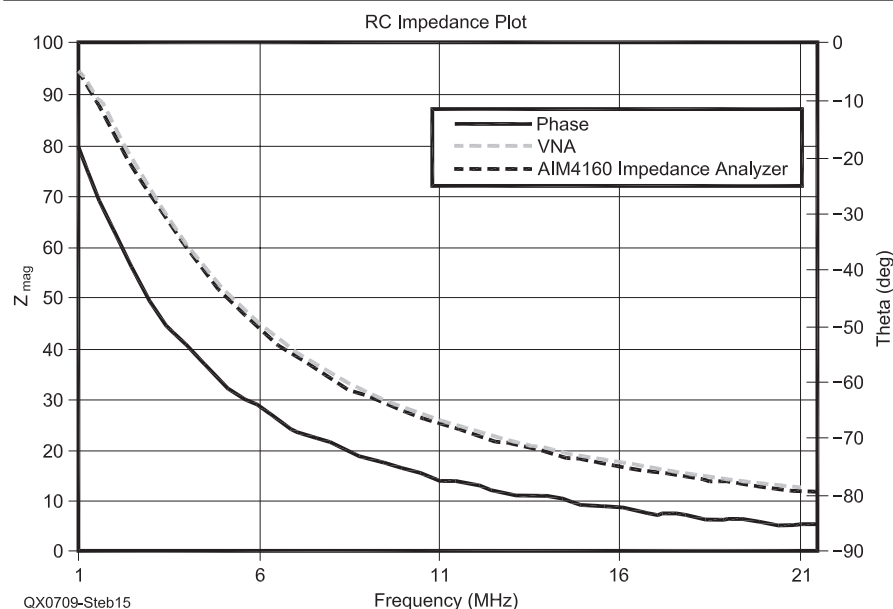


Figure 15 — This graph is an impedance plot of RC components. The author’s VNA plot is compared to a reference measurement from an AIM4160 impedance analyzer.

Table 3
Comparisons of Measurements with an AIM Impedance Analyzer and the VNA

Frequency (MHz)	AIM		VNA	
	Z	angZ	Z	angZ
3.5	65.6	-49.3	64.8	-49.9
7.0	39.6	-67.2	39.0	-67.9
10.0	28.3	-73.9	27.9	-74.5
15.0	18.7	-79.5	18.4	-81.5
21.0	12.4	-83.5	12.3	-85.0

Note: The slight discrepancies may be due to fixture or calibration differences.

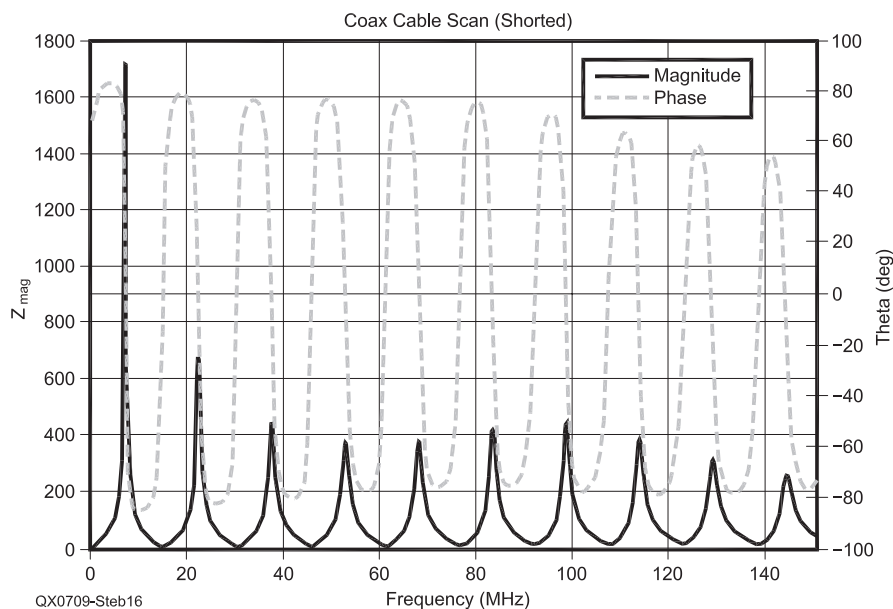


Figure 16 — This graph is an impedance plot of a shorted coaxial line. Both magnitude and phase are shown.

Summary and Conclusions

This article presents an alternate approach to vector network analyzers using a *sampler* type front end as opposed to the more conventional *mixer* type. This VNA is unusual since only a digital scope, frequency synthesized signal generator, measuring fixtures and a GPIB controller are needed. Granted, digital scopes are costly items but they can often be found on auction sites at bargain prices. (In my humble opinion, a digital scope is essential in today's advanced home lab.) Using conventional equipment has drawbacks in terms of dynamic range and noise floor but can produce useable results in the right situation. Examples were presented to show a number of useful applications.

One shortcoming of this system is that it is very slow at obtaining measurements. This is mainly because of the serial transfer speed of the controller and the capture time of the scope. With today's PCs, the calculation time for processing the data is negligible. Data capture and transfer to the PC are slow, however, and, in this case average from 1.0 to 1.8 seconds per data point depending upon the amount of data transferred. This could be improved considerably with faster hardware. It is not so bad waiting a minute or so for a scan, though, as it gives you time to sip your coffee and reflect on what you are doing. It also causes you to think more carefully about setting up scan limits and the starting frequency. As it turns out, most of my time is spent pouring over the data, reflecting on the measurement and planning the next test rather than just waiting for a scan. Anyway, in most cases, only a few scans are needed.

The software to get this system going took up most of the project time. This is because controlling hardware is fraught with little bugs that need to be found and fixed. (For example, my scope had a problem traced to a poorly seated GPIB connector.) Also, hardware doesn't always work exactly as described in the equipment programmers guide, and some trial and error measures are needed. Several weeks were spent exploring the fine points of GPIB control, because that was all new to me. Fortunately, programming is an enjoyable experience and it is always exciting when a piece of code actually does what it's supposed to do. Other weeks were spent exploring types of signal generators and learning to program them. While not overly complicated it does take some time to do all of this.

This homebrew VNA can be very useful in many situations where a more sophisticated instrument is not available. It's easy to set up and operate. But it took me several weeks of operating and testing to gain confidence in it. Now it's a pleasure to use and it seems that everything in my junk box needs measuring! Dynamic range is restricted to around 60 dB

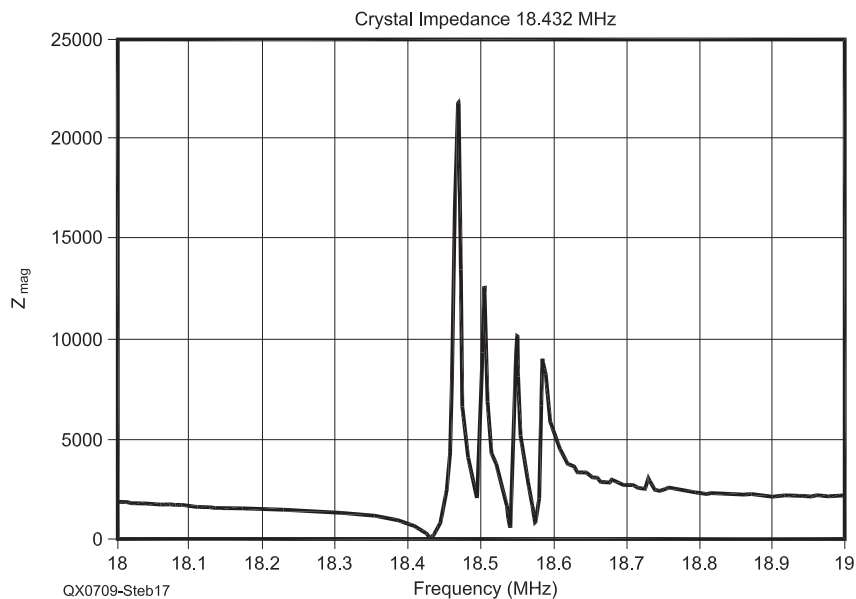


Figure 17 — Here is an impedance plot of an 18.432 MHz crystal. Notice that there are four high impedance peaks, similar to the S_{21} plot of Figure 12.

Table 4
Impedance Measurements of a Crystal Using the VNA

Frequency (MHz)	R_s	X_s	VNA Z_{mag}	VNA Z_{ang}
18.430	7.29	-88.9	91.7	-85.4
18.435	2.60	135.5	135.5	88.9

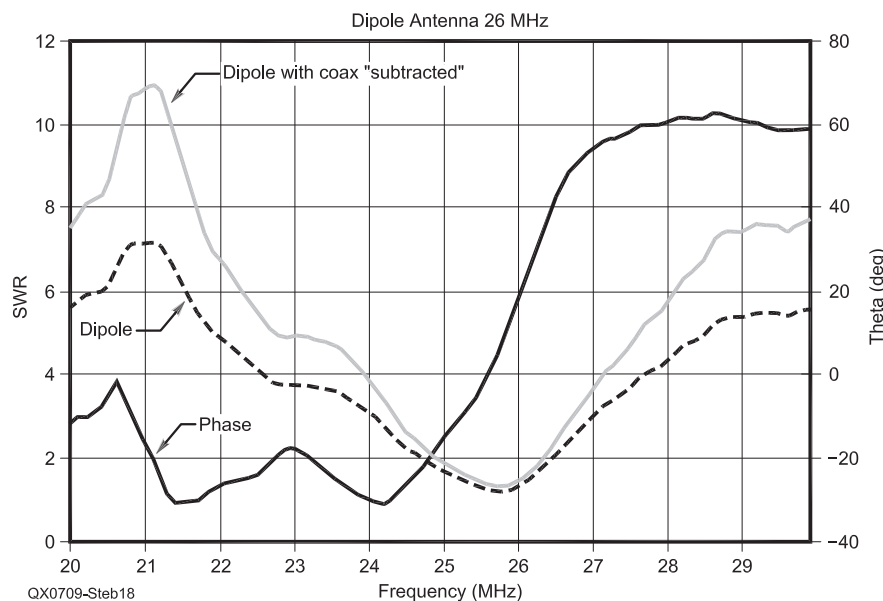


Figure 18 — Impedance plot of the first cut on a 10 m (28 MHz) dipole.

(depending on noise) and the accuracy and resolution are good over a large frequency range. Would a commercial VNA be a better choice? Of course. But until that day comes along I'll string along with this one.

Being able to make transmission type measurements is important. Many antenna analyzers on the market today only measure impedance and require twiddling the frequency to find the phase, which doesn't always work with a coaxial transmission line. They don't have the dynamic range, measurement capabilities or resolution of this unit. But, of course, this VNA isn't portable like most of those analyzers, either.

Building this VNA was an enjoyable experience. Its specifications are woefully short of a commercial VNA so don't sell your stock in Agilent! All the same, it was instructive putting it all together and getting it working. Hopefully you have also learned something from this project that will help you with your next activity. In any event, *analyze* your options, set your *vector* in the right direction, and don't be *phased* by the *magnitude* of your next project.

George R. Steber, PhD, is Emeritus Professor of Electrical Engineering and Computer Sci-

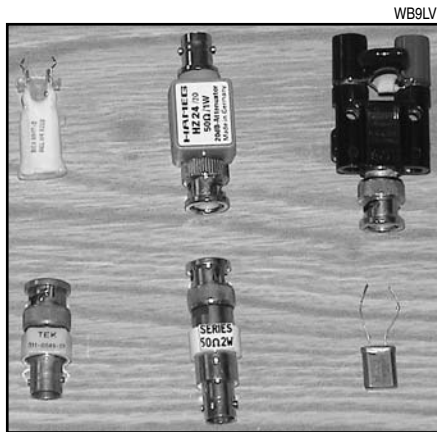


Photo 3 — This photo shows some of the items mentioned in the text. Top row, from left to right, are a delay line, a 20 dB attenuator and my RC component test unit. Bottom row, from left to right are a coaxial resistive termination, a commercial 50 Ω series resistor and an 18.432 MHz crystal.

ence at the University Of Wisconsin-Milwaukee. He was an active researcher there and also taught in the graduate program for 35 years before retiring a few years ago. George, WB9LVI, has an Advanced class license, is a

life member of ARRL and the IEEE, and is a registered professional engineer. Dr Steber has written several articles for QST such as "A Low Cost Automatic Curve Tracer" in the July 2006 issue, as well as several QEX articles. George has worked with NASA and the USAF on various projects and also has extensive industrial experience, with 18 patents issued. He still acts as a consultant and product designer occasionally. In his spare time he enjoys reading, racquetball, astronomy, Amateur Radio, music projects, video editing, and playing his trumpet in local bands. You may contact him about this article at steber@excepc.com with "vna" in the subject line and your e-mail mode set to text.

Notes

- ¹cp.literature.agilent.com/litweb/pdf/5965-7917E.pdf
- ²www.national.com/appinfo/adc/files/ABCs_of_ADCs.pdf
- ³www.ar.com.au/~softmark/
- ⁴www.control-systems-principles.co.uk/whitepapers/frequency-response-analysis2.pdf
- ⁵www.k6mhe.com/n7ws/AN77-3.pdf. Caution, this is a 13 MB file.
- ⁶www.weinschel.com/PDFILES/PowerS&DFAQ.pdf
- ⁷cp.literature.agilent.com/litweb/pdf/5950-

Two Big Winners from Array Solutions



PowerMaster Watt / VSWR Meter

- Sets the benchmark for all other SWR/Watt meters to follow
- Unheard of accuracy for the price
- Fast, bright, reading meter
- Application software included
- Upgradeable via Internet
- \$450



AIM 4170 Antenna Analyzer

- Most advanced vector impedance analyzer at a fraction of the cost
- Accurate and easy to use
- Application software included
- Lab instrument quality
- Upgradeable via Internet
- \$495

Just too many features to put in just one ad, see them on our website!

www.arrayolutions.com

Phone 972-203-2008

sales@arrayolutions.com

Fax 972-203-8811



We've got your stuff!

A DDS Based QRSS (and CW) Beacon

While experimenting with a DDS IC, the author added a PIC controller and QRP amplifier to create a really slow speed CW beacon.

Matteo Campanella, IZ2EEQ

Introduction

In early 2006 I became interested in the theory and applications of DDS (Direct Digital Synthesis), leading me to some experiments using Analog Devices ICs to better understand and evaluate this technology. Later on, during one of the usual Web-surfing sessions intended to find out something new to try out with the radio waves, I got in touch with the world of QRSS.

I knew little about these very narrow bandwidth modes, and I was convinced they were only used on the VLF bands. What I found on the Internet changed my vision about that, thanks to the contribution of a bunch of fellow hams belonging to a group called "The QRSS Knights."

These hams are active worldwide and they share a common interest: to break the micro-watt per mile record, renewing on a daily basis the challenge of being heard at the longest distance with the lowest power.

Most interestingly, a good part of the experimentation is done on the 30 m band, at about 10,140 kHz. This makes it accessible with the standard equipment and antennas an average ham usually owns (some traffic is done on 40 m, too, for an even wider audience).

What Is QRSS?

The term QRSS is derived from QRS — a CW abbreviation that means "You are sending too fast" or "Slow down." By extension, then, QRSS would imply a *very* slow sending speed. Another interpretation is that QRSS stands for "quasi-random signal source."

This definition has to do with the very long dot and dash times.

There is a lot of information on the Internet about QRSS. One interesting and informative article is at www.ussc.com/~turner/grss1.html.

Operating QRSS

Even though a commercial radio can be used to operate QRSS and related modes, usually the QRSS gear is home built, either on the basis of an existing project or starting from scratch, and the whole story works more or less like this: you build your QRSS/DFCW/FSKCW (more on these terms later) capable beacon, and put it on the air, possibly letting the fellow Knights know you're on the air. (There is a very active mailing list for this purpose: mail.cnts.be/pipermail/knightsqrss_cnts.be.)

The enthusiasm and participation on the list was so exciting that I decided to build my own beacon as well, and I couldn't think of a better way to put my recently acquired DDS knowledge to work.

Later on you will start receiving reports, but do not expect an RST report — a report is usually an e-mail or a posting onto the list, with a screen shot attached. This depends on the fact that, because of the very low power involved, the signal is not usually heard; it is buried in the noise. Given the very slow cadence of symbols, though, it is possible for some DSP enabled software to integrate over time and show the carrier on a frequency waterfall screen, much like the one we use with PSK31. One of the most-used programs for receiving QRSS is *Argo* (freely available on the Internet at digilander.libero.it/i2phd/argo/index.html). Even though this software has been developed with QRSS decoding in

mind, it works perfectly with the other modes as well, as they are small variations on the main theme.

A Brief Guide to Narrow Bandwidth Modes

QRSS mode is 100% good old CW, only very, very slow; so slow that one dot is usually 3 to 120 seconds long! Considering that the dashes and spaces are in the usual relationship with the dot, you can easily imagine how long it takes to send a simple word! FSKCW and DFCW are instead 100% duty emission modes, as the transmitter never stops transmitting a carrier: FSKCW is quite similar to CW, the only difference being that keying is not off during the pauses but it's just shifted down a few hertz. Suppose you're transmitting on 10,140,080 Hz, in FSKCW. You have to shift your frequency to 10,140,070 Hz during the pauses. DFCW is quite different: dots and dashes in this mode have the same duration, and the difference is made by the frequency of the carrier. Referring to the previous example, you will transmit your dashes on 10,140,080 Hz and your dots on 10,140,070 Hz. This is the most efficient of the three, as it takes the smallest time to transmit a message. It's also a bit awkward to recognize at a glance, as we are used to seeing dashes always much longer than dots.

Graphically speaking, QRSS will show up on *Argo* or any equivalent software as a brighter line over the blue noise background; the line will be dashed, with the long marks corresponding to dashes and short ones corresponding to dots. The blanks will obviously be the pauses. FSKCW looks more like a square view, with the top line of the signal representing dots and dashes as in QRSS, and the bottom line the pauses. Finally, DFCW

SS Dei Giovi, 41/A
Binasco, Italy 20082
iz2eeq@arri.net

looks like a square wave with 50% duty cycle, the dashes being on the top line of the signal and the dots on the bottom.

The Project

The most basic device to get on the air with QRSS is a crystal based oscillator followed by a buffer and a final amplifier. You want an output power that doesn't exceed half a watt most of the time (100 mW is the most common power). This allows for very simple circuit solutions and cheap components, but on the other hand there is a critical requirement — frequency stability. QRSS and similar modes are extremely narrow band, allowing many signals to be stacked close in the same 100 Hz frequency span (the range monitored by *Argo*). In such a condition it is very important to avoid as much drift as possible. This goal is normally

achieved using heated crystals and thermally stable enclosures for the VFO module. Let's see how a DDS will behave.

The approach I have used with this project was to think modular, and to design each module so that it could be reused in a number of different contexts from the original project, as an elementary building block for something more complex. According to this model, I have identified three modules: the DDS module (responsible for signal synthesis), the CPU control module and the amplifier module.

Choosing Module Cores

When it comes to DDS, there's a huge choice on the market today. The most modern devices are out of reach for the casual experimenter anyway, mainly because of the package that makes them unsolderable

by means of a simple iron. Luckily enough, Analog Devices makes a device that perfectly fits the needs at HF and low VHF bands — the AD9851. It's not exactly what you can consider easy soldering, having a pin to pin distance of 0.6 mm, but with some patience, a magnifying glass and a good low power iron it is possible to work it out.

This small wonder can be clocked at a maximum of 180 MHz, thus allowing synthesis of a sinusoidal signal up to 90 MHz for the Nyquist Theorem limit. (As a matter of fact you will want to limit synthesis to one third of the clock frequency, or 60 MHz, because of hardware limitations over theory.) The other interesting aspect of this chip is that it needs just one voltage (2.7 to 5.5 V) for operation, while some of the more powerful and modern solutions require different voltages for I/O

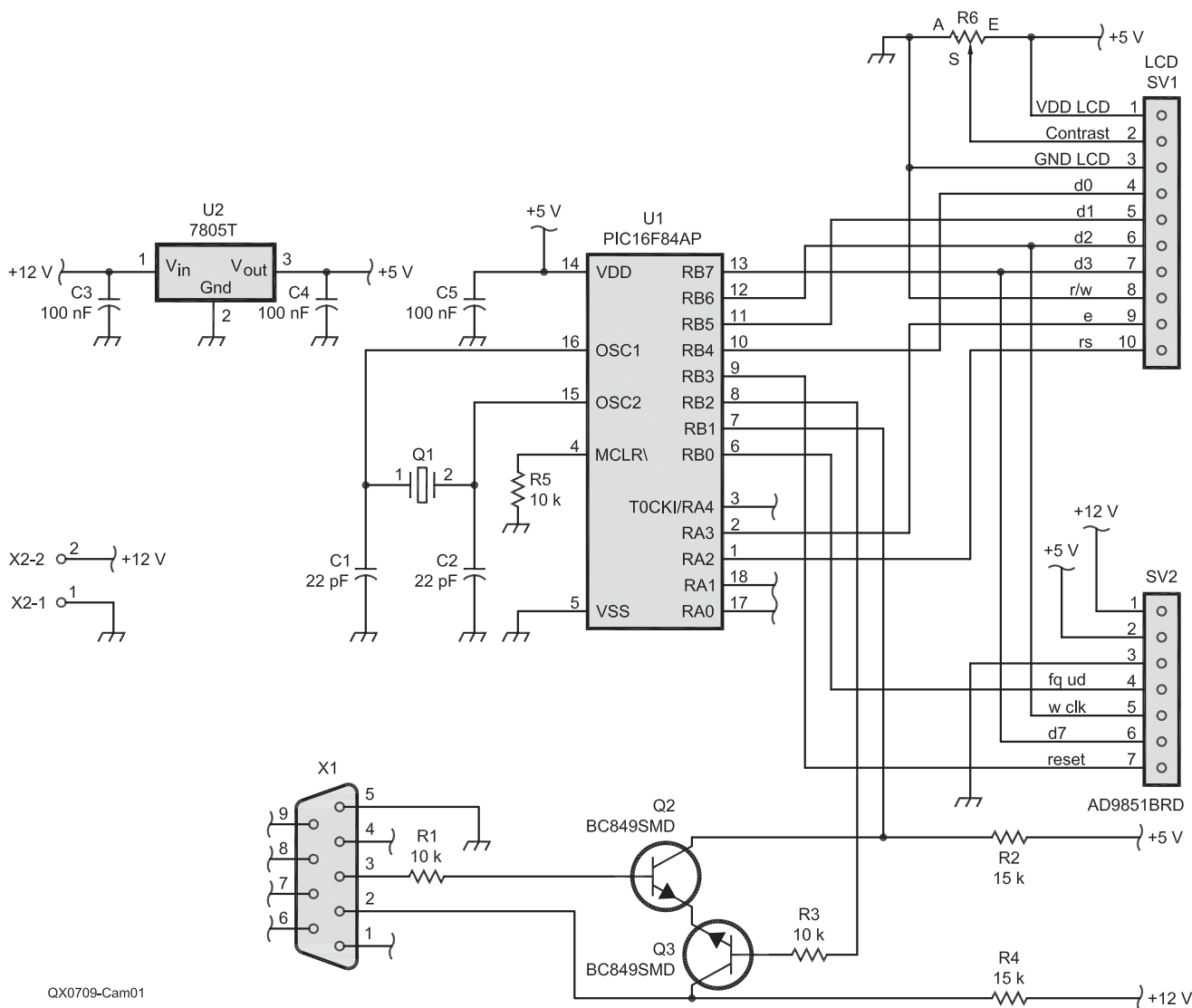


Figure 1 — This schematic diagram shows PIC controller module portion of the project.

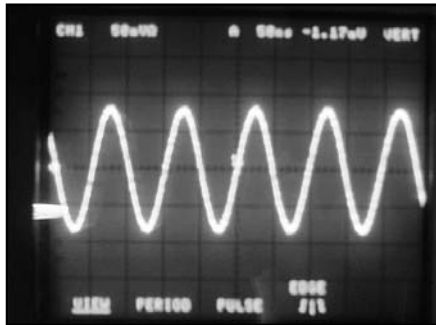
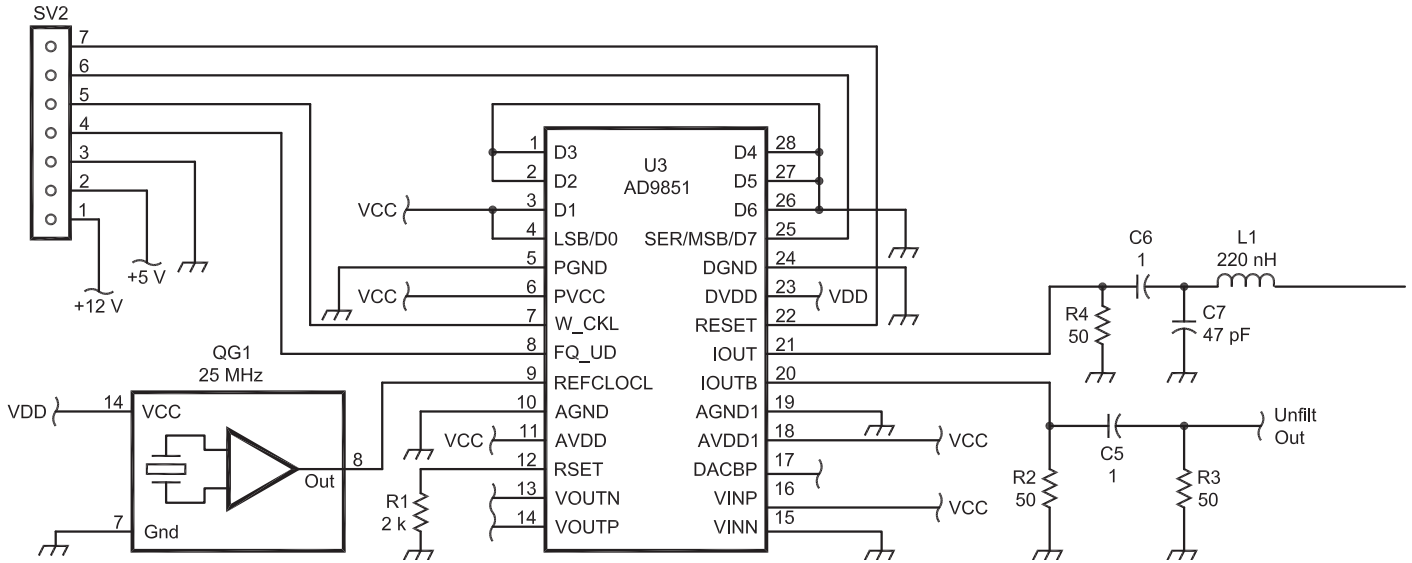
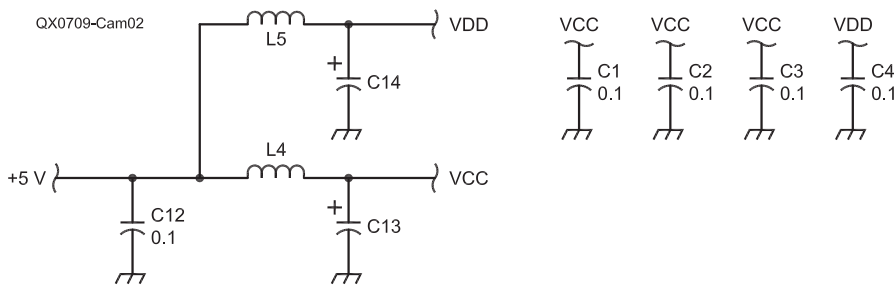


Figure 3 — The DDS output signal waveform is displayed on the oscilloscope CRT.

and core (as happens in computer processors). Ease of use, together with the advantages described above make this device very popular among Amateur Radio experimenters.

The choice of the microprocessor couldn't be easier: requirements are to control the device, drive some human readable interface (LCD) and manage input of commands. The PIC16F628 was chosen for this task, because it is small, versatile and abundant in my component box.¹

¹The PIC controller hex program file for this project is available for download from the QEX Web site at www.arrl.org/qexfiles. Look for the file **9x07_Campanella.zip**.

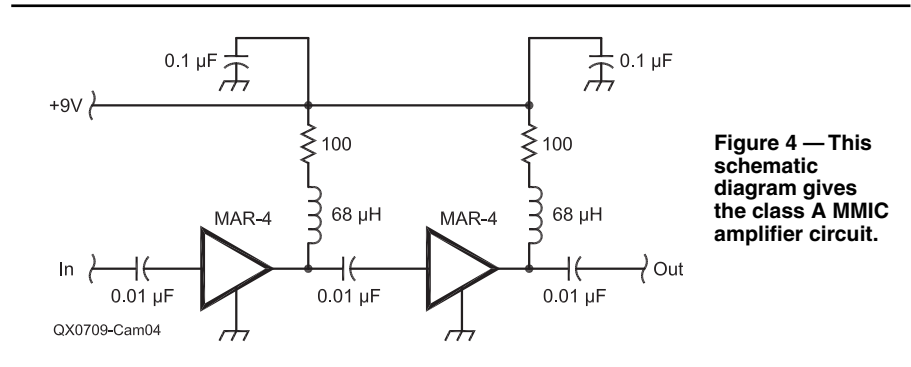


Figure 4 — This schematic diagram gives the class A MMIC amplifier circuit.

The CPU Module

There's really nothing special about the CPU module, with the possible exception of the serial interface. In this case, rather than using an ad-hoc device for doing CMOS to RS232 level conversion, I have used two transistors and a bunch of resistors to obtain a similar result. Even though this way the transmitted signal is going to be in the range 0 to 12 V and not bipolar (-12 / +12 V) as RS232 specification dictates, I have never found a computer serial input that got confused and garbled the serial stream.

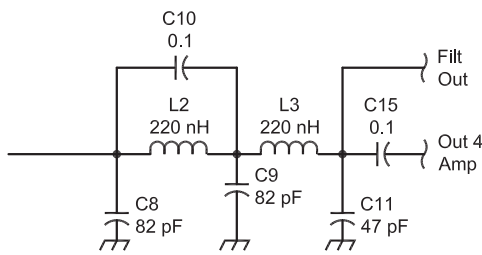
The crystal frequency for clocking the CPU is not critical at all; you can choose

any frequency in the range of 4 to 20 MHz for the 16F628.

Of the 13 bits available as inputs or outputs on the CPU, six are used for LCD control (I used a Hitachi HD44780 compatible LCD module) and four for DDS control, while three ports are still free for custom uses. In order to achieve the minimum number of wires around, a four bit control mode has been chosen for LCD and serial control mode for the DDS; that way only seven wires are required to control the LCD and four for the DDS.

The schematic diagram of this module is shown in Figure 1.

Figure 2 — The direct digital synthesizer (DDS) module is given in this schematic diagram.



QX0709-Cam02

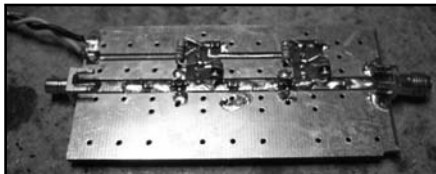


Figure 5 — Here is a photo of the MMIC amplifier construction.

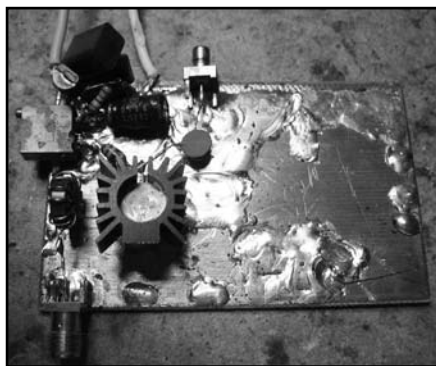


Figure 6 — This photo shows the 2N2259 transistor amplifier.

The DDS Module

This is the “trickier” module of the project, because it has a mixed nature of both analog and digital circuits. The recommendations

about the correct use and placement of decoupling capacitors near the power supply pins are very precise and peremptory on the DDS datasheet. In order to achieve the best spectral purity of the synthesized signal, there are separate pins for analog and digital power supplies for the internal circuitry. C12, L4, L5, C14 and C13 are aimed at this purpose, and there is a dedicated 0.10 μF capacitor for every analog power supply pin (C1 to C4). See Figure 2.

The AD9851 can be clocked either by providing the right final clock frequency or by using the internal 6 \times multiplier. The latter choice is to be preferred for non critical applications, as it dramatically reduces the cost, considering that a 30 MHz computer grade oscillator costs much less than a 180 MHz one. (Actually, surplus computer cards are good sources of 24 MHz oscillators.) I am personally using a 25 MHz oscillator, thus limiting my theoretical maximum output frequency to 50 MHz (rather than the maximum obtainable 60 MHz).

The output of the DDS chip is balanced, and it is a current output; this means that I_{OUT} is “pushing” current out of the chip while I_{OUTB} is pulling current into the chip. Balanced outputs are really useful for cancelling common mode noise, supposing that the noise is equally induced on the two wires — as the difference between the two signals is considered — the same-sign components simply cancel out. Given the balanced output, two solutions are possible: one uses a center tapped 1:1 transformer to couple the I_{OUT} and I_{OUTB} outputs into a single output, while the other terminates I_{OUT} and I_{OUTB} to the same resistive load, capacitively coupling I_{OUT} to the output connector.

The first has the advantage of pushing out some more power and being quite immune to common mode noise; the second is less expensive and gives a flatter response over the whole device frequency range, at the expense of less output power. This is due to the fact that, no matter how broadband a transformer is, it will be difficult to obtain a frequency response that is as flat as that of a chip capacitor, especially at low frequencies, where the transformer efficiency degrades dramatically. I tested both solutions, and in the end I chose the capacitive coupling because I plan to use the same module for experiments at the IF as well, not to mention the reduced costs implied.

In order to eliminate aliases from the output signal, the last stage is a low pass filter with a cut-off frequency of about 50 MHz. Some applications are based on the ability of a DDS to produce aliases, so an unfiltered output could come in handy sooner or later — that’s what you get from the I_{OUTB} circuitry. The important thing to remember is that the unused output *must* be terminated in 50 Ω for a correct operation of the device. The schematics show the DDS with the unfiltered output terminated, supposing you’re going to use the filtered output to connect the power amplifier.

The output current, and therefore the output power, is dependent on the value of R1, because, according to the datasheet, it is given by 39.93 divided by R1, and it cannot be bigger than 20 mA. The given value of R1, 2 k Ω , is set for maximum output current. It could be a good idea to place a variable resistor in series with R1, so that the output power can be fine tuned to give the final amplifier the correct input power. R1 alone gives about 1 V_{pp} on a 50 Ω load, or 4 dBm. A good practice is to keep the maximum output current near 10 mA, rather than to the rated maximum. This value is obtained using an R1 of 4 k Ω , and it gives an output power of -2 dBm on 50 Ω .

Figure 3 shows the output of the DDS modules tuned at 10,140,080 Hz.

The Amplifier Module

The amplifier is the most “independent” part of this project, because you can use any power amplifier to get on the air, just taking into account that it has to accept an input signal at -2 dBm, and be able to provide 10 to 27 dBm (10 mW to 500 mW) output for QRSS activity. I built three different amplifier modules. The first one was based on MMIC amplifiers, the second on a 2N2259 transistor and the third on a bunch of 2N2222 transistors.

The MMIC amplifier is a two stage class A amplifier, based on a MiniCircuits MAR-4, and provides a power gain of 16 dB (each device is capable of 8 dB power gain). The third harmonic is well below 35 dB, and at these output levels a low pass filter after the amplifier is not really needed. Figure 4 is the schematic diagram of this amplifier. Figure 5 shows my circuit board. There is a limitation with this solution though: the maximum output of a MAR-4 device is 12.5 dBm, and this limits the maximum possible input to -3.5 dBm. This is not really a problem if you adopted the variable resistor in series with R1, as mentioned earlier.

The 2N2259 solution is a very simple power amplifier in class AB configuration, using a multturn variable resistor to provide the correct bias to the base-emitter junction of the transistor. A low pass filter at the output of this circuit is mandatory because of the working class. An output power of about 100 mW is easily obtained with this solution. The transistor can reach quite high temperatures, so you will have to use a heat sink. Figure 6 shows my construction for this amplifier version. I haven’t provided a schematic diagram because there was nothing special about the construction or operation of this amplifier.

The last amplifier I tried is based on a design that I found on the Internet, and is part of an all 2N2222 transceiver that K8IQY designed to attend (and win) the 1997 NorCal QRP Club building contest. It does not need any active devices except a couple of diodes



Figure 7 — This amplifier uses 2N2222 transistors to produce about 2 W of output power on the 40 m band.

and a bunch of 2N2222 transistors. (Actually, I used a 2N2219 transistor for the final stage. That is a somewhat more rugged version of the 2N2222.) It produces 2 W at 7 MHz. The only thing I had to redesign was the output low pass filter, because I chose to use this amplifier on 30 m. The details of this interesting project are at www.k8iqy.com/qrprigs/2n240/2n240page.html and the schematics are available at www.k8iqy.com/qrprigs/2n240/2n2sche.html. Figure 7 is a picture of the amplifier I built from this design.

As I mentioned earlier, any power amplifier that is able to take a -2 dBm input signal is perfectly suitable.

Figure 8 shows the prototype assembly of the DDS board, Control board and LCD.

The Firmware

The firmware of the beacon implements three narrow bandwidth modes (QRSS, DFCW, FSKCW) plus standard CW, serial communication to a computer for calibration, mode/speed selection and a way to enter beacon text. The mode and frequency are displayed on a Hitachi HD44780 compatible LCD. The text shown

on the LCD, visible in Figure 9, indicates the mode (FSKCW in the example), the speed (03), and the frequency in hertz (10,140,080).

The serial port is always checked by the PIC processor during operation, so that commands can be sent to the beacon all the time; port setup is 57600,n,8,1. Valid commands are letters, as indicated in the following list.

- 1) q — switches to QRSS mode;
- 2) d — switches to DFCW mode;
- 3) f — switches to FSKCW mode;
- 4) c — switches to CW mode (fixed 16 wpm);
- 5) 1 — switches to speed 10;
- 6) 3 — switches to speed 3;
- 7) 6 — switches to speed 6;
- 8) a — increases frequency offset by 1 Hz;
- 9) z — decreases frequency offset by 1 Hz;
- 10) s — increases carrier frequency by 10 Hz;
- 11) x — decreases carrier frequency by 10 Hz;
- 12) h — increases calibration factor by 1;
- 13) n — decreases calibration factor by 1;
- 14) m — enables beacon message input;
- 15) r — resets device.

An echo is sent on the serial line for any key pressed, in order to give the user some sort of feedback.

Upon switching the unit on, if any digit is typed on the keyboard of a computer connected to the device, it enters the frequency programming mode, and expects a total of 8 digits (including the first one) that are the digits of the new frequency you want your beacon to operate on. The useful time frame during which the first digit is accepted is shown both on the serial line and LCD display by a ">."

Any variations to the settings are saved in the PIC flash memory, so the device will keep settings through resets or on/off cycles.

A calibration factor is used to fine tune the

output frequency, in order to compensate for small errors in the clock nominal frequency. Since calibration is saved on flash memory, calibration is a once in a while operation.

I will offer programmed PICs for \$15 US, plus shipping charges. I can also make the PIC source code available for \$20 US. I will accept payment by PayPal.

Conclusions

Even if not aimed at the assembly of a QRSS beacon, the solutions presented in this article are well suited for reuse wherever a direct radio frequency synthesizer is needed. Considering the spectral purity of the generated signal, as well as the incredibly small tuning step DDS are capable of, only your imagination will limit the possible applications. One future extension of this project will be to connect a DAC to the output current calibration pin, in order to make the output current vary according to some input signal. We're talking about amplitude modulation here! If you're rather interested in discrete frequency modulation (such as FSK), no additional hardware is needed. It will just take some CPU reprogramming.

Matteo Campanella has been a radio amateur since March 1999, when he earned a Tech Class license with the call IW2NGE. He upgraded to Extra in June 2001 as IZ2EEQ. He has been interested in electronics since he was 13, when he built his first FM radio. He received the Laurea degree in Electronic Engineering in 1994 from the University of Pisa. Since then his work has mostly involved software related activities. He presently is Senior Consultant on Java Enterprise Applications and Open Source Solutions. For now, electronics has become a spare time activity, when he enjoys digital signal processing and embedded systems programming.

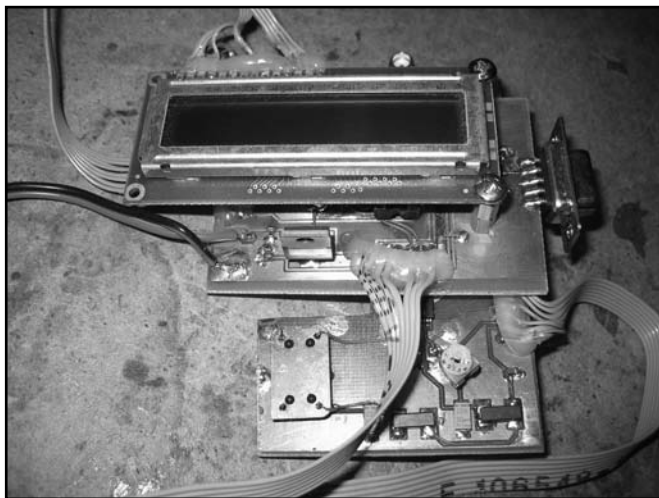


Figure 8 — Here is the combined PIC control module with LCD and the DDS module ready for testing.

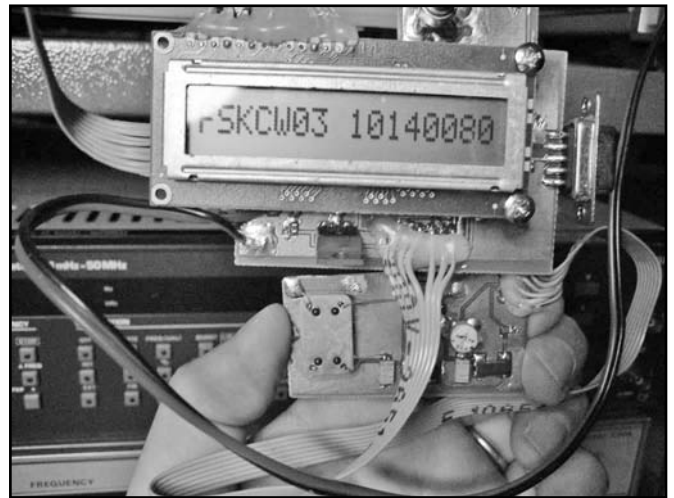


Figure 9 — With power applied, the LCD shows the operating mode (FSK CW), sending speed (03) and the operating frequency (10,140,080 Hz).

QEX

Very High Q Microwave Cavities and Filters

Design and Laboratory Test of Cylindrical Resonators with Quality Factor of 24000 in the 10 GHz band

Paolo Antoniazzi, IW2ACD, and Marco Arecco, IK2WAQ

On the HF bands, nearly all resonant circuits consist of a coil and a capacitor that are connected in series or in parallel. The resonant frequency of the circuit is changed by modifying the capacitance, the inductance, or both. When the inductance and the capacitance cannot be further reduced, this is the highest frequency at which a conventional LC circuit can oscillate.

The upper limit for a conventional reso-

nant circuit is in the low GHz range. At these frequencies, the inductance may consist of a half turn coil, and the capacitance may only be the stray capacitance of the coil. The quality factor, or Q, of these devices will be very low. Also, a $\lambda/4$ section of transmission line can act as a resonant circuit, but typical applications of these transverse electromagnetic (TEM) resonant lines are normally limited to VHF/UHF filters.

By definition, a resonant cavity is any space completely enclosed by conducting walls that can contain oscillating electromagnetic fields and have resonant properties. The microwave cavity has many advantages and uses: they have a very high Q and can be built to handle relatively large amounts of power. Cavities with a Q value in excess of 20,000 are not uncommon. The high Q gives these devices a narrow passband and allows very accurate tuning. Normally, simple and rugged construction is an additional advantage. Although microwave cavity resonators, built for different frequency ranges and applications, have a variety of shapes, the basic principles

Via Roma 18
20050 Sulbiate MI
Italy
paolo.antoniazzi@tin.it

Via Luigi Einaudi 6
Cologno Monzese MI
Italy
ik2waq@alice.it

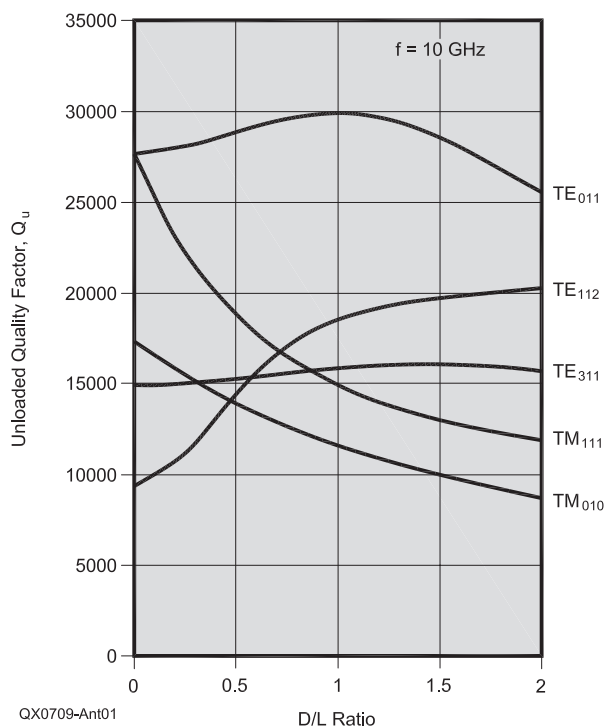


Figure 1 — Unloaded quality factor, Q_u , at 10 GHz of some TE_{mnp} and TM_{mnp} modes versus D/L ratio.

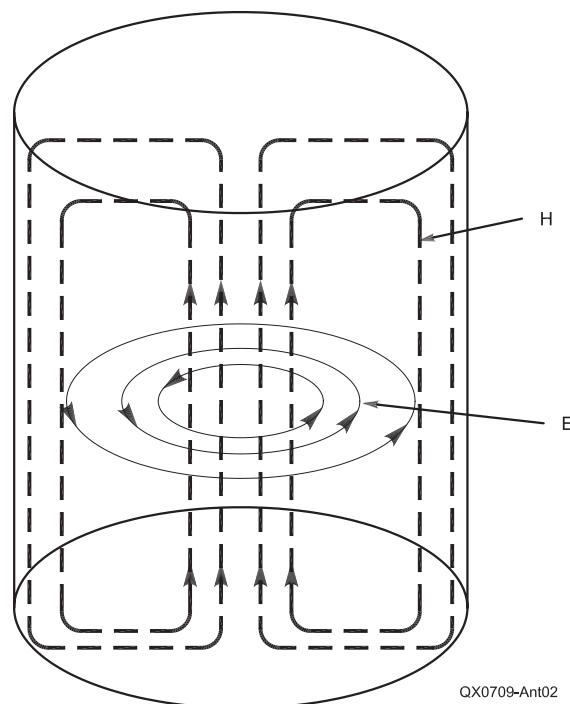


Figure 2 — The E and H Fields in a TE_{011} cavity at 10 GHz are shown in this drawing.

of operation are the same for all.

The TM_{010} mode, where the resonant frequency depends only on the inner diameter (about $f_0 = 229.5 / D$), is the most interesting for Amateur Radio use.^{1,2} Another advantage of this type of cavity is the reduced dimensions: about half the size of other cavities at the same frequency.

The tuning of TM_{010} cavities is very frequently realized with a tuning screw (Pipe-Cap), which, if screwed tightly into the cavity, modifies the working mode from transverse magnetic to TEM (no magnetic or electric field along the cavity axis). Also, the quality factor of the TM_{010} cavity is not as high.

Cavity resonators are energized in basically the same manner as waveguides and have a similar field distribution. A WR-90 $\lambda/2$ cavity has a $Q = 5490$ at 10 GHz, according to *The RSGB Microwave Handbook*, volume 2.³

When the cavity is energized, the electromagnetic wave reflects back and forth along the Z axis and forms standing waves. These standing waves form a field configuration within the cavity that satisfies the same boundary conditions as those in a waveguide. Modes of operation in the cavity are described in terms of the fields that exist in the X, Y, and Z directions.⁴

There are two variables that determine the primary frequency of any resonant cavity. The first variable is *physical size*. At any particular mode of resonance, the smaller the cavity, the higher the resonant frequency. The *shape* is the second controlling factor for the cavity.

Energy can be inserted or removed from a cavity by the same methods that are used to couple energy in and out of waveguides. The operating principles of probes, loops, and slots are the same whether used in a cavity or a waveguide. Therefore, any of the three methods can be used with cavities to inject or remove energy. The cavity mode selected for our paper analysis is the TE_{011} mode, the magnetic and electric field patterns of which

are shown in Figure 1. This type of cavity is quoted for a Very High Q Award.

The resonant frequency of a TE_{011} cavity can be varied by changing cavity volume. Varying the height, L, will result in a new resonant frequency. If the volume is decreased, the resonant frequency will be higher and vice versa.

Waveguide and Cavity Modes

In a waveguide, the “x” and “y” axes lie in a plane perpendicular to the waveguide length or the direction of the energy travel. The “z” axis is perpendicular to the previous two. See Figure 2. A cavity — either rectangular or cylindrical — is a portion of the waveguide enclosed by metallic walls at the two ends, along the “z” axis.

The TEM mode, or transmission line mode, is characterized by: $E_z = H_z = 0$. This means that the electric and magnetic fields are completely transverse to the direction of propagation of the wave. This mode cannot exist in hollow waveguide since it requires two conductors, such as the coaxial transmission line and open line wires. It cannot be propagated in a waveguide.

The TE_{mnp} modes are characterized by $E_z = 0$. In other words the “z” component of the magnetic field, H_z , must exist for energy transmission in the guide ($H_z \neq 0$). The peculiarity of TM_{mnp} modes is $H_z = 0$, so only the component of electric field, E_z , exists for energy transmission in the guide ($E_z \neq 0$).

In the rectangular waveguide resonator, the modes are named TE_{mnp} or TM_{mnp} where the integer “m” designates the number of half waves of electric or magnetic field in the “x” direction (the bigger dimension of waveguide cross section), while “n” denotes the number of half waves in the “y” direction (the smaller dimension of waveguide cross section) and “p” indicates the number of half waves in “z” direction (perpendicular to the waveguide cross section).

In the cylindrical cavity, the same type

of index system is used, but the meaning of the subscripts changes: “m” represents the number of *full wave variations* along the circumference that constitutes the base of the cylinder (as a function of its angle at the center), “n” expresses the number of *half cycles* along the base radius direction and “p” defines the number of *half waves* along the cylinder symmetry axis.

In the waveguide, there are only two mode subscripts: “m” and “n,” corresponding to the “x” and “y” axes, because the third direction is the direction of the wave propagation.

Design of a TE_{011} Cavity

To calculate the physical dimensions of a right cylindrical cavity resonating according to the TE_{011} mode, we suggest the use of the graph of Figure 3. The input parameter is the square of the ratio of diameter over height $(D/L)^2$ that must be chosen in order to have a suitable separation from the other possible modes to avoid unwanted resonances. With regard to this matter, it is useful to remind readers that a circular waveguide, shorted at the two ends, has an infinite number of possible resonances.

According to this consideration our choice was $D/L = 1.44$ corresponding to $f_0 D = \sqrt{(180000) / 424.3}$ GHz mm that allow us to calculate the resonant frequency, fixing the diameter or vice versa. Selecting $f_0 = 10.350$ GHz, the diameter becomes $D = 41$ mm and consequently the cavity height will be $L = 28.5$ mm. Now, with the cavity dimensions defined, we are able to more accurately calculate the resonant frequency in hertz by Equation 1.^{5,6}

$$f_0 = \sqrt{\left(\frac{2X_{mn}}{D}\right)^2 + \left(\frac{p\pi}{L}\right)^2} / 2\pi\sqrt{\mu_0\epsilon_0} \quad [\text{Eq 1}]$$

where:

$X_{mn} = 3.832$ is the propagation constant of TE_{01} mode into a circular waveguide.

$p = 1$, is the third index (integer) of the resonating mode

¹Notes appear on page 36.

Table 1
Resonance of Some Frequency Modes and Unloaded Quality Factor, Q_u , of a Cylindrical Cavity
(Diameter 41.0 mm, Height 28.5 mm)

Mode	Calculated		Measured				
	Resonance, f (GHz)	Quality Factor, Q_u	Resonance, f (GHz)	BW (MHz)	Quality Factor, Q_L	Insertion Loss (dB)	Quality Factor, Q_u
TM_{010}	5.598	13499					
TE_{111}	6.784	15189					
TM_{011}	7.681	11149					
TE_{211}	8.843	15304					
TM_{110}	9.012	17128					
TE_{011}	10.354	28356	10.326	1.9	5435	2.2	24290
TM_{111}	10.354	12944					
TE_{311}	11.103	15280	11.001	11.2	982	0.9	9977
TE_{112}	11.358	18421					
TM_{210}	11.954	19727					

Note: Cylindrical cavity diameter = 41.00 mm, height = 28.5 mm.

QX0709-Ant03

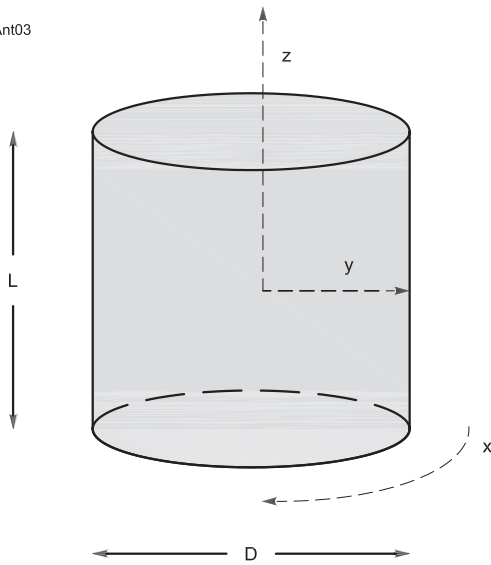


Figure 3 — This drawing shows the cylindrical cavity axes, X, Y and Z.

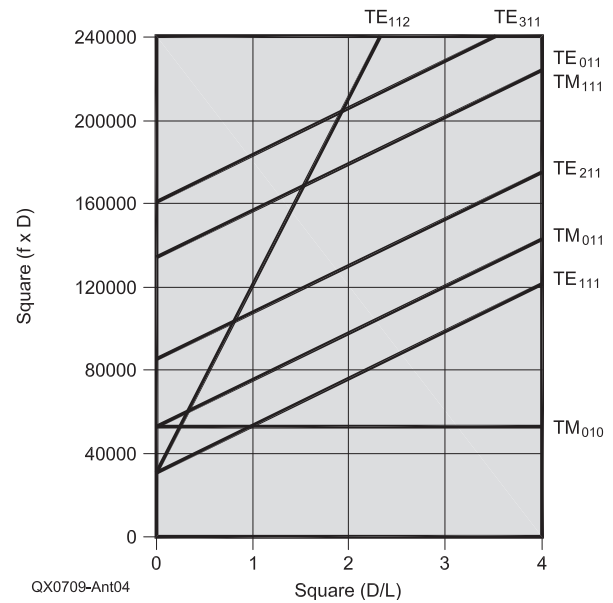


Figure 4 — Mode chart for microwave cavities (GHz and mm).

$\mu_0 = 4 \pi \times 10^{-10}$ H/mm is the absolute magnetic permeability of the air (or the vacuum)
 $\epsilon_0 = 8.85 \times 10^{-15}$ F/mm is the absolute dielectric constant of the air.
 D and L are in millimeters

Equation 1 can be applied both to TE_{mnp} and TM_{mnp} modes with an appropriate choice of the propagation constant shown by Table 1 for circular waveguide.

The quality factor, Q, is a measure of the frequency selectivity of a resonant (series) or an antiresonant (parallel) circuit. It is directly proportional to the ratio of the maximum energy stored and the energy dissipated per cycle, or simplifying, the ratio of the cavity volume over its inner surface area. The theoretic unloaded quality factor is the maximum possible value for the Q when the cavity surfaces are “mirror” polished. Using a massive copper block to manufacture the cavity, it can be calculated by Equations 2 and 3.^{5,6}

$$Q = \{ \lambda_0 \times 10^3 [1 - (m / X_{mn})^2] [X_{mn}^2 + (\pi D p / 2 L)^2]^{3/2} \} / \text{den} \quad [\text{Eq 2}]$$

$$\text{den} = 2 \delta \pi \{ X_{mn}^2 + [D (\pi D p / 2 L)^2 / L + (1 - D / L) (\pi D m p / 2 L X_{mn})^2] \} \quad [\text{Eq 3}]$$

where:

λ_0 is the resonant wavelength = $299.8 / f_0$ where the frequency is in gigahertz
 m = 0, for the TE_{011} mode, is the first index (integer) of the resonant mode
 p = 1, for the TE_{011} mode, is the third index of the mode
 $\delta = 6.6 \times 10^{-4}$ mm is the microwave skin depth of the RF into the copper

All of the linear dimensions in these equations are in mm.

The wavelength can be also calculated using Equation 1, if you remove the square root of $(\mu_0 \epsilon_0)$ in the denominator.

The skin depth, δ , is that distance below a surface of a conductor where the current density has diminished to $1/e \approx 0.368$ of its value at the surface. The skin depth in microns can be calculated by Equation 4.^{7,8}

$$\delta = \sqrt{\frac{10^{10}}{4\pi^2 f_0 \sigma}} \quad [\text{Eq 4}]$$

where:
 $\sigma = 5.8 \times 10^4$ S / mm is the reciprocal of the resistivity (1 / ρ) in Ω / mm.

Table 2 shows the calculated values of resonance frequency and the relevant

unloaded quality factor of TE_{011} and other possible TE_{mnp} and TM_{mnp} modes obtainable by a cylindrical cavity having diameter $D = 41.0$ mm and height $L = 28.5$ mm.

Using different materials than copper to manufacture the cavity or its surfaces, the skin depth will change and so the quality factor will be multiplied by the factors: 1.07 for silver plated copper ($\delta = 0.60 \mu\text{m}$), 0.75 for aluminum, ($\delta = 0.86 \mu\text{m}$) and 0.45 for brass ($\delta = 1.44 \mu\text{m}$).

Table 2
 Propagation Constants of Some TE_{mnp} and TM_{mnp} Modes

Mode	X_{mn}
TE_{11}	1.841
TE_{21}	3.054
TE_{01}	3.832
TE_{31}	4.201
Mode	X_{mn}
TM_{01}	2.405
TM_{11}	3.832
TM_{21}	5.136

Table 3
 Fine Frequency Tuning of the TE_{011} Cavity

Tuning Screw (mm)	Measured f_0 (GHz)	BW (MHz)	Q_L	Insertion Loss (dB)	Q_U
0.0	10.339	0.70	14770	11.3	20296
1.0	10.380	—	—	—	—
2.0	10.441	0.70	14910	11.5	20315
3.0	10.521	—	—	—	—

Note: Input/Output iris diameter, $D = 5$ mm

Figure 4 shows also that using the TE_{011} mode we can reach much higher quality factors than in the other modes. This is the main reason why we decided to investigate more about this mode.

For the TM_{mnp} modes, the quality factor is given by Equation 5. See Notes 5 and 6.

$$Q = \{ \lambda_0 \times 10^3 [X_{mn}^2 + (\pi D p / 2 L)^2]^{1/2} \} / [2 \delta \pi (1 + D / L)] \quad [\text{Eq 5}]$$

This Equation is valid for $p > 0$.

For $p = 0$ the equation simplifies to:

$$Q = (\lambda_0 \times 10^3 X_{mn}) / [2 \delta \pi (1 + D / 2 L)] \quad [\text{Eq 5A}]$$

At the end of the design phase and after creating the relevant mechanical drawing, we turned to a machine shop for the realization of the filter. The cavity has been manufactured by working a copper block, with the aid of a milling machine, to create the lateral surface

of our right cylinder. See Figure 5.

Two copper plates are made to completely close the cavity with metallic walls using four M4 machine screws. There is no need to use more screws, with the purpose of improving the contact between the different parts of the cavity, because there is no RF current between the cylinder walls and its top and bottom. In fact, no current circulates either in the radial (y axis) or longitudinal directions (z axis) with the TE_{011} mode. See Figures 1 and 2.

To excite the TE_{011} mode into the cavity and to collect the output signal, we used two WR-90 to SMA adapters along the diameter of the cylinder and at the center of its height. The adapters are fixed to the cavity body by two plates and M4 screws that push the waveguide flange, as shown in Figure 6.

This kind of adapter allows passing from

the TEM mode of the coaxial cable to the TE_{10} of the WR-90 waveguide. An electric probe that extends the central lead of the SMA connector into the waveguide performs the coupling between the waveguide and the coaxial line.

For a correct coupling of these adapters, put the largest dimension of WR-90 cross section parallel to the symmetry axis of the cavity. The optimum coupling with the resonant cavity occurs when the iris is placed at the point of the cavity where the magnetic field is strong and oriented in the same direction as the field in the waveguide. See Figure 7A. If the adapter is connected wrong, perpendicular with respect to the correct orientation, the TM_{010} mode shown in Figure 7B or the TM_{111} mode will be excited instead of the TE_{011} mode.

The input and output impedance of the



Figure 5 — Here is the cylindrical copper cavity for TE_{011} mode.

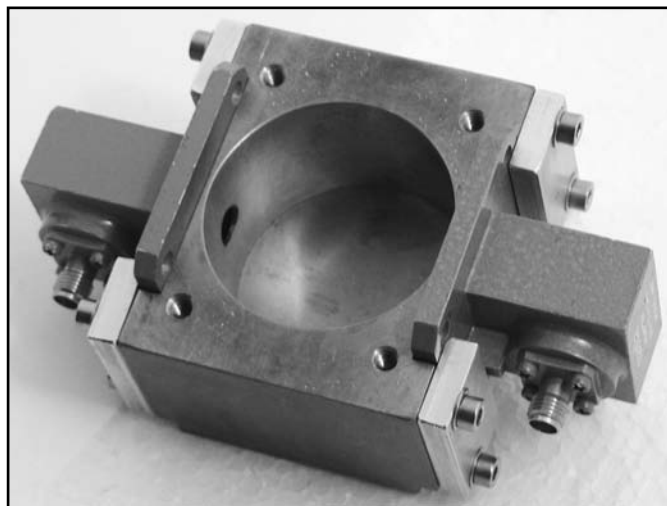


Figure 6 — This photo shows the cavity input-output coupling using WR-90 to SMA adapters.

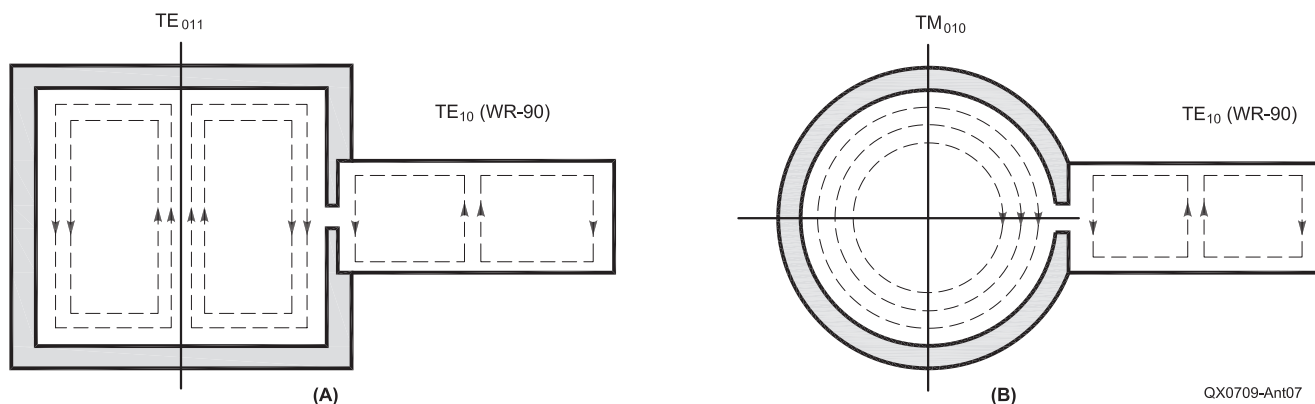


Figure 7 — Part A shows a waveguide coupling to a TE_{011} mode cavity. Part B shows a waveguide coupling to a TM_{010} mode cavity.

whole system is 50Ω (SMA connector and cable) and the matching between this low impedance with some hundreds of ohms of the waveguide characteristic impedance is achieved by placing a suitable antenna (probe) into the waveguide. The matching between waveguide and cavity is performed by a hole having 7 mm diameter drilled into the cylinder walls (iris).

The diameter of the iris has been optimized by drilling a small hole at the beginning and increasing it a little at time to reach a good tradeoff between the quality factor and the insertion loss of the cavity.

A Test Cavity

For the design of a resonant cavity it is desired to select values of L (28.5 mm in our cavity) and D (41 mm) such that there are no extraneous modes that have resonant frequencies near the designed ones. Modes have a maximum value of Q when the cavity length, L , equals (approximately) the diameter, D . A big advantage of the TE_{011} cavity is its small and compact volume that results in high energy density and the high magnetic

field strength in the center of the resonator. The strong magnetic field along the cavity axis makes the TE_{011} mode particularly useful for a sample cavity for laboratory test of materials. A large access hole in the top and the bottom of the cavity is feasible without a noticeable decrease of its Q -factor. Such a feature enables one to insert reasonably large samples into the resonator axially.

It is unnecessary to achieve good electrical contact between the tuning plunger (if one is used) and the cylinder. In such a cavity, there is no HF current between the cylinder walls and its top and bottom. In fact there is no current in either the radial (r) or longitudinal (z) direction, but only in the angular direction. This property enables one to tune the cavity using the plunger on the end of the cylinder (see Figure 8).

To obtain our target, or the best results in the quality factor, Q , a copper cavity was realized (Figure 5 is an open view) and the essential results are reported in Figure 9, where the resonance response is shown.

As described earlier, the input/output iris for the WR-90 adapter is two holes of diameter $D = 7$ mm. The surfaces of the cavity are per-

fectly polished (mirror like) to maximize the unloaded Q_u . These coupling holes are made experimentally, starting from a diameter, $D = 3.5$ mm. The final cavity has an insertion loss of 2.2 dB and a bandwidth of about 2 MHz at 10.325 GHz. This match, with a Q_L of 5435, corresponding to a Q_u better than 24000 (evaluated by the graph of Figure 16). Two Narda WR-90 to SMA model 4601 (8.2 to 12.4 GHz) adapters are used for input/output matching to the coaxial cable test system. See Figure 6.

To fine tune the cavity (Table 3), a big M20 brass screw has been put at the center of one of the upper cavity caps.⁹ See Figure 8. This screw cannot be plunged into the cavity more than a few millimeters to avoid a possible degeneration to the TEM mode. During this test the input/output coupling holes are with a diameter, $D = 5$ mm. The quality factor is lower than the maximum, but this specific check is only for demo purposes. The coarse tuning can be obtained using a milling machine to reduce the cavity height. Table 4 shows the relationship between the cavity height, L , and the frequency, f_0 . See Table 5 for the frequency variation versus diameter.

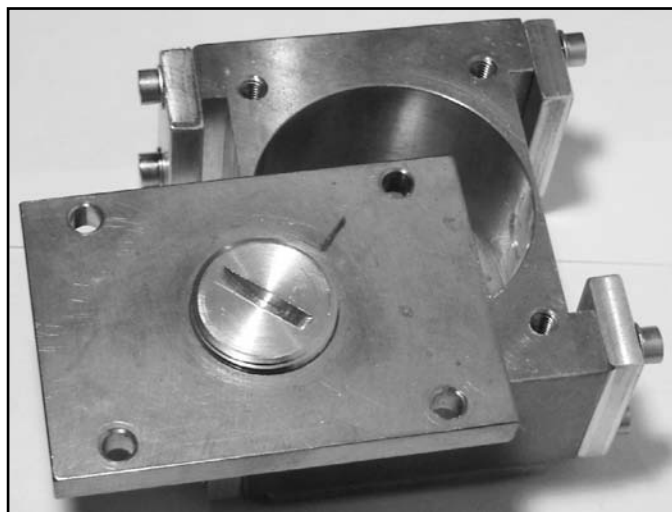


Figure 8 — The movable cylinder in the center of the cover plate is used for fine frequency tuning of the TE_{011} cavity.

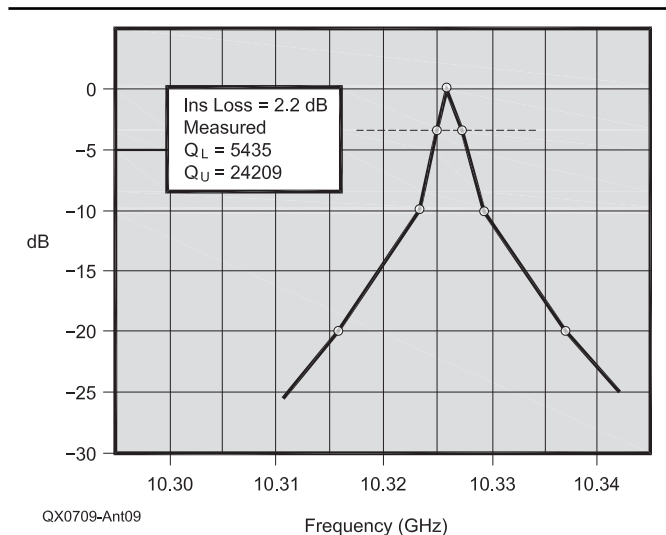


Figure 9 — This graph shows the response of a single TE_{011} cavity.

Table 4

TE_{011} Frequency Change Versus Cavity Height, L , for Diameter, $D = 41.0$ mm

Height (mm)	Frequency (GHz)	Δ Frequency (MHz)
28.5	10.3543	0
28.3	10.3733	+ 19.0
28.1	10.3926	+ 38.3
27.9	10.4122	+ 57.9
27.7	10.4323	+ 78.0
27.5	10.4528	+ 98.5

Note: Cavity diameter, $D = 41.0$ mm

Table 5

TE_{011} Frequency Change Versus Cavity Diameter, D , for Height $L = 28.5$ mm

Diameter (mm)	Frequency (GHz)	Δ Frequency (MHz)
41.6	10.2337	- 120.6
41.4	10.2802	- 74.1
41.2	10.3171	-37.2
41.0	10.3543	0
40.8	10.3920	+ 37.7
40.6	10.4301	+ 75.
4.04	10.4686	+ 114.3



Figure 10 — This photo shows the dual TE₀₁₁ cavity filter.

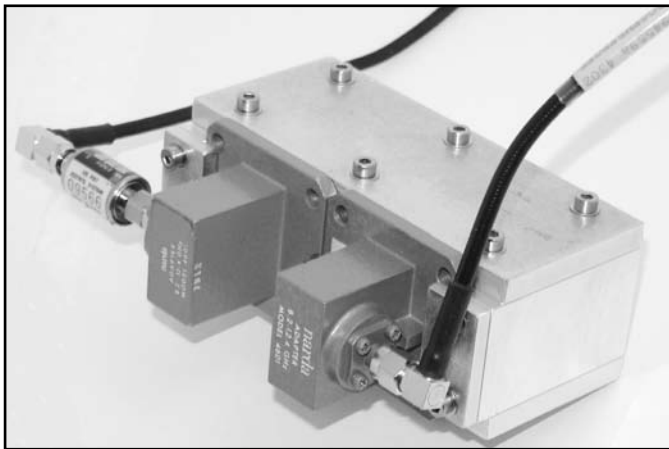


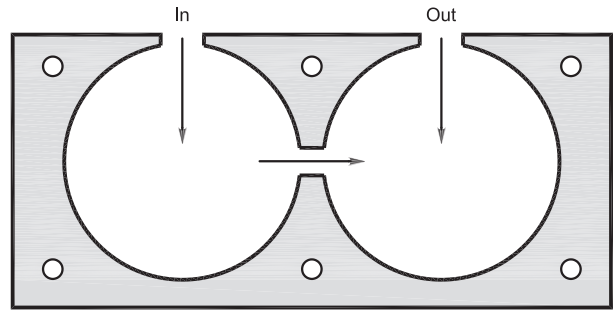
Figure 12 — In this photo, the dual cavity filter with WR-90 adapters attached uses 90° coupling of the coaxial lines.

We can control the degree of coupling between the waveguides and the cavity by means of the diameter and the thickness of the coupling apertures: the bigger the ratio of the diameter to thickness, the stronger the coupling. Nevertheless, the diameter of the coupling hole cannot be too large: it has been shown that the linear dimensions of the aperture must be less than $\lambda / 2\pi$, so that the electrical and magnetic field in its neighborhood are closely approximated by unperturbed fields.

Experimentally, the rule is that the optimal coupling apertures should be small, with a diameter of $\lambda_0 / 5$ or $\lambda_0 / 4$, where λ_0 is the wavelength corresponding to the working frequency (about 29 mm at 10.4 GHz).

A TE₀₁₁ Dual Cavity Filter

At this point we will discuss the design and performance of a narrow-band filter that uses two cylindrical TE₀₁₁ mode cavity resonators. This



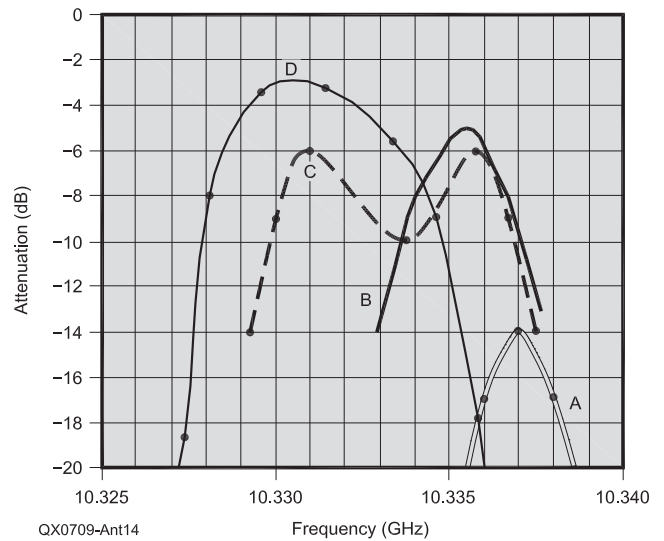
QX0709-Ant11

Figure 11 — Here is the mechanical layout of the dual TE₀₁₁ cavity filter.



QX0709-Ant13

Figure 13 — This drawing illustrates the electric field simulation in TE₃₁₁ mode.



QX0709-Ant14

Figure 14 — Here is a graph of the experimental responses of the dual cavity filter: (A) with input/output diameter $D = 7.0$ mm and coupling diameter $D = 2.5$ mm, (B) with input/output diameter $D = 7.0$ mm and coupling diameter $D = 3.5$ mm, (C) with input/output diameter $D = 7.0$ mm and coupling diameter $D = 4.5$ mm, (D) with input/output diameter $D = 7.5$ mm and coupling diameter $D = 4.5$ mm.

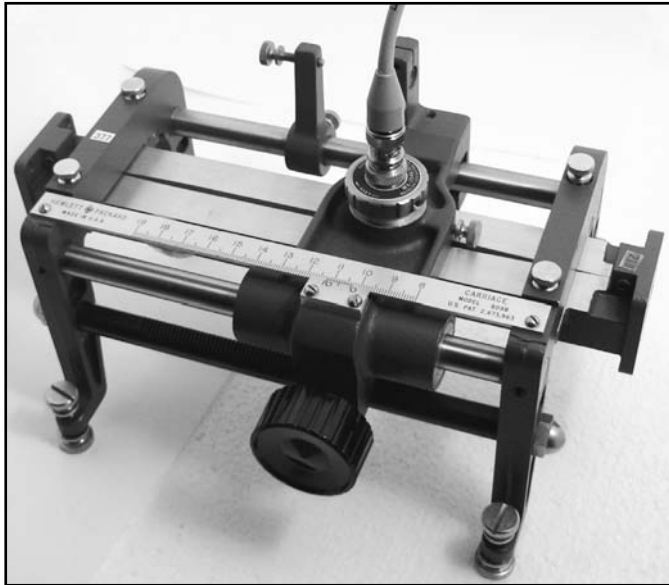


Figure 15 — This is the HP 809B slotted line used to make the SWR measurements.

type of filter is typical of the narrow-band, low-insertion-loss filter category. The main disadvantage of a TE_{011} cavity filter is that it has spurious passband responses at frequencies relatively close to the main passband; these spurious passband responses occur when the cavities resonate in other modes. By using particular techniques, however, the insertion loss of these spurious modes can be kept quite high over an appreciable frequency band. Figure 10 shows the experimental dual-cavity TE_{011} filter, which was built from aluminum and optimized for the 10 GHz band. The two cavities are coupled together by means of a small circular iris. The diameter ($D = 41.0$ mm) and length ($L = 28.5$ mm) of the two coupled cavities are exactly the same as the single cavity, and are selected to limit the spurious modes. See Figure 3. The terminating waveguide adapters (WR-90 to SMA, Figure 11) are oriented to couple strongly to those TE modes within the cavity that have components of magnetic field parallel to the cavity axes. TM modes, which have no components of magnetic field parallel to the cavity axes, are only weakly excited from the terminating waveguides. Some small problems with TM modes may exist, however, because of the coupling iris. It is very important to minimize the coupling at frequencies other than the design frequency, via the many modes that may be coupled by apertures. No matter how the iris is made, the edges of the iris opening will always have some electric field components perpendicular to the ideal TE_{011} , in the axial direction for example. One technique to limit the spurious modes consists of positioning the coupling apertures so they lie in the middle between the top and bottom of the cavities. This pro-

cedure minimizes the coupling of the TE_{211} mode from the external waveguide adapters and also minimizes the coupling of this mode between cavities.

Thinning the iris slot is found to reduce the size of spurious current components and thereby decrease the RF leakage, and in order to reduce the coupling of the TE_{311} mode between cavities, the coupling slots in each cavity are oriented at right angles to one another, resulting in the positioning of the cavities shown in Figure 12. This is clearer with reference to the simulated TE_{311} cavity mode shown Figure 13. See Note 5, which shows the electric field magnitude on cavity walls where the maximum levels of the electric or magnetic fields are at any 60° angle. Coupling the two filter TE_{011} cavities at 90° we obtain an important separation from the spurious TE_{311} mode. As you can see in Figure 14, the 3 dB-bandwidth is about 5 MHz, with a 20 dB attenuation at a 9 MHz bandwidth. These are very interesting values for the 10 GHz band.

Measurements and Conclusions

We don't have a sweep generator in the 8 to 12 GHz band to realize serious measurements on very high Q cavities. All the measurements were obtained with the "Galileo method" (step by step, manually). Normally, with Pipe-Cap resonators or similar filters, all the tests are easy and not reserved to skillful people, but this is not true with TE_{011} cavities. Another problem we had was that our Marconi 6058B signal generator does not have excellent frequency stability.

The dual cavity filter shown in Figure 11 was realized and optimized in a totally experimental way. The dimensions of the

cavities are exactly the same as that of the single cavity shown in Figure 5. As a starting point, the same input/output iris hole ($D = 7$ mm) was used and the internal coupling hole was modified starting from 2.5 mm to 3.5, 4.0 and 4.5 mm.

Figure 14 shows the effect of different input and coupling holes. The filter can be optimized by modifying the values of the input/output and coupling holes more gradually. We obtained an acceptable compromise with insertion loss = 2.8 dB at 10.330 GHz with $D1 = D2 = 7.5$ mm (input/output hole diameter) and $D3 = 4$ mm (coupling hole diameter). Figure 9 shows the response of the single TE_{011} cavity.

The beautiful HP 809B slotted line of Figure 15 was used along with an HP 415E SWR meter to confirm a good in-band filter SWR (< 1.2). We described the slotted line use in a May/June 2004 *QEX* article.¹¹ In that application, however, the filter was following a good 10 GHz preamplifier to be used with the future AMSAT-DL P3E satellite, but that's not a critical component. More work will be needed if the target is a filter with very-low insertion loss. All the measurements are made using the Marconi 6058B, which is an 8.0 to 12.5 GHz signal source and an HP 435B power meter.

The unloaded quality factor, Q_U , versus measured loaded Q_L and insertion loss was derived from the classic diagram of Figure 16, valid for all single resonators in a 50Ω system.

We conclude this paper with many thanks to Paul Wade, W1GHZ. Paul is the author of the many important articles that help us learn about the fantastic world of microwaves.^{12, 13}

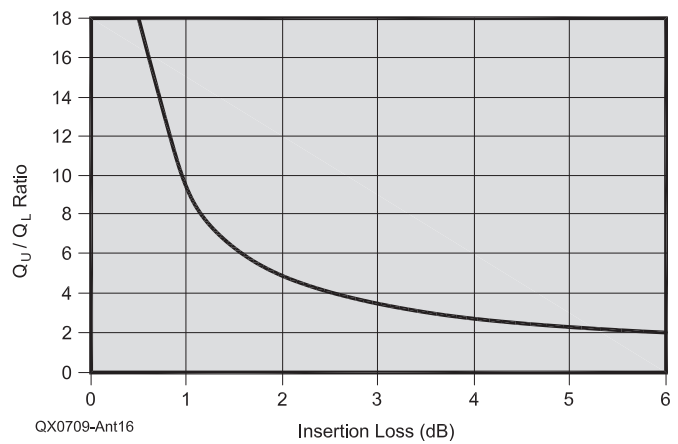


Figure 16 — This graph shows the ratio of unloaded to loaded quality factor (Q) versus insertion loss in a cavity.

Notes

- ¹Paolo Antoniazzi, IW2ACD, and Marco Arecco, IK2WAQ, "Easy Microwave Filters Using Waveguides and Cavities," *QEX*, Sep/Oct 2006, pp 37-42.
- ²H. J. Meise, DK2AB, "Complementation of Cylindrical Resonator Cavities, *DUBUS*, 2/1987, pp 95-97.
- ³*RSGB Microwave Handbook*, 1991, Vol 2, pp 12.13.
- ⁴Simon Ramo, John R. Whinnery and Theodore Van Duzer, *Fields and Waves in Communication Electronics*, John Wiley and Sons, 1984.
- ⁵L. F. Chen, C. K. Ong, C. P. Neo, V. V. Varadan

- and V. K. Varadan, "Microwave Electronics," *Measurements and Material Characterization*, John Wiley and Sons, 2000, pp 100-103.
- ⁶R. E. Collin, *Foundations for Microwave Engineering*, McGraw Hill, 1990, pp 326-329.
- ⁷Z. D. Farkas, Particle Acceleration with TE₀₁₁ Cavity, Linear Accelerator Conference, pp.14, Sep 1979.
- ⁸*Reference Data for Engineers*, Seventh Edition, SAMS, 1989, pp 6.5-6.10.
- ⁹John Share, "The Practicabilities of Microwave Cavities," *Electronics World*, Jan 2004, pp.24-27.

- ¹⁰R. R. Mett, "Microwave Leakage from Field Modulation Slots in TE₀₁₁ Electron Resonance Cavities," *Review of Scientific Instruments*, pp 1-11, Dec 2004.
- ¹¹Paolo Antoniazzi, IW2ACD, and Marco Arecco, IK2WAQ, "Measuring 2.4 GHz Helix Antennas," *QEX*, May/June 2004, pp 14-22.
- ¹²Paul Wade, W1GHZ, "Rectangular Waveguide to Coax Transition Design," *QEX*, Nov/Dec 2006, pp 10-17.
- ¹³Paul Wade, W1GHZ, "Understanding Circular Waveguide — Experimentally," *QEX*, Jan/Feb 2001, pp 37-48.



Down East Microwave Inc.

We are your #1 source for 50MHz to 10GHz components, kits and assemblies for all your amateur radio and Satellite projects.

Transverters & Down Converters, Linear power amplifiers, Low Noise preamps, coaxial components, hybrid power modules, relays, GaAsFET, PHEMT's, & FET's, MMIC's, mixers, chip components, and other hard to find items for small signal and low noise applications.


We can interface our transverters with most radios.

Please call, write or see our web site www.downeastmicrowave.com for our Catalog, detailed Product descriptions and interfacing details.

Down East Microwave Inc.
954 Rt. 519
Frenchtown, NJ 08825 USA
Tel. (908) 996-3584
Fax. (908) 996-3702


1010 Jorie Blvd. #332
Oak Brook, IL 60523
1-800-985-8463
www.atomictime.com

ATOMIC TIME




14" LaCrosse Black Wall WT-3143A \$26.95
This wall clock is great for an office, school, or home. It has a professional look, along with professional reliability. Features easy time zone buttons, just set the zone and go! Runs on 1 AA battery and has a safe plastic lens.

Digital Chronograph Watch ADWA101 \$49.95
Our feature packed Chrono-Alarm watch is now available for under \$50! It has date and time alarms, stopwatch backlight, UTC time, and much more!




WT-3143A - \$26.95



LaCrosse Digital Alarm WS-8248U-A \$64.95
This deluxe wall/desk clock features 4" tall easy to read digits. It also shows temperature, humidity, moon phase, month, day, and date. Also included is a remote thermometer for reading the outside temperature on the main unit. approx. 12" x 12" x 1.5"

WS-8248 - \$64.95



WS-9412U - \$19.95

LaCrosse WS-9412U Clock \$19.95
This digital wall / desk clock is great for travel or to fit in a small space. Shows indoor temp, day, and date along with 12/24 hr time. apx 6"x 6"x 1"

Tell time by the U.S. Atomic Clock -The official U.S. time that governs ship movements, radio stations, space flights, and war-planes. With small radio receivers hidden inside our timepieces, they automatically synchronize to the U.S. Atomic Clock (which measures each second of time as 9,192,631,770 vibrations of a cesium 133 atom in a vacuum) and give time which is accurate to approx. 1 second every million years. Our timepieces even account automatically for daylight saving time, leap years, and leap seconds. \$7.95 Shipping & Handling via UPS. (Rush available at additional cost) Call M-F 9-5 CST for our free catalog.

A Differential Leveling Microphone

This mic was designed to overcome some basic problems commonly associated with standard microphones.



J. R. Laughlin, KE5KSC

Some basic problems commonly associated with microphones are:

- 1) Background “clutter” pickup
- 2) Overloading with abnormally high inputs
- 3) Feedback squeal when used with speakers
- 4) Lack of volume control over excessively varying input levels

This design greatly reduces all of these problems. One basic approach is to use two differential cancelling mic inputs, which results in greatly reduced reproduction of sounds originating at short distances away from the mic. The other is automatic leveling of the output when the input reaches and exceeds a predetermined level. In this design, a method of leveling is used that is superior to some standard methods in respect to the distortion resulting from the leveling process.

Table 1 gives the leveling and distortion characteristics of the mic circuit. As you can see, the leveling is very good, and far beyond any expected input levels. The resulting distortion level is insignificant. There are undoubtedly many very useful applications for the leveling part of the circuit, using only one input. I believe that if you build this project you will enjoy it as much as I have. It has been very interesting.

How it works

U1B is an op-amp connected for a differential input. A differential amplifier has an output that represents only the difference of the two inputs. Figure 1 gives the schematic diagram for the circuit.

You can see that each mic element feeds into one of the differential inputs of U1B. So, for any sound to be reproduced as an output, the incoming sound needs to be delivered more to one mic than the other.

For good cancellation of equal-sound inputs, the mic elements, as well as the phase and frequency response of both input circuits need to be carefully matched. Mic elements vary as to characteristics so the two

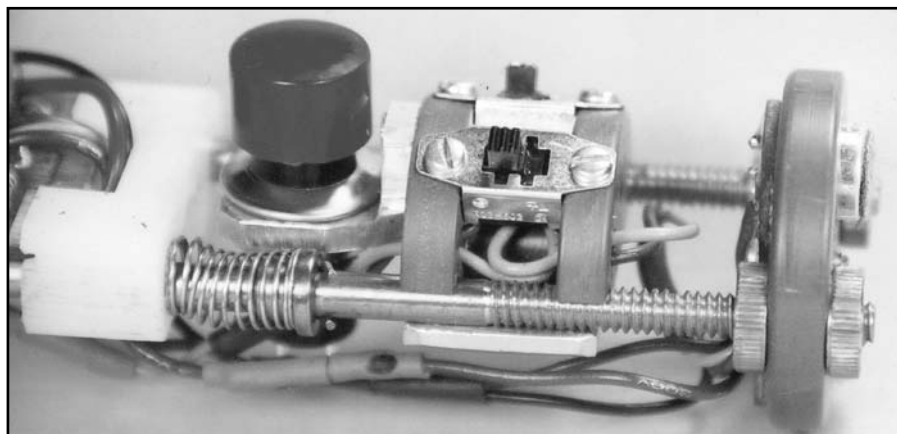


Photo A — This photo shows the PTT push button switch on the left, the mic selection switches in the center and the microphone element mount on the right.

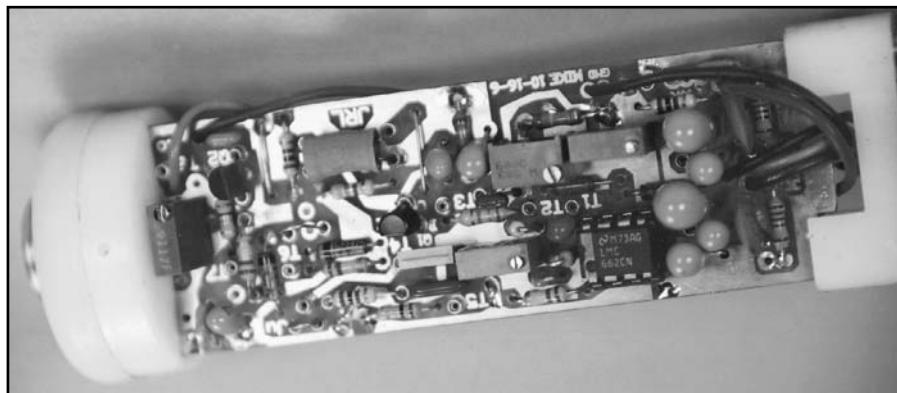
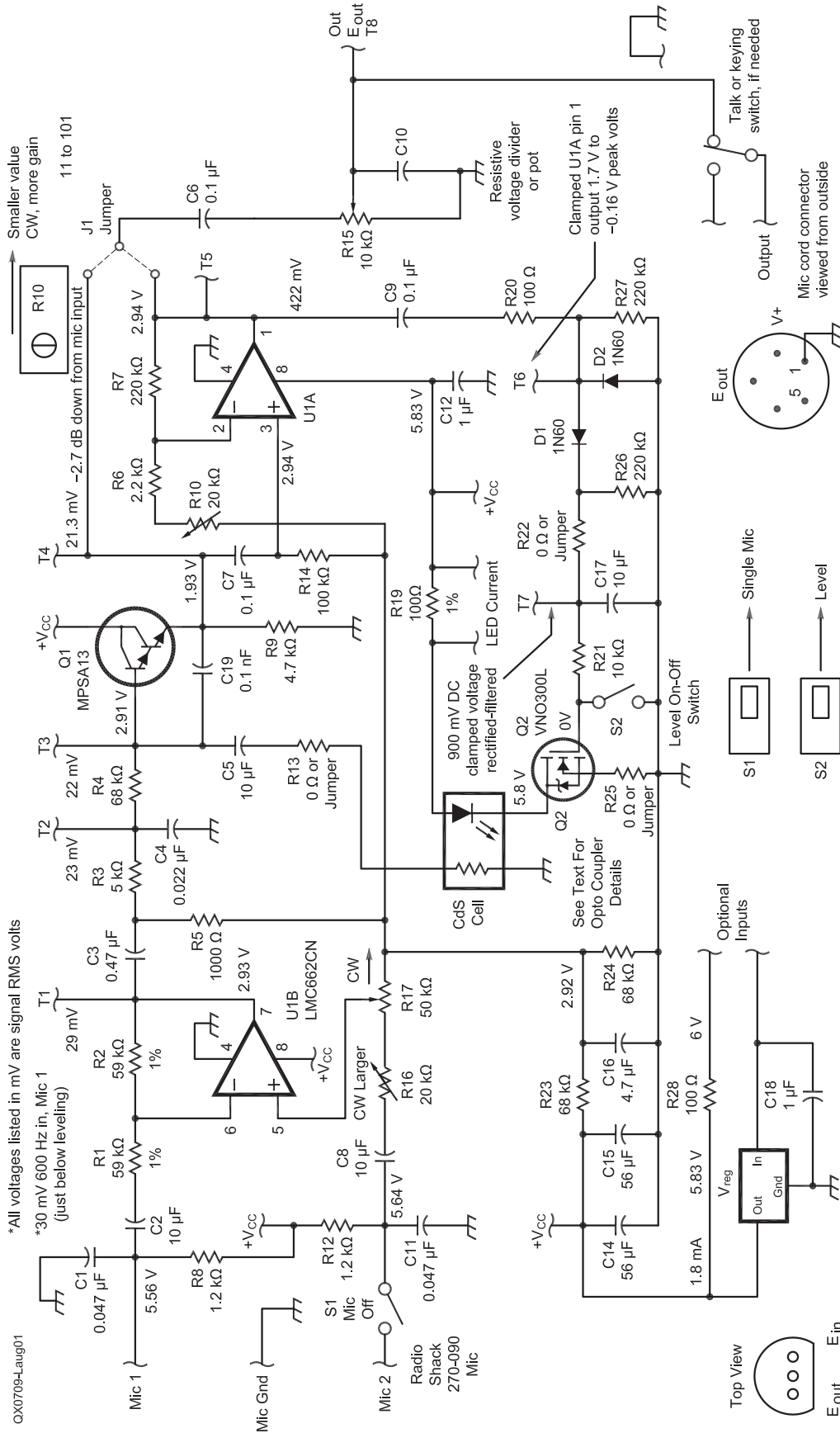


Photo B — The main circuit board is held between two pieces of plastic that have been machined to fit inside the drain-pipe tubing.

11918 Pompano Ln
Houston, TX 77072
johnel@earthlink.net

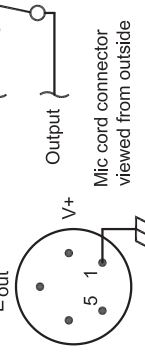
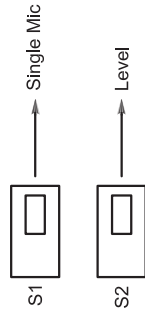
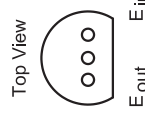


*All voltages listed in mV are signal RMS volts
 *30 mV 600 Hz in, Mic 1 (just below leveling)

QX0709-Laug01

Figure 1 — This is the complete schematic diagram of the differential microphone circuit. Note that circuit voltages listed in V are dc values and those listed in mV are signal values.

- Parts List**
Resistors all 1/4 W
 R1, R22 — 59 kΩ metal film, preferably 1%
 R3 — 4700 Ω metal film
 R4, R23, R24 — 68 kΩ, preferably 1%
 R5 — 1 kΩ metal film
 R6 — 2.2 kΩ metal film
 R7 — 220 kΩ metal film
 R8, R12 — 1.2 kΩ metal film
 R9 — 4.7 kΩ metal film
 R10, R16 — 20 kΩ potentiometer, Bourns 3292 or equivalent
 R13 — 0 Ω or wire jumper
 R14 — 100 kΩ metal film
 R15 — 10 kΩ potentiometer, Bourns 3292 or equivalent
 R17 — 50 kΩ potentiometer, Bourns 3292 or equivalent
 R19 — 100 Ω, preferably 1%
 R20 — 220 Ω
 R21 — 10 kΩ
 R22 — not used, jumpered
 R25 — not used, jumpered
 R26, R27 — 220 kΩ
 R28 — 100 Ω
Capacitors all at least 10 V dc
 C1, C11 — 0.047 μF, Matched
 C2, C8 — 10 μF Tantalum, Matched
 C3 — 0.47 pF film or Tantalum
 C4 — 0.022 pF film or ceramic
 C5 — 10 μF tantalum
 C6, C7, C9 — 0.1 pF film
 C10 — Not used
 C12, C18 — 1 μF film
 C13 — 0.1 pF ceramic.
 C14, C15 — approximately 56 μF tantalum, not critical
 C16 — 4.7 μF tantalum, not critical
 C17 — 10 μF tantalum
 C19 — 0.1 nF
Semiconductors
 Q1 MPSA13 Darlington or equivalent
 Q2 VNO300L or similar with no more than 1Vdc turn-on must be enhancement type
 D1, 2 1N60 or similar Ge diode
 U1 LM66CN or close
 CdS cell components, see text
Voltage regulator, if used, 78L05 to 78L08
Switches
 Mic and level - small slide switch. RadioShack 900-7597 or equivalent.
 push-to-talk - SPST pushbutton RadioShack 275-644 or equivalent.
Mic Elements
 Mic elements, electret with leads or circuit board mounting, RadioShack 270-292 - 270-290
Mechanical
 Approximately 20 inches of 0.185 inch diameter brass rod
 Approximately 3 inch length of 2 inch diameter plastic rod



Piece of chrome plated brass drain pipe,
1.5 inch OD with 0.022 inch thick wall
Circuit boards
Compression spring, approximately
0.3 inch OD
Molex 0.062 inch crimp terminals,
RadioShack 910-2720 and 910-2722
Various colored no. 22 to 24 AWG wire
and 1/8 inch various colored heat-shrink
tubing
Mic windscreen, RadioShack 33-4001
Machine contact sockets, Jameco
102200CB or equivalent. See text.
Right angle bracket for PB switch, made
to order.
Four-pin jack and plug, RadioShack 274-
002 and 274-001

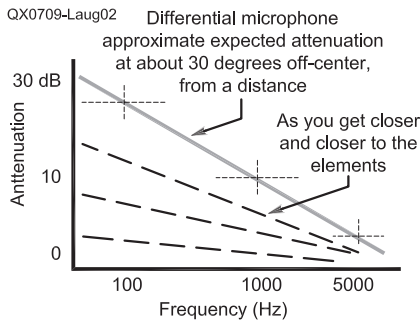


Figure 2 — This graph shows an approximation of the differential attenuation you can expect from the circuit. Note that higher frequencies and shorter distances from the microphones produce lower attenuation.

elements for my mic were carefully selected, from a group, to match. The plug-in feature for the mic elements was greatly helpful in matching the two. The circuit impedances and resistances presented to each mic were carefully matched.

C1 and C11 are used to help roll-off frequency response above the 3 kHz region. The capacitors should be matched closely. The output impedance of the mic elements is equal to their load resistance, R8 and R12, which here is 1.2 kΩ.

Again, you should pay special attention to careful matching of frequency and phase characteristics of the two op-amp inputs. A phase difference between two equal amplitude inputs will cause an output to occur.

C2 and C8 were selected to be very close to their stated value. This will insure very close phase matching for both inputs at the lower frequency end of the audio spectrum. Being as large as the ones I used, there is not much of a problem here. The voltage division and phase characteristics of C2, R1 and R2

Table 1
Leveling, Distortion and RMS Levels

Frequency at Mic 1 input 600 Hz
U1A gain adjusted for a start of leveling at Mic 1 60 mV RMS

Measured RMS Levels:

Input (mV)	T3 (V)	T5 (V)	T7 (V dc)	LED Current (mA)	Second Harmonic Distortion (dB)
20	0.015	0.17	0.25	0	-58
80	0.042	0.48	1.0	0.059	-50
160	0.045	0.496	1.04	0.13	-50
360	0.047	0.513	1.08	0.28	-45
1 V	0.058	0.534	1.12	0.74	-45

At limiting, T6 exhibits approximately a +1.7 V and -0.16 V peak (clamped voltage).

Input level from 80 mV to 1000 mV = 22 dB increase = 156 to 1 power increase

T5 level from 0.48 mV to 0.534 mV = 0.92 dB increase = 1.2 to 1 power increase

Frequency response from input to T8 (C6 = 0.1 μF and RL = 10 kΩ):

-1 dB at 397 Hz and 1233 Hz

-3 dB at 265 Hz and 1797 Hz

-6 dB at 181 Hz and 2570 Hz

Approx. input (RMS) for leveling:

Gain Minimum -124 mV

Gain Maximum -12.8 mV

need to exactly match that of C8, R16 and R17. To obtain this precisely, R16 was made variable to adjust the total series resistance of R16 and R17 for phase matching with C2, R1 and R2. To match the voltage division of R1 and R2, R17 is adjusted to give input amplitude to pin 5 equal to that of pin 6.

If you wish to roll off the lows more by reducing these two capacitors, a smaller value will increase the phase shift and they will need to be very carefully matched and the phase adjustment of R16 will be more important for the low frequencies. These considerations ensure that for equal mic outputs, both inputs to the differential amplifier are equal as to phase and voltage, causing cancellation at the output, pin 7. Now, if you speak into one mic more closely than the other, its output will be greater, resulting in an output at pin 7.

Distant sounds will arrive at the two microphones with nearly the same amplitude and phase, and be cancelled. Figure 2 gives a rough idea of attenuation versus distance and frequency that you can expect. This can vary considerably, depending upon room acoustics.

From pin 7, the resulting audio is rolled off on the high end by R3 and C4, and the low end by C3 and R5. The most interesting part of the circuit continues from this point. Note that R4 and the resistance value of the cadmium sulfide (CdS) element, often referred to as a "light dependent resistor" or LDR, in the opto coupler, form a voltage divider that determines the audio input level at the base of Q1. R13 was not used and was jumpered. It was made available in case some alteration to the resistive characteristic of the CdS cell

would be desired.

The mic input level to U1B that results in the beginning of the leveling action depends upon the gain of U1A. This gain is adjusted by R10. Output from U1A is directed through C9 to the two diodes, D1 and D2. D2 acts with C9 to form a positive "clamping" action of the audio waveform. D2 and D1 are germanium diodes resulting in the negative excursion of the audio to be "clamped" at a maximum negative excursion of approximately -0.14 V and the positive excursion of approximately +1.7 V from an RMS value of about 0.65 V at pin 1. This results in a higher positive amplitude being delivered to D1 from the output of U1A. D1 rectifies the positive value of the waveform and this rectified voltage is filtered and smoothed by C17 and applied to the gate of Q2, which at a certain level causes Q2 to turn on. As Q2 turns on, light is delivered to the LDR whose resistance decreases from virtually an open circuit to a value which now reduces the input to the base of Q1.

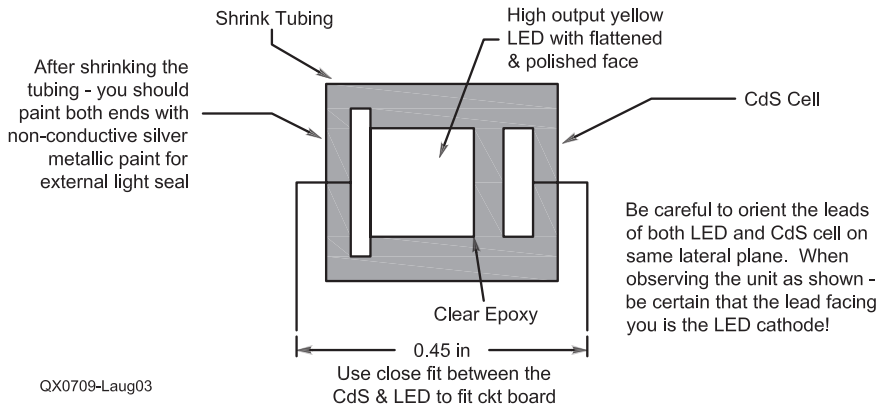
When a mic input reaches a level sufficient to cause leveling, two things happen.

1) More mic voltage to the base of Q2 results in more light to the LDR.

2) More light to the LDR results in a reduction of voltage to Q1 base.

The two actions work "against each other," which results in a much more controlled amplitude at the base of Q1 compared to that being produced by the mic input, resulting in a relatively constant audio level delivered out to the final destination. The T3 and T5 voltage columns of Table 1 demonstrate this action. So, you can "Holler and Scream" into the mic all you want to, but you will not be

CdS - LED Construction

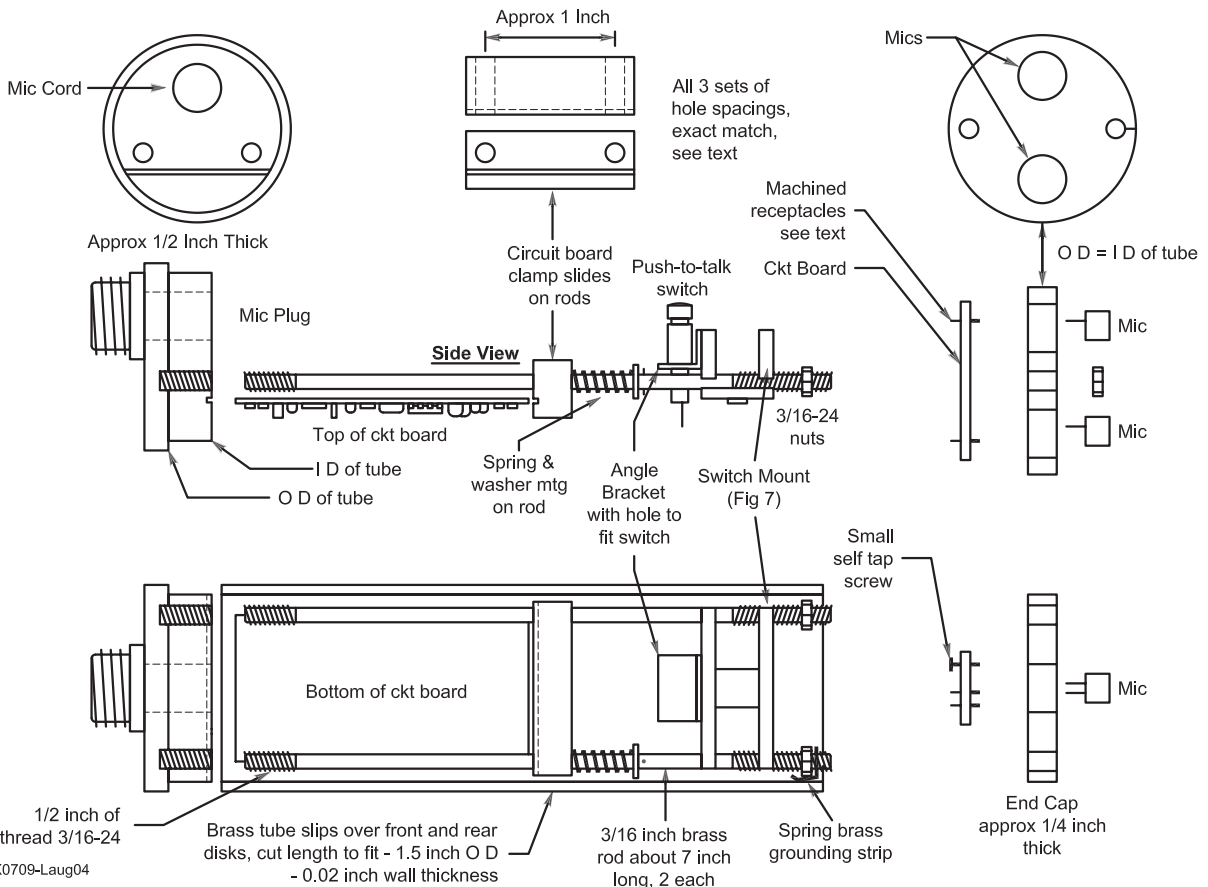


QX0709-Laug03

**Table 2
LED - CdS Relationship**

LED Current (μA)	CdS Cell Resistance (Ω)
20	1.025 M Ω
30	472 k Ω
40	279
50	187
60	137
70	106
80	85.6
90	71
100	60.3
120	46
230	18.8
250	16.9
400	9.6
800	4.5
1.00 mA	3.6
2.00 mA	1.85
4.00 mA	1.00

Figure 3 — This drawing shows how a cadmium sulfide photo cell and high output LED are epoxied together to form an opto-isolator.



QX0709-Laug04

Figure 4 — Here are the mechanical details of how the author packaged his microphone into a length of chrome-plated brass drain pipe.

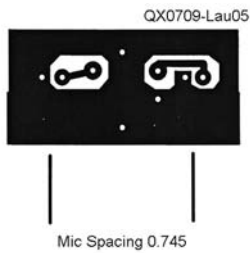


Figure 5 — This small circuit board makes it easy to plug in various mic elements to test for the best balance.

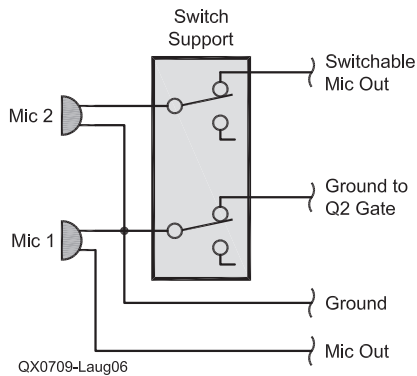


Figure 6 — The details of wiring a DPDT switch to allow Mic 2 to be included or removed from the circuit.

any louder when someone hears you! For a lot of places I have been, listening to microphone users, this would have been a blessing and I'll bet you will agree!

Two outputs are available to be delivered, one at T4 and one at T5. The T5 output is naturally larger than the one at T4 due to the voltage gain of U1A, so if you desire a relatively large output use T5. The Jumper will select your choice. The voltage divider, R11 with R18 or R15, can be selected to obtain whatever output level you may desire and is especially useful to "trim to order" the larger output from T5, if it is used.

For Q2 I used an FET for its extremely high input resistance, and it must be of the "enhancement" type. Using the FET means that the discharge time constant of the filtered dc is controlled only by the values of R26 and C17. R22 can be used to alter the charge time of C17 if desired. You can see, from the T7 voltage column of Table 1, that the particular FET I used begins to conduct at approximately +1 V dc gate voltage and the output leveling begins. These FETs can be selected for the turn-on voltage level, and I recommend using one with not more than 1 V. Note that voltages are listed at pertinent points on the schematic. To distinguish dc voltages from signal voltages, all signal voltages are in millivolts (mV). The dc voltage at T7 is a result of the signal voltage from pin 1 being clamped positive,

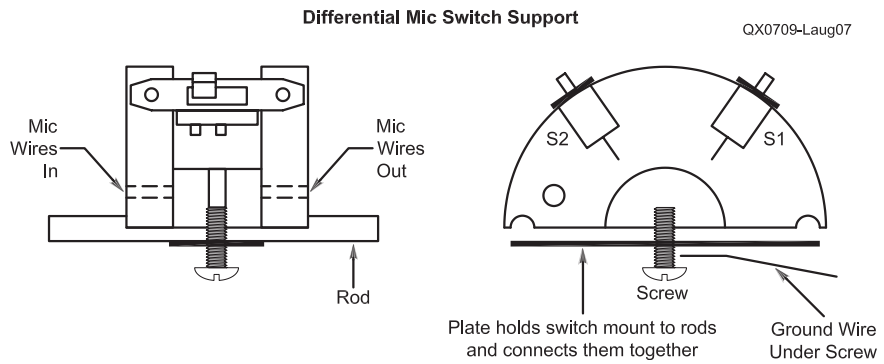


Figure 7 — This drawing shows the details of the differential mic switch support structure.

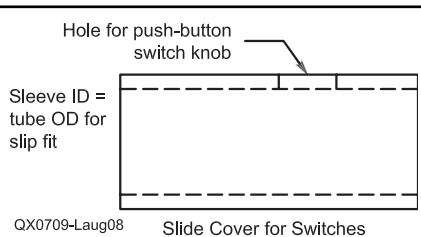


Figure 8 — A piece of tubing slides over the main microphone tube housing to cover the mic selection switches. A cut-out provides access to the PTT switch.

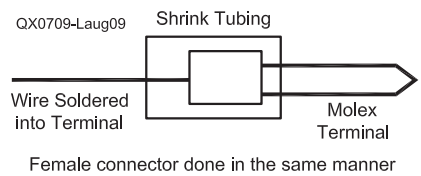


Figure 9 — I soldered the connecting wire to a Molex terminal, then used a piece of heat-shrink tubing to cover the connection. The mating female Molex terminal is wired the same way.

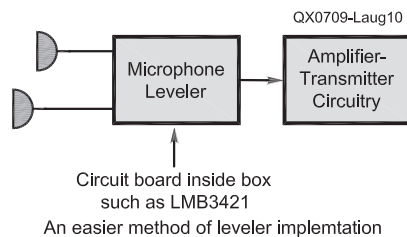


Figure 10 — There are many packaging options for a differential leveling microphone.

rectified and filtered to a dc level.

CdS Cell and LED Construction

Figure 3 shows how I constructed a type of optoisolator by epoxying a cadmium sulfide (CdS) cell and an LED together. You should be certain to provide an LED with the highest light output for the driving current. This greatly reduces operating current consumption and results in more efficient operation overall. Notice that the average current drain of the circuit is approximately 1.8 mA. A yellow LED falls closest to the maximum response frequency of CdS cells. The cadmium sulfide light dependent resistance element (LDR) was used for the light receiving element here instead of a commonly used semiconductor device. CdS cells are extremely linear compared to a semiconductor element. This

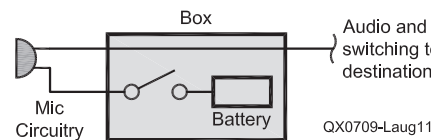


Figure 11 — If the operating voltage is not available from your transceiver or other circuit, you can build a battery and ON/OFF switch into the enclosure.

results in virtually immeasurable nonlinear distortion. See Table 1.

I found some small CdS cells that measured 0.185 inch in diameter and measured approximately 5000 Ω at normal room lighting levels. This parameter is not critical because the circuit can automatically adjust itself. The CdS and LED items are available from many sources. RadioShack has a five-pack of CdS cells (276-1657) for \$2.79. They also have a high output yellow LED (276-351) for \$2.69.

You should somewhat flatten the face of the curved LED and polish it. Carefully hold the LED and CdS cell facing each other and touching, with a fixture. It is important that the leads for both LED and CdS cell be orientated on the same lateral plane so they can be bent down properly in relation to each other.

This bending must be done exactly correct in order for the unit to plug into the circuit board properly! Study Figure 3 carefully to determine this.

Now, you should apply a small current to the LED and adjust the position of the two in respect to each other for maximum resistive response of the CdS cell. At this point a clear epoxy is allowed to seep between the two surfaces and harden. The overall length of mine measured 0.365 inch. This allowed the two leads from both to be bent straight down to match the circuit board pad spacing.

Table 2 shows the variation in CdS cell resistance versus LED current that my particular combination exhibited. Again, note that the leads *must* be bent the correct way so as to align with the *proper* pads on the circuit board. You need to be very careful of this. Review Figure 3. You should shrink a short piece of black heat-shrink tubing over the two. Then you should paint the ends with some nonconductive silver paint for external light blocking.

This circuit was designed for an approximate 5 to 6 V power source, but this is not at all critical. The tantalum capacitors should have a voltage rating of 16 V dc or higher, so I included a position for a voltage regulator for use with higher supply voltages that I might need or want to use sometime.

Try the “machine tooled sockets” like found on some IC sockets such as a Jameco IC socket no. 167003CB. Another source is Aries X518 collet sockets or their pin-line sockets with “break” feature. See www.arieselec.com/Web_Data_Sheets/12020/12020.htm. These little sockets are widely available from other sources. I carefully free the individual sockets from the plastic and place them in a circuit pad hole of 0.051 inch, where it might be desired to have a removable item such as resistors, transistors and so on. Plug-in parts can really be a great asset at times.

Construction

Figure 4 and the photos show the construction details of how I packaged my micro-

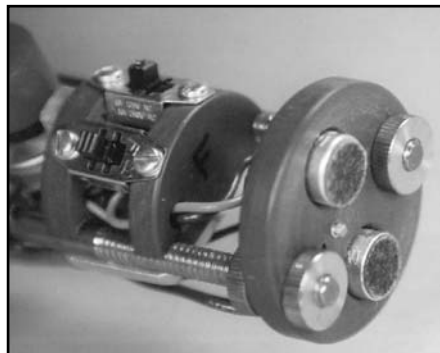


Photo C — The mic elements plug into a small circuit board behind this plastic block that forms one end of the package.

phone. The supporting rods are of 3/16 inch brass, approximately 7 inches long, threaded about 1 inch on the mic end and about 0.5 inch on the cord end. The housing is 1 1/2 inch diameter chrome-plated-brass sink drain pipe with approximately 0.02 inch wall

thickness. This is available at many hardware stores. All of the plastic pieces were turned from a 2 inch PVC rod. Of course nearly any plastic will do. The cord end was indented as a stop for the tubing, with the mic end diameter turned for close fit into the tube.

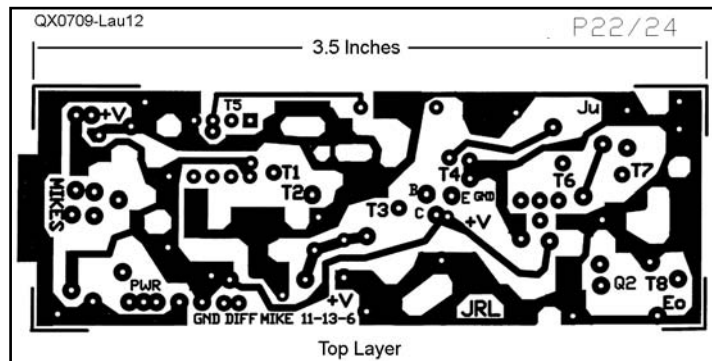


Figure 12 — A full-sized etching pattern for the top (component side) of the circuit board.

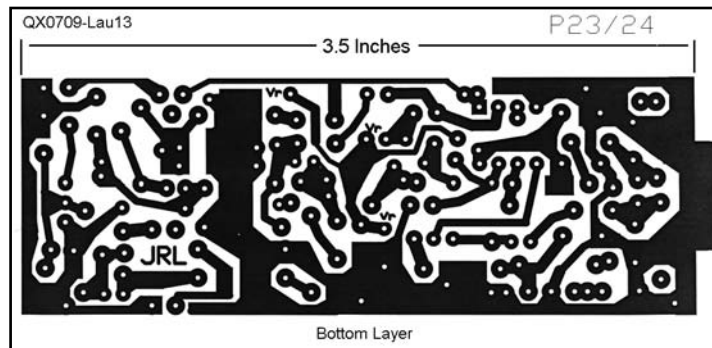


Figure 13 — A full-sized etching pattern for the bottom of the circuit board.

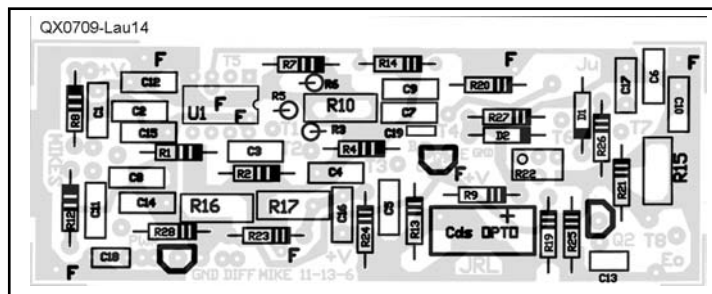


Figure 14 — Parts placement diagram for the differential leveling microphone circuit.

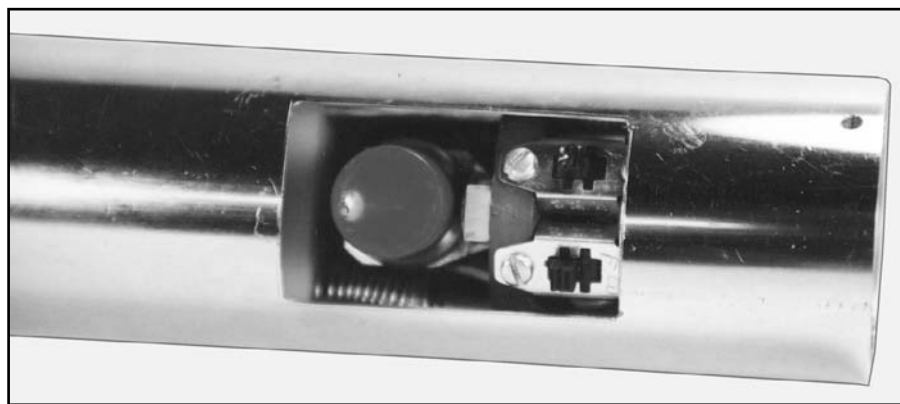


Photo D — This photo shows the mic selection switches and PTT push button switch inside the drain-pipe tubing. In the finished microphone, a piece of tubing slides over the opening, with the PTT switch protruding through a hole in that cover.

The center piece (circuit board clamp) was trimmed from round to rectangular as shown. Holes in all pieces must be drilled with very accurate spacing. I ensured this by drilling two guide holes (smaller than the rods) in the 2 inch rod before it was machined into the separate pieces. The holes must then be drilled with a diameter suitable for the rods used except for the cord end, which was drilled with a smaller diameter suitable for threading to fit the threaded rod. Some small nuts were used to hold the mic end in place.

I made a small circuit board to plug the mics into for easy removal. Figure 5 shows the board pattern. You may prefer to simply wire them instead. Note that the circuit board clamp is loose fitting on the rods, and a spring was used to press it against the end of the circuit board, the board fitting into shallow grooves in the clamp and cord end. Figure 6 shows how I wired Mic 2 to be disconnected if desired, to disable the cancellation feature. Another switch was used to ground the gate of Q2, to disable the leveling feature if desired. These two switches are mounted on the "switch mount." See Figure 7.

Note that the plate electrically connects the rods together and all are grounded by a wire placed under the screw. I used a small terminal on the end of the wire. The switch support was machined as a round piece then cut almost in half. Its diameter needs to be such that the switch handles just reach the inner wall of the brass tube. Appropriate cutouts were made in the tube to accommodate the switch handles. A spring brass clip was formed to clamp between one of the front nuts to ground the case.

A thin wall tubular cover was made to slip over the switch cutout in the tube, as shown in Figure 8. I machined this to size and thickness from a piece of PVC tubing. A hole in this tube accommodates the switch push knob and this knob "locks" the cover in place. To change switch settings, simply press the switch knob in and slip the cover down to expose the switches.

For the push-to-talk switch, a small right angle support was made to be bolted to the end of the switch support, as shown in Figure 4. It must be carefully positioned so that when the case is in place the button projects above the case so as to be easily pressed for transmitting. This switch can be wired to disconnect the audio output or to transmit. Because the switch button projects above the case, care should be taken so that the switch is mounted at a correct height, which will allow the case to be slipped on and off when the button is held down hard.

All wires going to the circuit board were connected through the Molex crimp terminals. This allows easy and complete removal of the board if needed. The connectors were greatly shortened by removing the normal wire-crimping ends. The connecting wires

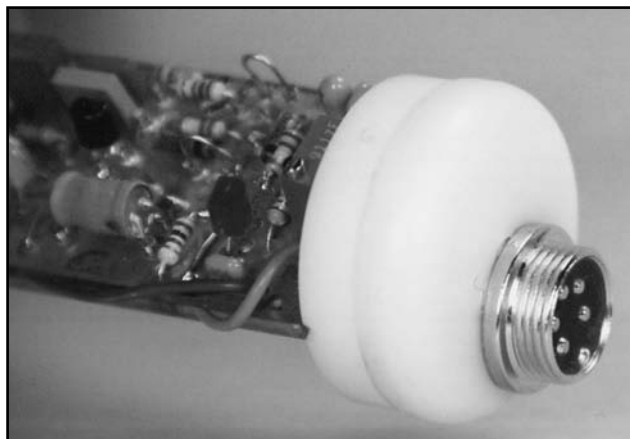


Photo E — The plastic block at the back of the microphone holds the circuit board and includes the connector for the mic cable to your rig.

were simply soldered to the small remaining end of the terminal. See Figure 9. I used different colors of wire and matching shrink tubing for each wire. Figure 7 shows that the mic wires were run through a small hole in the switch mount, both from the mics and from the switches to the board connectors. This was not necessary but made a bit neater layout.

I am sure that you have noted that my particular construction technique used here involves a small amount of machine work. An easier method would be to "box" the circuit board as shown in Figure 10. The mic was designed to be powered by the instrument into which it is connected. A small battery box can be used to power it in the absence of any other source, as indicated in Figure 11. A local machinist should be able to construct parts similar to the ones I used if you like my layout but do not have a machine lathe.

Adjusting for Proper Operation

First, you should check dc voltages at T1 through T5. These should be close to those shown on the schematic. If these check out, you can proceed to adjustments.

Adjusting R16 and R17 for Null

1) Feed in an input signal of about 400 Hz at about 0.1 V amplitude into one input.

2) Check for signal presence at T1 through T6, and check for signal dc voltage at T7.

3) Trim R10 for a U1A gain of about 10 to 15. This is done while comparing the level of signal at pin 3 and pin 1. The correct level should be approximately 60 to 80 mV. You test this by observing T5 and see when its output level stops rising as the input level is adjusted up and down. You must be sure to have S2 open while doing this!

4) If okay, jumper both mic inputs together, disable leveling (close S2). Be certain that the input signal level is not causing any clipping. Close the Mic2 disconnect switch, S1.

5) Adjust R17 for the lowest reading at T1.

6) Alternately adjust R16 and R17 for

best null. This can be a bit tricky because you are adjusting R17 for amplitude and R16 for phase and amplitude. Actually, capacitors C2 and C8, both 10 μ F, result in very small phase shift at the lower frequencies and virtually none at higher frequencies, so adjustment is quite easy for good cancellation, even at the low frequencies. Face the mic directly toward a radio playing music at about 1 foot away. Carefully check the adjustment of R17 and R16 for minimum output at pin 1. Be certain the radio is directly in front of the two mics, so they will receive equal sound. You can observe the degree of cancellation by alternately opening and closing switch 1.

Table 1 is a rough idea of what to expect of the differential response at differing distances and frequencies. Note that higher frequencies are not attenuated nearly as well. Closer mic spacing will improve this. I designed the circuit to roll off the higher frequencies that are not as important, to help with the attenuation of them.

For a practical test, I connected the output through a small amplifier feeding a pair of headphones. By listening to various sound sources both inside and outside, I got an evaluation of the performance. The mic worked wonderfully well on both the leveling and prevention of feedback.

John Laughlin, KE5KSC, holds a BS in Electronic Engineering Technology from the University of Houston. He has been employed in the electronic industry for 25 years, and also was a college instructor for 25 years. He holds six CET certifications, along with a Radio-Telephone license, First Class, with radar endorsement. John is a member of the Brazos Valley Amateur Radio Club in Sugarland, TX.

John has published numerous articles in Popular Electronics, ham radio magazine, 73 Amateur Radio and other electronics magazines. Other hobbies include walking across the Grand Canyon (three times so far, with more to come!), sailing, billiards and making fine custom billiard cues.

QEX

Turbo Delphi Explorer: Develop Amateur Radio Projects for Windows with a Free Compiler

It's free but you can't tell from the great performance.

Steve Gradijan, WB5KIA

Turbo™ Delphi® Explorer is a free Windows development tool available from CodeGear (Borland). This compiler might be one of the most useful “freebies” you will ever find for Amateur Radio. Stop complaining about the availability of commercial and freeware Amateur Radio software, and start writing your own applications to do what you want the programs to do. The example source code provided in this article and the Web links mentioned will help even novice programmers get started.

Turbo Delphi Explorer allows you to experiment with coding Windows programs at the cost of only your time and a little patience. The Turbo Delphi Explorer compiler is available as a free download.

What Is It?

Turbo Delphi Explorer is a full featured Windows compiler. The Explorer edition comes with a fixed set of over 200 software components for building hundreds of different types of applications, limited only by your imagination. The Turbo Professional edition, which CodeGear hopes some individuals will migrate to (and pay for), has additional components and allows you to customize the included components, create new components and add third party custom controls

and components to the compiler.

You get a Delphi compiler capable of writing professional quality software at no cost. The “one hundred year” license allows you to use the Explorer Edition for developing software for both personal and commercial use. Several years ago, a similar product retailed on the order of \$100 and did not have a fraction of the capabilities of Delphi Explorer. You also get a few features related to databases previously available only on the very expensive Delphi Professional or Enterprise editions!

If you are experienced in other programming languages, CodeGear provides several other programming tool options. There are also free Turbo Delphi for .NET, Turbo C++ and Turbo C# compilers available. A caveat of this free deal is you can only have one of these compilers resident on your PC at a time.

Microsoft also has a free version of their VB.Net compiler available, called Visual Studio Express. This offering uses a variation of the Visual Basic language that some experimenters may prefer to Delphi. I haven't tried Visual Studio Express but be aware, it has fewer features than Delphi, and the Pascal code provided with this article will not work with it. Download Visual Studio Express at msdn.microsoft.com/vstudio/express/. It is a 35 to 70 MB download.

Is Program Coding Hard?

Coding Pascal is not easy but is certainly doable for anyone who has even minor experience with other programming languages.

Programming in Pascal (in this case, actually the Delphi visual object Pascal) is an easy transition if you are blessed with C or C++ coding experience. Even Visual Basic programmers should find learning this tool to be relatively easy.

There is plenty of programming help on the Internet for both beginners and experienced programmers. Numerous examples of Delphi source code are also available on general topics. Amateur Radio oriented Delphi source code examples are available from various resources, including the example source code files accompanying this article. Figure 1 shows the Explorer main screen, with programming window and various tools.

You can easily change the programs to look like you want them to look, and you can add additional features you want. Program modifications are possible if you have the Delphi source code.

Visual Basic, the standby programming tool for many amateur coders is no longer available at retail. (See the earlier note about Visual Studio Express, the Visual Basic replacement.) Even if Visual Basic 6 still could be purchased in stores, Delphi is a superior programming tool and a great fit for a beginner. “Porting” Visual Basic source code to Delphi requires some knowledge of both programming languages so some ports to Delphi are not trivial.

It's Free So What Are You Missing?

Unlike the Delphi compiler versions you

1902 Middle Glen Dr
Carrollton, Texas 75007
steve_jg@msn.com

pay for, *Turbo Delphi Explorer* does not come with an installer program like *InstallShield Express*. For simple and even many involved programs, an installer is really not necessary. If you are installing other features along with the application, however, an installer might be necessary to deploy your creations to other users' PCs. Free installers like *Inno Setup* are available and work well. (See www.jrsoftware.org/isdl.php.) The free installers I am aware of do not handle Microsoft *.msi install files (which may be necessary to support some program features on a user's PC). A program like *Inno Setup* has provisions for installation of .ocx, .DLL and the Borland Database Engine (.BDE) files, and that is all most coders will ever need.

You are limited to the visual components provided by *Explorer* (about 200). The free version does not allow installation of third party components. If an example source code uses controls that are not available on the *Explorer* control pallet, you will have to

write appropriate code, which may or may not be a simple task.

I use *AsyncPro* or *TComport*, free *Delphi* add-in controls, with *Borland Delphi 5 Professional* to provide control of the COM port on PCs. My expensive program allows third party controls, and I save a lot of time by using them instead of coding my own serial port communication routines. With *Turbo Delphi Explorer* it is necessary to write any code to access your PC COM ports in native *Delphi* Pascal, since *Explorer* does not support add-in controls. Is this important? It could be if you intend to develop an application that controls a transceiver, rotator or other device that needs to receive signals from the program, or if you will write programs to communicate over the Internet or a network. You will have to write your own routines or buy a different version of *Delphi*.

As long as the program you develop works within the framework of a PC, even advanced programmers will have enough

tools to work with. The two hundred provided controls will allow you to do plenty of amazing things. The files provided on the *QEX* Web site and discussed later show how to provide even COM serial port control using type libraries (.TLB files).¹ The free *Explorer* can handle TLB files. I have provided a native code example to use serial port control as part of the zip file available on the ARRL *QEX* files Web site. Additional *Delphi* code is available on my Web page, at www.qsl.net/wb5kia/.

Serial Communications Solved

The source code needed by *Turbo Delphi Explorer* to command a Kenwood radio or other transceiver using serial ports is "easy" to write. Capturing the transceiver's feedback

¹The example program files mentioned in this article are available for downloading from the *QEX* Web site. Go to www.arrl.org/qexfiles and look for the file **9x07_Gradijan.zip**.

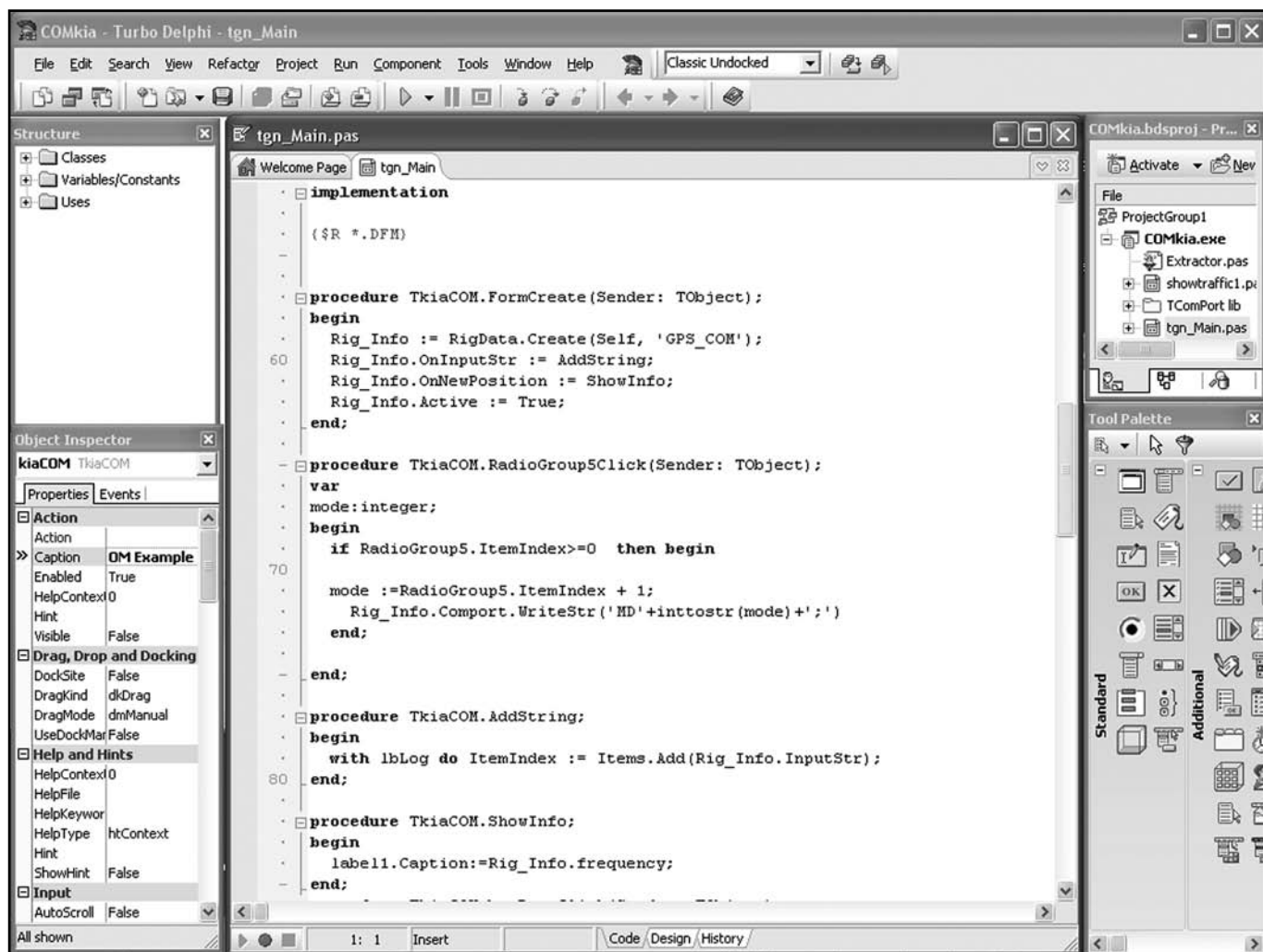


Figure 1 — Screen shot of *Turbo Delphi Explorer* main development screen showing the code writing screen in the center with various tool boxes to the sides.

over the serial line back to the PC is complicated. The example source code provided on the *QEX* files download page shows a simple approach to serial communications. You have to be able to exchange information with your equipment. The routines I use with *Explorer* to provide the serial communication between the transceiver and PC are highly commented and will especially help novice programmers do something many programmers think is moderately difficult. Figure 2 is a screen capture from the Kenwood CAT control program I wrote.

You'll have to figure out how to use *Explorer* to communicate over the Internet and to use it with special USB ports on your own. USB/Serial adapters, however, do work fine with *Explorer* and use the same code required for normal COM ports.

Check the **Resources** compilation listed in Table 1 for places to find *Delphi* source code and programming tutorials. Have fun.

How to Get the Compiler

The CodeGear compiler application is a very large download. The compiler uses quite a few Microsoft programming tools in its operation, and they also need to be loaded on

your PC. The Microsoft tools are also free. The non-CodeGear required tools are contained in over 228 MB of files. Most of the Microsoft tools are probably already loaded on your PC, however. Table 2 lists the required Microsoft files you will need. The *Turbo Delphi Explorer* install is a 325 MB file. My slow DSL connection took nearly two hours to download everything (over 550 MB). The program installation took another half hour.

Download the necessary files from the mirror site at turboexplorer.com/mirror. Click on the entry for *Turbo Delphi Explorer* or obtain the program from a friend. After you have the program and prerequisites, go to www.borland.com/downloads/download_turbo.html to register your program. The second link does not indicate *Explorer* is free, but it is. These URLs have both the *Explorer* and the necessary Microsoft files (or links to them). It is necessary to visit the CodeGear Web site (www.codegear.com/downloads) as linked from the www.borland.com/downloads/download_turbo.html Web site to obtain a registration key if you obtained a disk elsewhere.

The prerequisite "helper" programs listed in Table 2 can be downloaded from either of

these sites. My experience is that it is easier to download only what you need from Microsoft at www.microsoft.com/downloads.

CodeGear encourages users to burn CDs containing the *Explorer* download and take the CDs to their local clubs to share, but individuals need to visit the CodeGear Web pages to obtain their own free registration key to activate the programs on their PCs.

Loading the Example Code Available on the *QEX* Web Page

After you have loaded the *Explorer* compiler on your PC, download the files accompanying this article from the *QEX* files at www.arrl.org/qexfiles/. (See Note 1.) Find either the file COMkia.bdsproj or COMkia.dpr (both files will work) in the "catsimple" folder for an example using Windows API calls to provide serial communications with Kenwood radios. More complicated but usable with many radios, use the files catcomplicated.bdsproj or catcomplicated.dpr in the catcomplicated folder. The specific catcomplicated example is used in conjunction with a free utility program called *Omni-Rig* developed by Alex Shovkopylas,

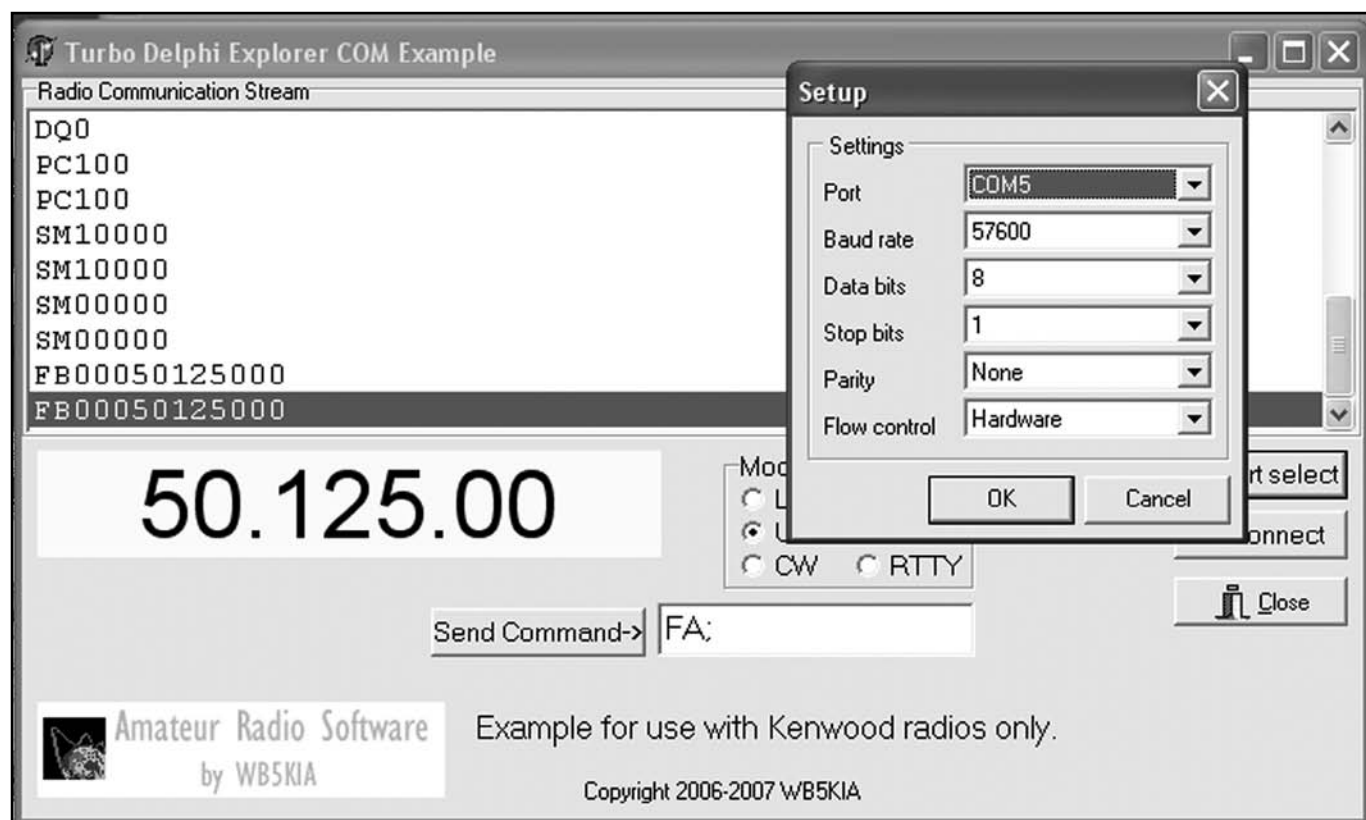


Figure 2 — You get around the few limitations of the compiler by writing code the old fashioned way. An example program shows how to handle the lack of a serial port control in the *Explorer*'s provided controls. It demonstrates code required for a simple CAT program to "talk" to your computer controllable Kenwood radio. A similar example is provided for use with other manufacturer's radios.

Table 1**Resources***Compilers and Installers*

S. Gradijan, WB5KIA, "Beginners' Computer Programming for Ham Radio — Part 1," *QST*, Feb 2003, pp 32-37 describes other programming options. *Turbo Delphi Explorer* by CodeGear and its registration is available at www.borland.com/downloads/download_turbo.html. The mirror site at turboexplorer.com/mirror is the easiest place to download. It still is necessary to visit the CodeGear Web address to obtain a registration key if you obtained a disk with the software elsewhere.

The Microsoft tools described in Table 2 are available at www.microsoft.com/downloads as individual downloads. The entire package is available at turboexplorer.com/mirror.

The Inno Setup installer is available at innosetup.org/isinfo.php. This is an excellent free tool, but it is only needed if you will deploy elaborate programs.

Microsoft's *Visual Studio Express* is available for free at msdn.microsoft.com/vstudio/express/. It is a lightweight version of Microsoft's *Visual Basic 6* replacement, called *VB.Net*. You code in a version of the Visual Basic language but will not be able to use the example *Delphi* code.

Software and Source Code

QEX files www.arrl.org/qexfiles/. Look for the file **9x07_Gradijan.zip**.

AsyncPro is a free *Delphi* add-in control used with a CodeGear *Delphi* or C++ compiler to provide control of the COM port. It is available from: sourceforge.net/projects/tpapro/. Unfortunately it will not work with the free version of *Turbo Delphi*.

TComport is another free *Delphi* add-in control. Authored by Dejan Crnila, it is available from sourceforge.net/projects/comport/. The source code is provided. I used Dejan's source code as the basis for "native" routines you can use to embed serial port control within your software projects in the "COMkia" example (Figure 2).

S. Gradijan, WB5KIA, "Amateur Radio Software: It Keeps Getting Better," *QEX*, Sept/Oct 2002, pp 19-29.

A. Shovkopyas, VE3NEA. Free rig control engine called *Omni-Rig* provides serial control. It is available at www.dxatlas.com/omnirig/. *Omni-Rig's* use with *Explorer* is described in the source code accompanying this article.

Programming Amateur Radio Software with Delphi

M. E. Erbaugh, N8ME, "Customize the Ten-Tec Pegasus — Without Soldering," *QEX*, Sept/Oct 2002, pp 3-9.

S. Gradijan, WB5KIA, "Command and Control: Talk to Your Radio and Your Radio May Talk Back," *QEX*, Nov/Dec 2006, pp 40-48.

S. Gradijan, "A Talking Logbook with Rig Control," *QEX*, May/June 2006, pp 40-44. Routines from the Microsoft SDK might be usable with *Turbo Delphi Explorer*.

S. Gradijan, WB5KIA, "Build a Super Transceiver — Software for Software Controllable Radios," *QEX*, Sept/Oct 2004, pp 30-34.

S. Gradijan, WB5KIA, "Beginners' Computer Programming for Ham Radio — Part 2," *QST*, Mar 2003, pp 36-42.

S. Gradijan, WB5KIA, "Beginners' Computer Programming for Ham Radio — Part 3," *QST*, Apr 2003, pp 39-44.

The www.qsl.net/wb5kia Web site has numerous examples of *Delphi* code that have application to Amateur Radio activities.

Beginning and intermediate *Delphi* coders will find a great general coding Web site at www.efg2.com/Lab/Library/index.html.

The Web page at www.delphiforfun.org/ is WONDERFUL for beginners. It contains lots of non-Amateur Radio projects that can be modified for use with your radio projects.

Table 2**Delphi Explorer Prerequisites**

Microsoft .NET Framework SDK Version 1.1 (23.1 MB)

Microsoft .NET Framework 1.1 Redistributable Package (10.1 MB)

Microsoft .NET Framework 1.1 Service Pack 1 (106.2 MB)

Microsoft Explorer 6 Service Pack 1 (9-77 MB)

Microsoft Visual J# v1.1 Redistributable Package (6.6 MB)

XML Core Services (MSXML) V4.0 SP2 (9.8 MB or less)


These files MUST be installed on your PC before installing *Turbo Delphi Explorer*. The links in Table 1 explain how to download and install these files.

VE3NEA, which must be loaded before you experiment with the project. With *Omni-Rig* and *Explorer*, you can control almost any PC controllable radio without a lot of coding. Double left click on the file and the compiler will load automatically. *Explorer* can also use the *.dpr files created by other versions of *Delphi*.

More Projects?

An article in a future edition of *QEX* will describe how to build a voice keyer/recorder using *Explorer*. The Resources Table 1 directs you to places that have source code you can use in your projects. You can sell the programs you develop but you also can develop them as freeware

for other radio amateurs to benefit.

Steve Gradijan, WB5KIA, is a Geoscience Consultant in the Dallas, Texas area. He holds an Extra Class license and has BS and MS degrees in geology. He has been involved in recreational programming in various programming languages for over 25 years. 

Using Gain-Probability Data to Compare Antenna Performances

Use readily available software to make antenna and propagation comparisons before you build your next antenna.

Fred Glenn, K9SO

When designing a backyard antenna system, the physical reality of available space, antenna height zoning issues, and available support structures must be taken into consideration. The reality of a typical backyard means that most of us have to rule out a three element 80 meter beam up at 120 feet. We all know that this beam will outperform most other antennas, and if you can put that up you don't need to read any further. If your backyard reality means that you can either put up a 30 foot high dipole or a vertical, however, then a method of predicting comparative performance is needed. This article introduces a simple method of comparing two or more antennas and evaluating them in terms of the *probability* of their relative performance into particular parts of the world. The Gain-Probability concept combines antenna pattern performance with published propagation probabilities to evaluate relative antenna performances. The analysis will aid in the antenna building decisions for your backyard reality.

As an example of this approach, I will show a comparison between two simple 80 meter antennas that could possibly be built in a typical backyard like mine: a $\frac{1}{2} \lambda$ dipole at 30 feet and a simple $\frac{1}{4} \lambda$ ground-mounted vertical with radials. Then I will show how these comparisons relate to the probability of success for DX on a path from Chicago, Illinois to Europe on 80 meters. You can easily use this approach for other antennas and other propagation paths.

The good news is that all of the data you

will need is generated by software programs that come bundled with the CD included in *The ARRL Antenna Book: EZNEC ARRL and HFTA*.¹ Once you have the data, the simple spreadsheet program described in this article will generate the gain-probability bar graphs for your analysis.

The typical methods for comparing antenna performances involve the generation of antenna gain patterns as shown in Figure 1. This shows the standard elevation patterns for the 30 foot high dipole (broadside) compared to the vertical.

While informative, these standard plots do not show the relative importance of 80 m propagation into Europe or other parts of the world as a function of elevation angle. At first glance it even looks like the dipole might be

the antenna of choice except for just a few of the lower elevations. This is where the *HFTA* program comes in. You don't actually use *HFTA*, just some of the files that come bundled with it. These are the *.PRN files, and they include data that shows the elevation angle of incoming signals as a percentage of the overall number of band openings. Select the file appropriate to your location and path(s) of interest. Table 1 shows a detailed breakdown of antenna gains (in dBi) generated by *EZNEC* for the two example antennas, combined with the elevation angle data for the Chicago to Europe path from the *HFTA* *.PRN files. In this case, "w9-il-eu.prn" is the propagation file name.

The data in the table shows that during 8.3% of the band openings from Chicago to Europe on 80 m, signals come in at an elevation angle of 10°. At that elevation angle,

¹Notes appear on page 50.

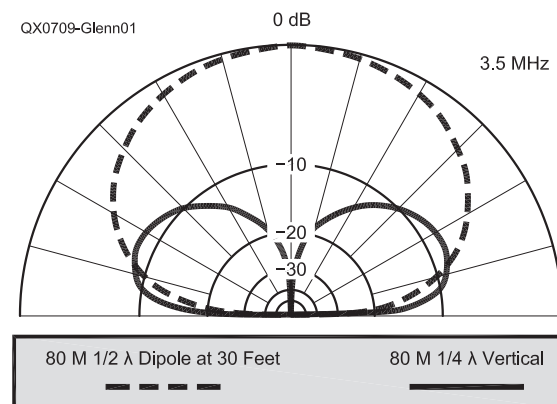


Figure 1 — Elevation pattern comparisons generated by *EZNEC* between the 30 foot high dipole at broadside and the vertical, both tuned for 80 meters. These plots were generated using real *MININEC* grounds. In the case of the vertical, this approximates a ground system using 120 radials to essentially eliminate near-field ground losses from this comparison. Details of the models used are included on the author's Web site: www.k9so.net.

320 Castlewood Ct
Palatine, IL 60067
k9so@arrl.net

Table 1
80 m Comparison Data Chicago-
Europe Path (Vertical is Ant1 and
Dipole is Ant2)

Elevation (Degrees)	Ant #1 (dBi)	Ant #2 (dBi)	Propagation Data (% of openings)
1	-16.47	-24.34	0.1
2	-11.1	-18.34	4.1
3	-8.21	-14.85	6.1
4	-6.31	-12.38	3.7
5	-4.94	-10.47	3.9
6	-3.9	-8.92	3.7
7	-3.09	-7.61	2.1
8	-2.44	-6.49	1.4
9	-1.9	-5.5	5.1
10	-1.45	-4.62	8.3
11	-1.08	-3.83	7.4
12	-0.77	-3.12	3.7
13	-0.5	-2.46	2.3
14	-0.28	-1.86	2.9
15	-0.09	-1.3	6.7
16	0.07	-0.79	6.5
17	0.2	-0.31	5
18	0.31	0.14	3.1
19	0.41	0.57	2.7
20	0.48	0.96	3.7
21	0.53	1.34	5.2
22	0.57	1.69	3.5
23	0.6	2.02	2.8
24	0.62	2.34	2.2
25	0.62	2.64	1.5
26	0.61	2.92	1.1
27	0.59	3.19	0.3
28	0.56	3.45	0.2
29	0.53	3.7	0.2
30	0.48	3.93	0.3
31	0.42	4.15	0.1
32	0.36	4.37	0.1
33	0.29	4.57	0.1
34	0.21	4.77	0
35	0.12	4.96	0
36	0.03	5.13	0
37	-0.07	5.31	0
38	-0.18	5.47	0
39	-0.29	5.63	0
40	-0.42	5.78	0
41	-0.54	5.92	0
42	-0.68	6.06	0
43	-0.82	6.19	0
44	-0.97	6.32	0
45	-1.13	6.44	0
46	-1.29	6.56	0
47	-1.46	6.67	0
48	-1.63	6.78	0
49	-1.82	6.89	0
50	-2.01	6.99	0
51	-2.2	7.08	0
52	-2.41	7.17	0
53	-2.62	7.26	0
54	-2.84	7.34	0
55	-3.07	7.42	0
56	-3.31	7.5	0
57	-3.55	7.57	0
58	-3.81	7.64	0
59	-4.07	7.71	0
60	-4.35	7.77	0

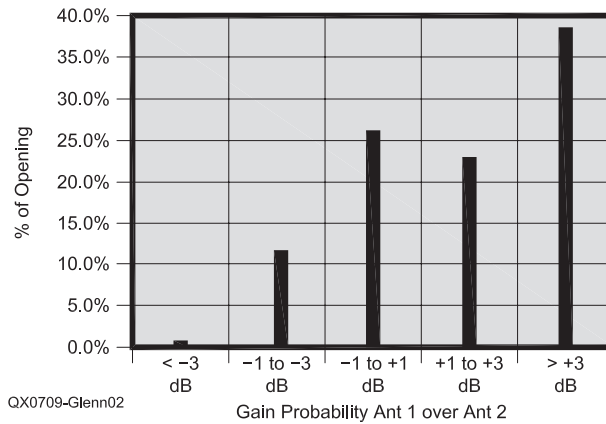


Figure 2 — Gain-Probability comparison into Europe for 80 m $\frac{1}{4} \lambda$ vertical (Ant1) versus 80 m broadsided dipole at 30 feet (Ant2).

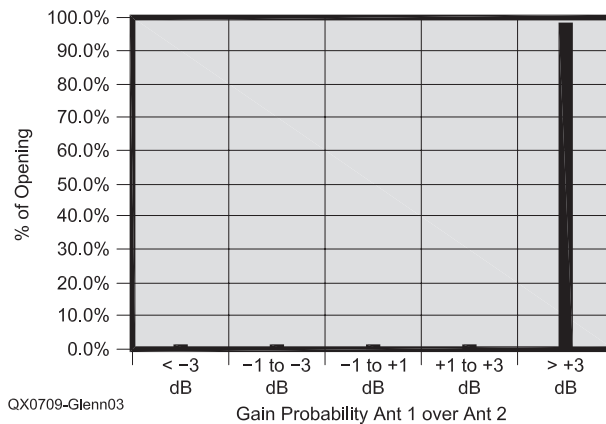


Figure 3 — Gain-Probability comparison into South Africa for 80 m $\frac{1}{4} \lambda$ vertical (Ant1) versus 80 m dipole (Ant2) at 30 feet and pointed at Europe. Here, the vertical is the clear winner.

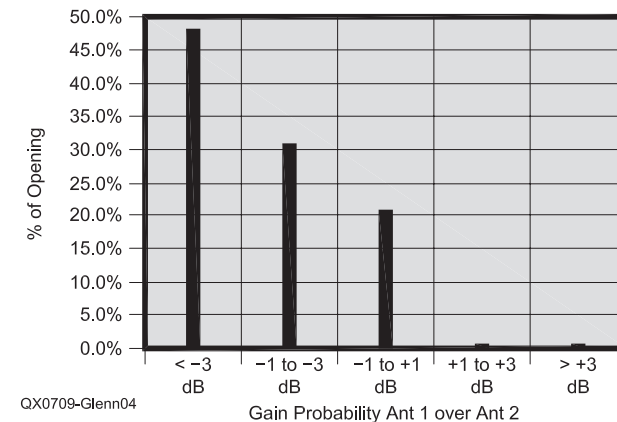


Figure 4 — Gain-Probability comparison for the path between Europe and Chicago for 20 m $\frac{1}{4} \lambda$ vertical (Ant1) versus 20 m broadsided dipole at 30 feet (Ant2). This shows that the vertical has negative gain probability over the dipole and that the dipole would be better.

the vertical has a 3.17 dB advantage over the 30 foot high dipole at broadside, and is clearly the better choice. During 1.5% of the openings, though, the signals will come in at an elevation angle of 25°. Here, the broadside dipole has an advantage of 2.02 dB. Assessing the relative importance of these numbers is where the Gain-Probability charts come in.

Generation of the gain-probability data is done using a simple spreadsheet calculator. For convenience, I have posted an example spreadsheet at www.k9so.net.² You will need to input the propagation elevation data used by *HFTA* for your location into this spreadsheet. The example spreadsheet will require you to input the data in the same format as shown. You can either do that manually or use the IMPORT DATA feature of Microsoft *Excel* to import the data into a temporary spreadsheet and then copy and paste.

The gain-probability output graph for the example antennas is plotted in Figure 2. Here, Ant1 is the vertical and Ant2 is the 80 m dipole at 30 feet. Gain-Probability data is all about designing antennas to maximize the probability of success over a given path on a given frequency. The G-P chart clearly shows that for a whopping 61.5% of the band openings into Europe, the vertical will be the clear winner by 1 dB or more (sum of the two right hand columns). For 38.5% of the openings the vertical will outperform the broadsided dipole by more than 3dB, and 26.2% of the time they will be about equal (within 1 dB). The decision is now clear: 87.7% of the time the vertical will be as good as or better than a 30 foot high dipole aimed directly at Europe. For much of the time it will be significantly better.

The G-P spreadsheet allows you to easily run this comparison for different parts of the world, too. Compare the antennas for propagation into South Africa using "w9-il-af.prn," for example. If you live in Fiji, use "3D2-AF.prn" instead. There are literally hundreds of propagation paths included on that *Antenna Book* CD.

See how the vertical compares to a dipole at 40 feet instead, if you could put that up. G-P will also let you compare a "sloper" to a vertical or an inverted V to a full wave loop. How will changes in your antenna farm relate to the probability of success on the air? The antennas simply have to be modeled in *EZNEC* and the data inserted into the G-P spreadsheet.

As a second example, let's use G-P to evaluate how a fixed 80 m dipole at 30 feet aimed at Europe might perform into Africa (52° off of the direction to Europe from Chicago) and compare it to a vertical's omnidirectional pattern. You would need to

calculate the *EZNEC* elevation data at 52° off broadside for the dipole, and then include the propagation data for Chicago to South Africa ("w9-il-af.PRN" file). Import both sets of data into the G-P spreadsheet. The dramatic G-P result is shown in Figure 3.

The vertical was looking pretty good for my backyard 80 m antenna, given the fact that I couldn't mount a dipole any higher than 30 feet, and certainly would not be able to turn it.

As a third example, consider that as frequency increases, the 30 foot height of the (retuned) dipole becomes a higher percentage of a wavelength. We all know that higher is better and by the time we reach 20 m, the results clearly favor the 30 foot high dipole. First, generate the elevation data in *EZNEC* for the azimuth angle of interest. Then paste in the *.PRN file for 20 m for the path from your QTH to the desired DX location. On 20 m, the dipole at broadside is predicted to be better than the vertical during 79.2% of the openings into Europe from Chicago. The 20 m G-P comparison graph is shown as Figure 4.

Use Gain-Probability to assess changes to your system in terms of the probability of producing a stronger signal where you want it. Is it really worth raising that dipole up another 10 feet? Would a delta loop be better?

Learning how to use *EZNEC* is easy and is all part of the fun. Using the Gain-Probability


approach will give you great predictive insight into the performance of your proposed or existing antenna systems. Detailed instructions for the *EZNEC* software program are given in *The ARRL Antenna Book*. An example G-P spreadsheet is posted at www.k9so.net.

Incidentally, using Gain-Probability data, I ended up with elevated trap verticals for 80 to 30 meters and 30 foot high dipoles for the higher frequency bands. That was the reality for my backyard. Use G-P to see what you can do to maximize your signals where you want them.

Fred Glenn, K9SO, has BS and MS degrees in Electrical Engineering and was first licensed in 1964 as WA9MVZ. He is an active CW DXer, an Extra-Class licensee, and a Life Member of the ARRL.

Notes

¹R. Dean Straw, N6BV, Ed., *The ARRL Antenna Book*, 21st Edition, 2007. *The ARRL Antenna Book* is available from your local ARRL dealer, or from the ARRL Bookstore, ARRL order no. 9876. Telephone toll-free in the US 888-277-5289, or call 860-594-0355, fax 860-594-0303; www.arrl.org/shop; pubsales@arrl.org.

²The example Microsoft *Excel* spreadsheet file and the *EZNEC* antenna model files mentioned in this article are available for downloading from the *QEX* Web site. Go to www.arrl.org/qexfiles and look for 9x07 Glenn.zip. 

WANTED: C++ PROGRAMMER

We need a part time C++ programmer who likes to work at home but lives in the Orange County/Los Angeles area. We need to automate our test procedures, which involve RF transmitters and receivers to determine if production products pass or fail. Tests include determining RF output, current consumption, PLL lock range, frequency accuracy, and receiver sensitivity by checking each section with a fully or semi-automated test program.

We need the following:

- Someone with experience writing Visual C++ programs allowing the PC to control the test equipment with RS-232 and or GPIB.
- You need to be familiar with RF test equipment such as spectrum analyzers, oscilloscopes, signal generators, and frequency counters.
- Be familiar with troubleshooting of RF and digital circuits.
- Be able to control relays, switches, etc. through PC I/Os with Visual C++.
- Have TCP/IP programming experience with Visual C++.
- Have CGI programming experience in any language.
- Robotic experience a plus.
- We would like to see examples and or samples of your past work.



COMMUNICATIONS SPECIALISTS, INC.

426 WEST TAFT AVENUE • ORANGE, CA 92865-4296

714.998.3021 • FAX 714.974.3420

US & CANADA 800.854.0547 • FAX 800.850.0547

www.com-spec.com E-mail: spence@com-spec.com

Circularly Polarized Aimed Satellite Antennas

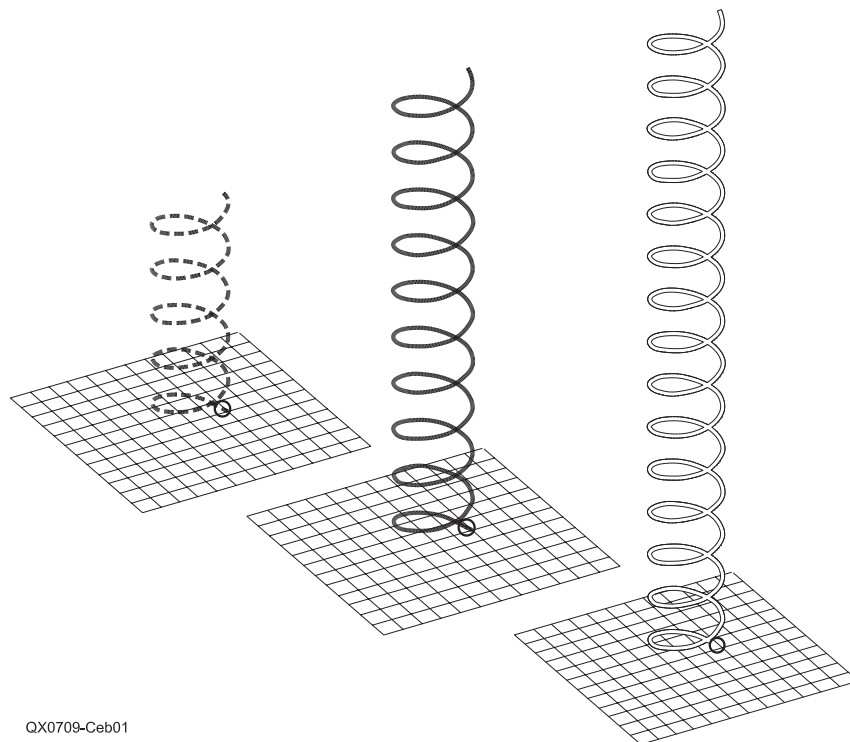
Among steerable satellite antennas, we generally have two options. The axial-mode helical antenna has become a favorite among some satellite and other operators, especially at UHF (435 MHz and up). However, the crossed and turnstiled Yagi remains in favor among other operators. Let's explore these options, at least to a small extent.

The Axial-Mode Helical Antenna

The following notes on axial-mode helices summarize parts of my longer study "Notes on Axial-Mode Helical Antennas in Amateur Service," which appeared in the 2005 *Proceedings of the Southeastern VHF Society*. There I examined NEC-4 models of 5, 10 and 15 turn helices, both over perfect ground and over ground plane wire-grid screens. Figure 1 shows the general outline of the models, as well as their relative sizes, using a $1.2 \lambda \times 1.2 \lambda$ screen that is 1λ above ground. The test frequency is 299.7925 MHz, where 1 meter = 1λ . You may scale the designs for other frequencies by using the ratio of 299.7925 to the new frequency times each of the critical dimensions, including the wire diameter but excluding the pitch angle. For uniformity, all models point straight up.

The need for such a study is a function of the classical literature on axial-mode helices. Researchers tend to treat the antenna as a broadband array and extrapolating data useful to amateur spot frequency use is somewhat daunting. (See the final notes for some references, especially VE3NPC's more recent empirical measurements.) Modeling this type of antenna also requires considerable care.

Perhaps the two most critical dimensions are the *pitch angle* and the *circumference*. In fact, basic helix theory tends to restrict axial-mode operation of the helix to pitch angles between 12° and 14° . The smaller the pitch angle (within limits), the higher will be the gain of a helix, given a fixed number of turns. As well, various texts restrict the circumference to ranges from either 0.8λ to 1.2λ (Kraus) or from 0.75λ to 1.33λ (Balanis). The number of turns in a helix is up to the builder, since gain (for any given pitch and circumference) rises with the number of turns. Furthermore, selection of a wire diameter is also a builder choice. Although not mentioned in any serious way in most literature, conductor size does make a difference to helix performance. The larger the wire diameter as a fraction of a



QX0709-Ceb01

Figure 1 — Approximate proportions of 5, 10 and 15 turn helices over ground planes 1.2λ per side.

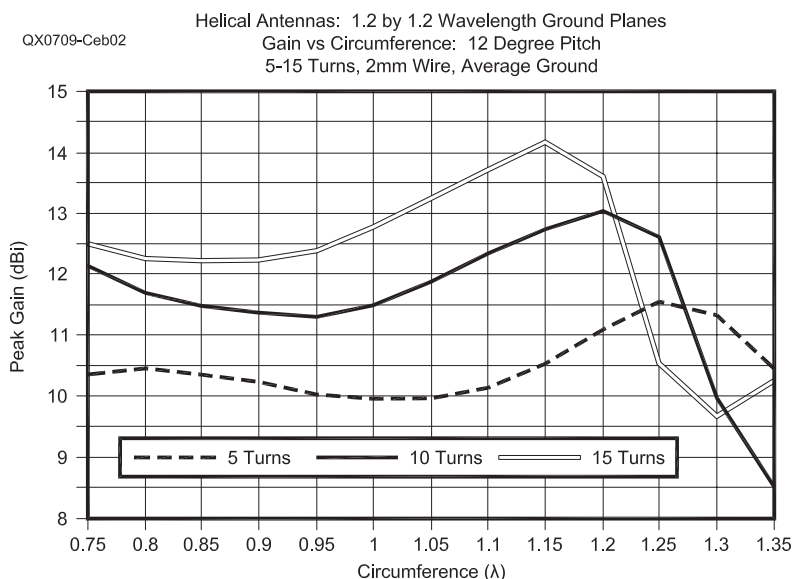


Figure 2 — Modeled gain of 5, 10 and 15 turn helices over ground planes 1.2λ per side.

wavelength, the higher the gain for an otherwise fixed helix size. The sample models that we shall explore use 2 mm diameter wire.

There are two major issues with modeling an axial-mode helix. The first issue arises from the fact that *NEC* must use straight wires to simulate a circle. The difference between the circumference of a circle and that of a polygon inscribed within the circle only reaches relative insignificance as the number of sides on the polygon passes about 16 or so. A 16 sided regular polygon inscribed within a circle has a circumference that is about 99.4% that of the circle. For a more rounded number in my *NEC-4* helix models, I used 20 segments per turn. Using 2 mm diameter wire, the segment length-to-radius ratio remained well above modeling minimums.

The second major issue involves the reported vs the actual gain of the helix models. For both the perfect ground and the wire-grid plane models, I assigned the source to the first segment, the one in contact with the ground surface. Because this segment does not have equal length wire segments on either side of the source segment, the initial reports of gain and source resistance will be erroneous but correctable. By moving the source segment to other segments, I ascertained that applying standard Average Gain Test (AGT) adjustments to the gain values would yield very reasonable corrected reports.

Figure 2 shows the results of gradually increasing the circumference of 5, 10 and 15 turn helices (12° pitch, 2 mm diameter

wire) over wire-grid planes that are 1.2 λ on a side and 1 λ above average ground. The gain curves are similar to those produced by the *NEC-2* models created by Paolo Antoniazzi, IW2ACD, and Marco Arecco, IK2WAQ, in "Measuring 2.4 GHz Helix Antennas," *QEX*, May/June, 2004. The major difference is that the ground beneath the helix in my models yields a moderate rise in gain below the generally accepted optimal circumference range. Both sets of curves show that as the helix grows longer, the optimum circumference for maximum gain decreases. Exceeding the optimal circumference results in a steep loss of gain potential. With a constant pitch angle (12°), the peak-gain circumference decreases by about 0.05 λ with each 5 turn increase in helix length.

The dimensions for three sample axial-mode helical directive arrays appear in Table 1. The arrays correspond to 12° pitch 5, 10 and 15 turn antennas at 299.7925 MHz, where 1 meter = 1 λ. The modeled performance data appears in Table 2. The gain values have been corrected for the average gain test (AGT) score, and the raw reports will be somewhat lower. The peak gain of the helices is about 11.7, 13.0, and 14.2 dBi for the 5, 10 and 15 turn antennas, respectively. Note that the gain increases almost linearly with the increase in the number of turns. This fact is important to keep in mind when comparing axial-mode helices with alternatives to them as circularly (or nearly circularly) polarized antennas.

Modeling the helix itself is simplified by

the GH entry in *NEC*. However, the *NEC-2* and the *NEC-4* versions of that geometry command differ radically. Therefore, modelers need to consult the appropriate manual for guidance. (The commands are available in *NEC-Win Pro* and in *GNEC*, by Nittany-Scientific, with entry-formation assistance screens.) An alternative method of creating a helix appears in *EZNEC Pro*, which allows helix creation as a set of individual wires batch-created by entries similar to those used in the GH command. The termination of the helix on perfect ground is simple enough, but mating the lowest wire end to a wire-grid junction may call for the modeler to displace the wire end to meet the closest junction. The size of the elevated ground-plane surface for a given helix does make a difference in the performance of the antenna, although gain changes are small. There is an optimal size that varies with the length of the helix. The ground screens in the sample models are close to optimal.¹

An axial-mode helical antenna rarely yields perfect circular polarization. Instead, it yields elliptical polarization, with a *major* and a *minor axis* and a *tilt angle*. The antennas approach perfect circularity most closely along the axis of the helix. Applications needing something closer to circular perfection tend to

¹Models for the antennas discussed in this article are available in *EZNEC* format at the ARRL web site. Go to www.arrl.org/qexfiles and look for **9x07_AO.zip**.

Table 1
Dimensions of three sample axial-mode helical directional arrays for 299.7925 MHz. All dimension in meters or in wavelengths. Wire diameter = 2 mm. Helix pitch angle (α) 12°.

Number of turns	Circumference λ	Total Length λ
5	1.25	1.33
10	1.20	2.54
15	1.15	3.66

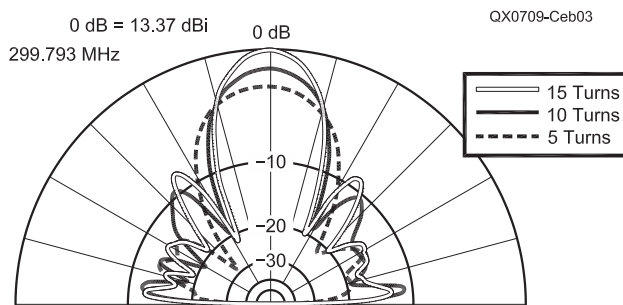


Figure 3 — Comparative elevation patterns of 5, 10 and 15 turn helices over ground planes 1.2 λ per side

Table 2
Modeled *NEC-4* relative performance of the sample axial-mode helices. All gain values are corrected for the average gain test (AGT) score. Raw reports will be lower.

Number of Turns	Gain (dBi)	Beamwidth (Degrees)	Sidelobe Ratio (dB)	R-H Gain (dBic)	L-H Gain (dBic)	Source Impedance Resistance (Ω)
5	11.69	44	-10.5	11.53	-3.19	314
10	13.03	33	-8.0	13.02	-13.16	312
15	14.16	28	-7.8	14.16	-13.48	316

work with quadfilular designs, although they are impractical for amateur satellite service. The sample models improve their circularity with increased length. More pertinent to amateur use is the fact that an axial-mode helix does not produce a perfect single-lobe pattern. Figure 3 shows the total field patterns of the 5, 10 and 15 turn helices over an elevated ground screen. In each case, we can see a considerable collection of side lobes. Each model uses the circumference that produces the best gain, but that circumference does not yield the lowest level of side lobes. Reducing the circumference produces lower gain (from 1 to 2 dB, depending upon the length of the helix), but results in a cleaner pattern. Circumferences below about 0.85λ rarely have any sidelobes at all through the 15 turn limit in my investigation.

As well, there are remnants of opposite-direction polarization within the total field of the axial-mode helix. Figure 4 shows the dominant right-hand polarized component of a 15 turn helix over a ground-screen elevated above average ground. The left-hand component is down by 25 dB, with some of the lower lobes being composed mainly of left-hand components. All of these facets of axial-mode helix performance have a bearing on the sensitivity of such antennas to off-axis signals, whether at high or low angles relative to the axis that marks the centerline of the helix. How much side lobe and oppositely polarized lobe suppression is enough, of course, you must determine based on your application and your local circumstances.

These notes have not addressed the question of actually constructing a helical antenna. Chapter 19 of *The ARRL Antenna Book* provides some of the general schemes used. For UHF, the most common technique is to use a nonconductive central shaft with periodic side projections to support the helix turns at critical points. (Fowler also uses a conductive center support rod with no degradation of performance.) The number of supports per turn depends upon numerous factors, including the inherent stiffness of the wire or tubing used to form the helix. A central shaft has a mechanical advantage by allowing attachment to the ground-plane screen, cup or grid. Hence, the wire turns do not experience much stress, except for the inevitable attachment to a connector. Standard references give the impedance as 140 times the helix circumference in wavelengths. However, the impedance will vary with the helix structure at the terminating end and with the diameter in wavelengths of the element wire. As the impedance varies, so too will the matching method selected for use with the coaxial cable. In such applications, the coax used for the main feed line may be 50Ω , or (for those using surplus solid sheath varieties) 75Ω .

The dimensions for an axial-mode helical

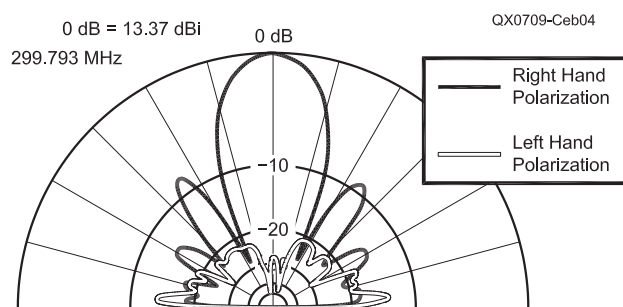


Figure 4 — Right-hand and left-hand polarized components of the elevation pattern of a 15 turn helix over a ground plane 1.2λ per side.

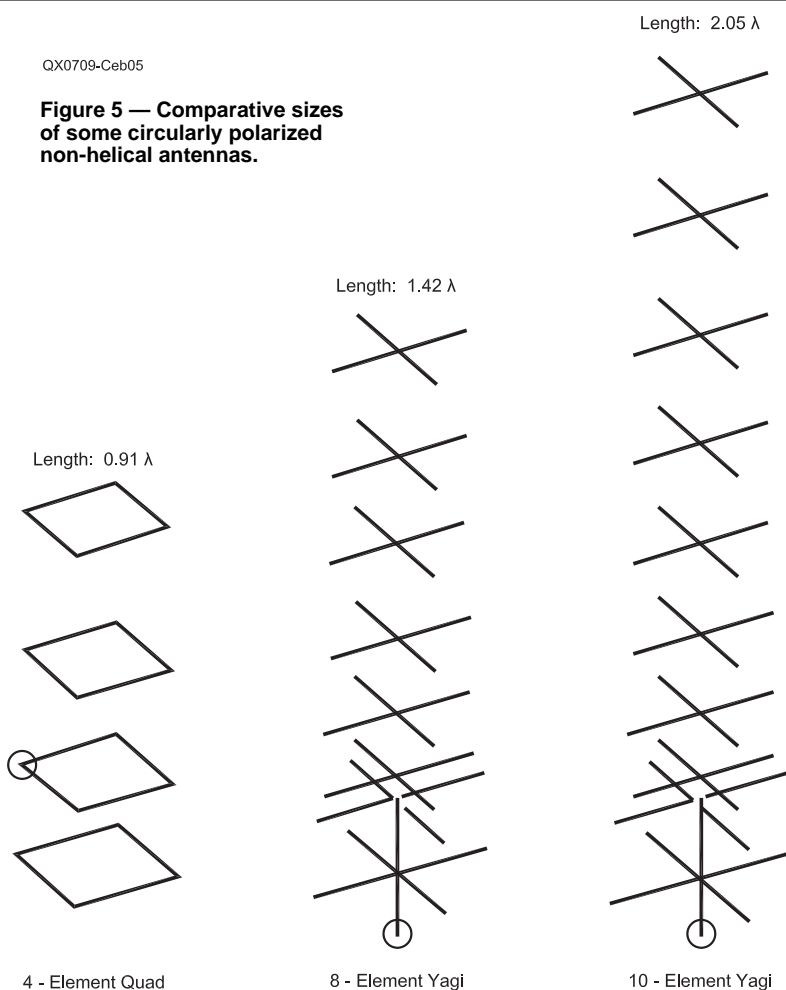


Figure 5 — Comparative sizes of some circularly polarized non-helical antennas.

Table 3

Dimensions Defining a Helix

R = radius of the helix, wire-center to wire-center	
C = circumference of the helix	$C = 2 \pi R$
S = spacing between turns	$S = C \tan \alpha$
α = pitch angle	$\alpha = \tan^{-1} (S/C)$
N (or n) = number of turns	
L = axial length of helix	$L = n S$
D = conductor diameter	
L' = conductor length for a single turn	$L' = \text{SQRT}(C^2 + S^2) = C/\cos \alpha = S/\sin \alpha$

array are implicit in the set of design criteria to which we build. Hence, I have given only overall dimensions, although you may easily derive more specific dimensions from the graphs shown and the basic trigonometry for the design work. Table 3 gives dimensions — many of which are interdependent — that define a helix.

All dimensions refer to center-to-center distances relative to the wires. The last two items in the list are relevant to the physical planning of the helix design.

If these notes give the impression that the axial-mode helix is somewhat imperfect, the impression is correct. However, it is not so far from perfect to bar its effective use in satellite applications. The antenna originated as a broadband array and has been pressed — sometimes uncritically — into spot-frequency or narrow-band uses. Understanding the fundamental properties of axial-mode helices in this context is an essential ingredient to producing an antenna that fulfills its promise.

Alternative Parasitic Arrays

An alternative to the axial-mode helical array is a parasitic array with turnstiled or quadrature fed drivers. Up to a point — but not necessarily beyond that point — such arrays offer some advantages over helical arrays. Not the least of these advantages is our familiarity with the construction techniques involved in building them and matching them to standard coaxial cable feed lines.

Unlike the helix and its design equations, most parasitic arrays are designed by model or experiment — or both — for a certain level of performance at a given frequency, within some overall size constraint. Therefore, we shall offer some dimension tables for our samples without in the least claiming them as the best possible designs. The goal will be to note some significant differences between parasitic and helical arrays designed for circular polarization. The design models are for 299.7925 MHz to coincide with the helix designs that we have so briefly surveyed. Like the helices, the parasitic arrays can be scaled to other frequencies.

When most folks think of parasitic arrays with circular polarization (or an approxi-

mation thereof), the *crossed Yagi* comes to mind. Although that antenna is certainly one of our alternatives, it is not the only one. Neglected is the *quad beam*, which we may convert to circular polarization without adding any further elements beyond those needed for ordinary or linear polarization.

Figure 5 shows three of our samples to illustrate their comparative sizes. For moderate gain levels, the parasitic arrays have boom lengths that are much shorter than corresponding helical arrays. For example, a 10 turn helix with a gain of about 13 dBi is almost a half-wavelength longer than a 10-element Yagi with about a half dB higher gain. However, we have noted that helices tend to increase in gain almost (but not quite) linearly with added turns, while adding more directors to a parasitic array results in a decreasing gain-per-new-element value. Hence, there is a crossing point at which the helix shows more gain than a parasitic array of the same overall length.

That crossover point most likely occurs when the arrays approach 5λ in overall length.

The first non-helical candidate is a 4-element quad, the dimensions for which appear in Table 4. The quad is only 0.91λ long from reflector to the last director. Using 1-mm diameter wire for the elements, it has a gain of 10.6 dBi when placed 1λ above average ground. The quad's beamwidth is 58° . The performance of the quad is more completely summarized in Table 5, along with the other sample candidates as alternatives to the helix. Two sets of values are especially significant. One is the high value of front-to-sidelobe ratio (listed as a negative value of dB below the main lobe gain value), when compared to the much smaller ratio shown by the helices. In fact, Figure 6 shows the elevation patterns for the quad overlaid with two of the Yagis for direct comparison with the helix patterns shown in Figure 3.

Because a quad allows some flexibility

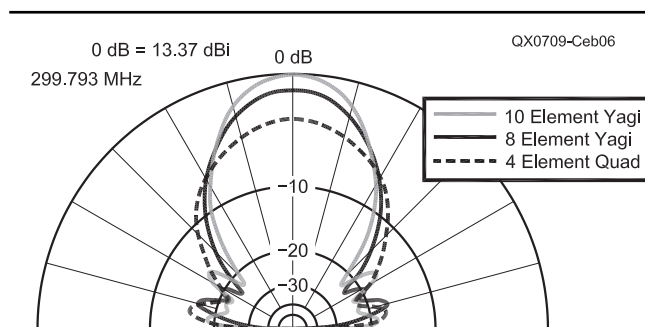


Figure 6 — Comparative elevation patterns of a circularly polarized quad and two circularly polarized Yagis: a 10-element Yagi, an 8-element Yagi and the 4-element quad.

Table 4

Dimensions of a 4-element circularly polarized quad array. All dimension in meters at 299.7925 MHz or in wavelengths. Wire diameter = 1 mm.

Element	Circumference	Side Length	Space from Reflector
Reflector	1.084	0.271	—
Driver	1.028	0.257	0.240
Dir 1	0.964	0.241	0.540
Dir 2	0.948	0.237	0.910

Table 5

Modeled relative performance of the parasitic arrays at 300 MHz. Quad gain values are corrected for the AGT score. Raw reports will be lower.

Array	Gain (dBi)	Beamwidth (Degrees)	Sidelobe Ratio (dB)	R-H Gain (dBic)	L-H Gain (dBic)	Source Impedance $R \pm j X \Omega$
4-El Quad	10.58	58	-11.9	10.58	-18.21	49.7 - j 0.0
8-El Yagi	12.58	44	-14.9	12.57	-13.88	44.7 + j 7.7
10-El Yagi	13.57	40	-15.5	13.54	-9.04	44.7 + j 7.0
12-El Yagi	14.17	37	-14.9	14.15	-8.69	44.5 + j 7.0

in the placement of the driver without undue adverse effects on the array gain, we may arrive at a single source impedance of about 95 Ω resistive. Hence, a $\lambda/4$ section of 93 Ω cable forms a proper phase line run between successive corners of the driver. The result is a circularly polarized antenna. This technique first came to my attention in a sample model that Brian Beezley, K6STI, included in the model collection that accompanies his *AO* program. We should not run the phase-line coax parallel to the active element. Hence, it is likely that we would use a $3\lambda/4$ section of line running from one corner to the center nonconductive boom and back to the adjacent corner. We may reverse the polarization simply by connecting the main feed line at one or the other end of the phase line. Higher isolation feeding methods have appeared from time to time. For this simple system, the result is a 50 Ω impedance for the main feed line. The 4-element quad in the outline sketch has a 2:1 50 Ω SWR bandwidth of more than 25 MHz, which eases the problems associated with construction variables. (Redesigning the antenna for fatter elements would yield an even larger bandwidth.) Obviously, longer versions are possible for the quad if you desire more gain. However, in our survey of alternatives, let's turn now to some Yagi designs.

Table 6 provides the dimensions of three sample Yagis, all derived indirectly from normal Yagis of DL6WU vintage. The short 8-element version is 1.42λ long, while the 10-element version has a boomlength of 2.05λ . The 12-element version is 2.60λ long. The last sample Yagi appears mostly to demonstrate that as we add new directors, the increase in gain dwindles per added element. Nevertheless, the 14.2 dBi gain of the 12-element Yagi compares well to the peak gain of the 15 turn helical antenna with a total length of over 3.6λ .

Since *NEC* uses only axial currents in calculating the antenna fields, you may model crossed Yagis with each crossed parasitic element pair joined at the center. If there are any interactions, they will not show in the model. In practice, it is likely that one will use a pair of independent linear elements. Since the drivers require separation, if only by a small distance, to establish their independence, it will not harm construction to use the same separation between parasitic elements. The modeled dimensions in Table 6 presume the use of a nonconductive boom.

Table 5 summarizes the potential performance of the Yagis. The total field patterns for the 8 and 10-element versions appear in Figure 6, along with the quad. I omitted the 12-element Yagi lest the morass of pattern lines become unreadable. Each Yagi shows close to the same front-to-sidelobe ratio — about 15 to 16 dB. As well, all of the Yagis show the same high ratio of right-hand gain to left-hand gain.

Figure 7 shows the polarized components of the 10-element Yagi for illustration of the difference. You may wish to compare this pattern with Figure 4, the comparable pattern for a 15 turn helical design.

All of the Yagis use identical feed systems to establish quadrature and a match to a 50 Ω feed line. In this particular design, the single driver source impedance is 50 Ω. Hence, the turnstile phase-line is also 50 Ω. The result-

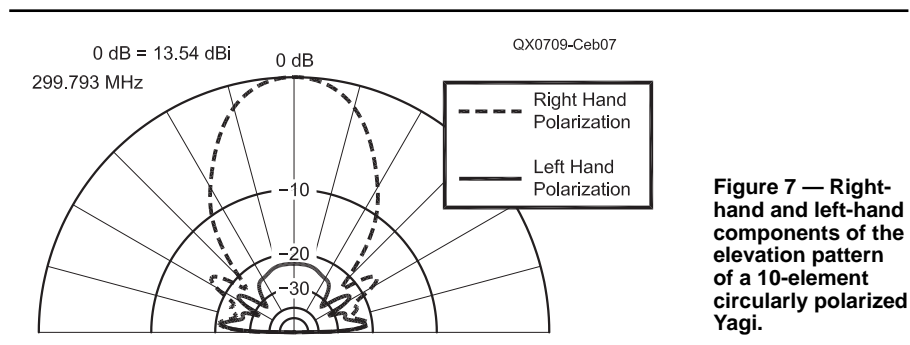


Figure 7 — Right-hand and left-hand components of the elevation pattern of a 10-element circularly polarized Yagi.

Table 6

Dimensions of three sample cross-element Yagis. All dimension in meters at 299.7925 MHz or in wavelengths. Wire diameter = 12.7 mm (0.5 inch or 0.0127λ). Each element entry represents two elements at right angles to each other.

A. 8-Element Yagi

Element	Element Length	Spacing from Reflector
Reflector	0.469	—
Driver	0.452	0.205
Dir 1	0.404	0.267
Dir 2	0.398	0.437
Dir 3	0.392	0.640
Dir 4	0.386	0.876
Dir 5	0.382	1.141
Dir 6	0.367	1.424

B. 10-Element Yagi

Element	Element Length	Spacing from Reflector
Reflector	0.469	—
Driver	0.452	0.205
Dir 1	0.404	0.267
Dir 2	0.398	0.437
Dir 3	0.392	0.640
Dir 4	0.386	0.876
Dir 5	0.375	1.141
Dir 6	0.369	1.424
Dir 7	0.363	1.731
Dir 8	0.356	2.052

C. 12-Element Yagi

Element	Element Length	Spacing from Reflector
Reflector	0.469	—
Driver	0.452	0.205
Dir 1	0.404	0.267
Dir 2	0.398	0.437
Dir 3	0.392	0.640
Dir 4	0.386	0.876
Dir 5	0.375	1.141
Dir 6	0.369	1.424
Dir 7	0.363	1.731
Dir 8	0.356	2.052
Dir 9	0.350	2.347
Dir 10	0.350	2.607

ing impedance presented to the main feed line is close to 25Ω . A length of 35Ω line (or a pair of 75Ω lines in parallel) provides the required match for a 50Ω main feed line. As with the quad, you may change polarization simply by swapping phase-line ends for the junction with the matching section and main feed line. Removing the phase-line altogether converts the array to linear polarization, with the unfed elements having little if any effect on operation in this mode.

To center the design frequency within the overall 2:1 50Ω SWR passband, the line lengths for both the phase line and the matching line are not true quarter wavelengths electrically. The electrical length of the phase-line is a bit over 0.22λ , while the matching line is close to 0.215λ . The 2:1 SWR passband, as illustrated in Figure 8, runs between 270 and 330 MHz, a 60 MHz spread that should make home construction less critical. However, as with any antenna based upon turnstiled dipoles, the SWR bandwidth will be far wider than the operating bandwidth for which the patterns hold their desired shape. Hence, it remains good design practice to optimize the performance of the crossed Yagis for the desired range of operation. An SWR meter alone is not sufficient to optimize any circularly polarized antenna.

The physical implementation of a parasitic design will require considerable effort. Never assume, but actually measure the actual velocity factors of the lines. Construction will require close attention to line dress and to the potential effects of any connector installed. For UHF and upward, one should use certified connectors rather than hamfest specials and bargains. Even the solder lumps that close the wire loops of the quads can create detuning effects from 70 cm upwards. Whether you are building a helix or a Yagi, the casual and careless construction techniques that are harmless at HF become potential plagues to UHF antennas.

Conclusion

As always, we have looked at alternatives for antennas meeting a certain set of needs. In this case, we selected satellite communications, with its need for circular polarization — or as closely as we may approximate circular polarization using standard construction techniques. The key alternatives for antennas that we steer with respect to both azimuth and elevation are axial-mode helical arrays and turnstiled parasitic arrays.

Both techniques will produce able arrays. Our survey and samples do not exhaust the designs that we may bring to bear on the communications need. However, they should open the door to relevant considerations in

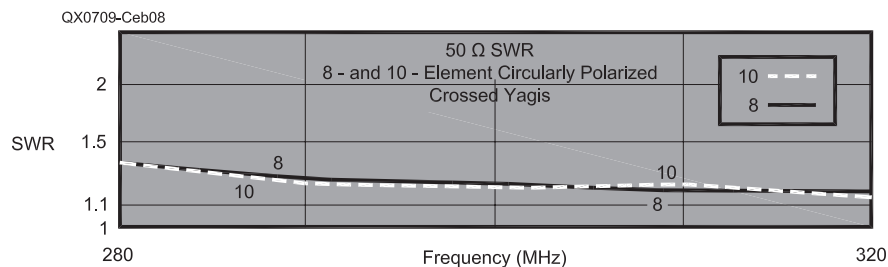


Figure 8 — $50\text{-}\Omega$ SWR curves for the 8 and 10-element circularly polarized Yagis.

making a choice between the two major routes to circularly polarized antennas and to some of the considerations when designing an antenna within either general category.

References

There are a number of background sources for information on axial-mode helices. The following list is a start, with most of the items having extensive bibliographies.

J. D. Kraus, *Antennas*, 2nd Ed. (1988), pp 300-310.
 H. E. King and J. L. Wong, "Helical Antennas," Chapter 13 of *Antenna Engineering Handbook*, 3rd Ed., R. L. Johnson, Ed. (1993), pp 13-1 ff.

D. Emerson, AA4FV, "The Gain of an Axial-Mode Helix Antenna," *The ARRL Antenna Compendium, Vol. 4* (1995), pp 64-68.
 C. A. Balanis, *Antenna Theory*, 2nd Ed. (1997), pp 505-512.
 W. L. Stutzman and G. A. Thiele, *Antenna Theory and Design*, 2nd Ed. (1998), pp 231-239.
 P. Antoniazzi, IW2ACD, and M. Arecco, IK2WAQ, "Measuring 2.4 GHz Helix Antennas," *QEX*, May/June 2004, pp 14-22.
 L. B. Cebik, W4RNL, "Notes on Axial-Mode Helical Antennas in Amateur Service," *Proceedings of the 2005 Southeastern VHF Society Meeting*, pp 82-121.
 C. Fowler, VE3NPC, "Real World Helix Antenna Measurements," *The AMSAT Journal*, May/June, 2006.



ELECTRONICS OFFICER TRAINING ACADEMY

The Complete Package To Become A Marine Radio Officer/Electronics Officer

ELKINS, with its 54-year history in the radio and communications field, is the only school in the country providing all the training and licensing certification needed to prepare for the exciting vocation of Radio Officer/Electronics Officer in the Merchant Marines.

Great Training | Great Jobs | Great Pay



Call, Fax or Email for More Information:

ELKINS Marine Training International
 P.O. Box 2677; Santa Rosa, CA 95405
 Phone: 800-821-0906, 707-792-5678
 Fax: 707-792-5677
 Email: info@elkinsmarine.com
 Website: www.elkinsmarine.com

Letters to the Editor

Voltage-Magnitude Impedance Measurement (Jul/Aug 2007)

With regard to Figure 3 on page 15: For the equation given for “resistor inductance”, I calculate the result to be 0.104 microhenrys, or, 10.4 nanohenrys, not 13 nanohenrys. Also, in the equation for R_0 , I believe the denominator of the radicand incorrectly shows the value of the inductance instead of the capacitance.

—73, Jim Olsen, W3KMN, 5905 Landon Ln, Bethesda, MD 20817; w3kmn@aol.com.

Hi Jim,

Thank you for pointing out my errors in Figure 3 of the Voltage-Magnitude Impedance Measurement article. I agree that the numbers provided give a calculated inductance of 10.4 nH rather than 13 nH.

I had modified the equation given originally by Dr. Eddy, based on the equation for inductance of a straight wire that I found in F. E. Terman’s *Radio Engineer’s Handbook* as well as *The ARRL Handbook*. Then I failed to correct the calculated value, as given in the original manuscript.

In the equation for R_0 near the bottom of Figure 3, I missed an error made when the ARRL Graphics Department created that Figure. You are right that the value for C should have been 4.2×10^{-13} F. When I run through that final calculation, if I use the calculated values of 1.04×10^{-8} H and 4.2×10^{-13} F then I get an R_0 value of 236 Ω rather than the original 264 Ω .

—73, Larry Wolfgang, WR1B, QEX Editor; lwolfgang@arrl.org

Hi Jim,

I confess that I am quite red-faced with embarrassment, especially as Larry pointed out the problem with my original inductance of a straight wire equation early in his editing work on my article. Somehow I managed to overlook the loose end, for which I have no excuse.

I fear that much of this work on real 1/4-W resistor capacitance and inductance was done many years ago and my recollections of both measured parameters (using a Q-meter, and using extremely low value and extremely high value resistors for determining inductance and capacitance, respectively) and my own theoretical calculation (at the time) of L and C are blurry and based upon all too sketchy notes made at that time. Back then, I believed that the agreement between theoretical and measured Boella parameters was extremely good — perhaps even too good to be believable considering the crudeness of the experimental set-up.

I could weasel and say that in the real world these differences are no greater than the uncertain disposition of the resistor with the local ground plane. But I really cannot avoid taking responsibility for what surely appears on the surface to be an error in calculation, or measurement, or both. Because of the apparent agreement with the later network-analyzer measurements carried out by Les Besser (*RF Design*, July 1993, p 66, with unknown resistors in an entirely different set up), I have greater confidence in the measured 0.43 pF and 13 nH values than in my calculations (which may have been unknowingly skewed by my earlier measurements).

Before saying anything beyond this, I think I am obligated to repeat both my measurements and my theoretical estimates. To be sure I do not repeat any prior errors I think I should do this more carefully than is possible in a few days time.

[A few days later, in another e-mail, Dr Eddy continued:]

I repeated my earlier measurements, added to them, and between times tried to think over what was said (and not said) in the paper.

Larry and I both missed the failure to have the calculation jibe with the given formula. (We also failed to notice the misspelled “impedance” instead of impedance in the second line above the block, $R_0 \cong \sqrt{L/C}$, and the omission of any reference to Terman or Grover for the inductance calculation). But more importantly, I fear that the long ago measurements and their apparent agreement with crude, back-of-the-envelope estimates had acquired a misplaced aura of sanctity in my brain. I would nonetheless now argue that, on the basis of my ability to repeat them, the measurements themselves were quite accurate under the circumstances.

I adopted the following component lead-swallowing stratagem. On my Q meter and on a reference inductor I mounted brass tubing with an ID just able to “swallow” the resistor’s leads to with 2.5 mm of the resistor shell. The test resistor end of the tubing had a short section filed away so that the resistor (or a shorting wire the same diameter as the resistor’s wire leads) could be tack soldered in place. Basically, this configuration enabled me to make differential measurements, resistor-in versus resistor-out. I used resistors with a resistance very much smaller and very much larger than 270 Ω with the implied presumption that their distributed capacitance and inductance would be the same. For the very high resistance measurements, I mounted the resistor in parallel with an inductor resonant at the upper frequency limit of the VHF Q-meter. The brass, lead-swallowing

tubing was mounted so as to occupy the same position whether the resistor was inserted or not. I then adjusted the resonant frequency (with the Q-meter’s vernier tuning capacitor) to a suitable, easy-to-record value, with the resistor in place, and again with it removed. I measured the effective capacitance by noting the change in vernier capacitance setting required to regain resonance.

The inductance measurements were made similarly, but at a lower frequency, and with a resistor value smaller than the inductor’s series resistance. I substituted a shorting wire in place of the resistor with the two lead-swallowing sections of brass tubing butted against one another. Using the vernier capacitor, I noted the change in capacitance to maintain a constant resonant frequency. For dL and dC (changes in inductance and capacitance) small compared with L and C such that the dL dC cross term is negligible, the differential inductance is then given by $dL = dC / (L C)$.

I made the foregoing measurements (this time) with $R_1 = 100 \Omega$, and $R_2 = 6.8 \text{ k}\Omega$ using 5% 1/4-W Allen-Bradley resistors, arguing that the internal design of these resistors was sensibly identical with, say, that of a 270 Ω resistor. To the extent that is correct, I would argue that the foregoing measurements are accurate to something on the order of 5%. I repeated the measurements at several different frequencies to obtain independent estimates (different settings of the vernier and main tuning capacitor dials). These measurements showed no significant difference relative to my earlier experimental results (the published 0.43 pF and the 13 nH values, with now forgotten resistor values). Fortuitously or not, these measurements are roughly consistent with those published much later by Les Besser (using a much more expensive network analyzer in place of my antiquated Q meter!).

I hope that QEX readers understand that the theoretical analysis presented for estimation of resistor inductance and capacitance is no more than a back-of-the-envelope calculation running rough-shod over the complexities of butting reference resistors with only 5 mm separation available for soldering — not to mention the inductive and capacitive coupling between contiguous components and a possible ground plane, and so on.

In retrospect, I would argue that my initial gloating in having achieved what seemed to be a fortuitous agreement between experimental measurement and theoretical prediction was inappropriate. Agreement to within 25% would have been satisfying; to within 50%, perhaps not unreasonable. I

am surely derelict to the extent that I may have implied any greater accuracy for the theoretical calculations. Somewhat chastened by all this, I do think I should have made it clear that while useful measurements can be made at 2 meters, and possibly even 1 meter, operation above a few hundred MHz is questionable.

— *Sincerely, F. Neal Eddy, 40 Finn Rd, Harvard, MA 01451; fneddy@charter.net*

High-Performance Audio Speech Low-Pass and CW Band-Pass Filters in SVL Design

The elliptic audio filters in DC8NR's article meant for use on CW would be found to be unusable were they truly elliptic filters. Due to the very low inductor Q ($Q = 7$), the CW filters presented, while designed as elliptic function filters, do not have the characteristics of an elliptic filter and that is what makes them usable. If high-enough Q inductors were used in these filter designs to realize the response of an elliptic filter, the ringing would make the filters useless on CW. It is interesting that for the given number of components, I don't know of any other filter that would have the steepness of this filter's skirts.

— *Sincerely, Joseph F. Bagdal, W8AVD, 645 Cascade, Cincinnati, OH 45240; jfb45240@yahoo.com*

Hi Joseph,

Thank you for writing with your comments about the filters presented in this article.

— *73, Larry, WR1B*

Letters (Jul/Aug 2007): On the Crossed-Field Antenna Performance, Parts 1 and 2 (Jan/Feb and Mar/Apr 2007)

Hello Larry!

Please allow me to reply to two "Letters To The Editor" in the Jul/Aug 2007 issue of *QEX*.

One writer complains that you carried an article about the "Crossed-Field Antenna." Of many articles I've read about this antenna, this one was the most complete, straightforward, clearly set forth, and understandable by Amateurs of many levels of technical proficiency. Our Broadcast Engineering weekly lunch group in Albuquerque, of which nearly everyone is a licensed Amateur, spent an hour discussing the reports in your article, and appreciate very much its publication (and debunking!).

Another writer complains that you carried "another IEEE article reprint." For the many of us who are not members of IEEE, having *QEX* republish "the best of the best" articles from other publications is a welcome "digest" service for us, your readers.

I recognize that the personal circumstances of the two letter-writers leads them to feel *QEX* wasn't speaking to them with these two articles. Take heart, however, as these

articles and others like them speak directly to the vast majority of your readers, and we are most appreciative.

— *73, Mike Langner, K5MGR, 929 Alameda Road NW, Albuquerque, NM 87114; mlangner@swpc.com*

Thanks Mike. I am trying to learn how to gauge our reader's interest in the various articles we publish. I hope we can provide several articles in each issue that will be particularly interesting to each individual reader, but certainly recognize that not every reader will enjoy every article.

I have heard from several other readers who either did or did not like these two articles, either for technical reasons or because they were picked up from an IEEE publication. I certainly do not intend to make it a common practice to pick up previously published works for *QEX*. We may do that occasionally, however, to share a particularly interesting article.

— *73, Larry, WR1B*

Congratulations to our new QEX Editor

Hi Larry:

First, let me offer my hearty congratulations to your appointment as editor of *QEX*. I feel very confident that you will continue the *QEX* legacy and will forge new and more interesting aspects of Amateur Radio to be explored and published.

My purpose in writing is to provide a couple of suggestions for you to consider as you move into *QEX* leadership. I am retiring at the end of the year and will again be able to delve more fully into the realm of Amateur Radio. Licensed and continuously active since 1958, I am an avid HF user, devoted primarily to CW operation. I enjoy QRP and have built several of my own rigs. I have been an ARRL member and supporter for many years, with a few intervening "off" periods due to work and family raising responsibilities. Amateur Radio is, and continues to be my primary hobby and I hope to take it to another level in the years to come.

Last Christmas, at my request, my daughter gave me a subscription to *QEX*. I have often felt that many of its articles and explanations of radio phenomenon were quite above my ability to understand, and to some degree I have found that to be true. Given that I am a business administrator professionally, however, and not engaged in electronics except as a hobby, I have been forced to learn more. That is a very good thing, and has expanded both my horizons and my mental abilities.

To me, *QST* provides Amateur Radio theory and construction material in very limited quantities. The explanations are often times somewhat clipped, because of publishing space and costs, I am sure. I look forward to each month's issue with as much anticipation

today, however, as I did in the late 1950s!

I understand that "outstanding" articles are not always available in quantity, but perhaps some of the articles that are easier to understand for the average ham could be included. Quite frankly, many of the articles in *QEX* thus far are over my head. I have learned a lot and each issue I do read each article in its entirety. I get lost, try to regroup, head to my extensive ARRL library for reference work and do my best to at least understand what the author is saying.

If some of those less technical or theoretical articles that are not suitable for *QST* publication could be included, I would find the mix to be more to my liking. I would still be pushed hard to understand the real geniuses who know electronics, but I would be rewarded for my patience and hard work with articles that I could perhaps master the contents and really take something away for use at my station.

As I said, Larry, I really have enjoyed reading *QEX*, and even if there are no changes I plan on continuing my subscription. I sincerely wish that I had the expertise to contribute at this time, but sadly that is not the case. But, hope springs eternal and with some more years of *QEX* exposure under my belt, I just might have something to offer.

Again, my congratulations and I wish you the very best in your new responsibilities.

— *73, Bob Brock, K9OSC, 1816 Chapman Dr, Waukesha, WI 53189; k9osccw@yahoo.com*

Hi Larry,

I just read that you have taken over the reins of *QEX*. I would like to offer best wishes, and a few words of encouragement for this important work.

As I see it, *QEX* is the place for articles that are aimed for a narrower, more technical audience than *QST*, require many more pages, or describe works in progress that invite participation at a high technical level by the community. My favorite recent article is the one by Fritz Raab describing the 500 kHz experiments.

I will do my best to encourage some new, sharp young authors to send interesting articles in your direction. I am currently mentoring three of them in that direction.

Technical publishing within the ham community is a great tradition, and it's not just hard work, it's a real honor. Once again, congratulations and best regards.

— *Rick Campbell, KK7B, 4105 NW Carlton Ct, Portland, OR 97229; kk7b@arrrl.net*

Dear Readers,


I was both surprised and honored by the number of congratulatory e-mails that I received after the announcement of my new responsibilities was posted on the ARRL Web page. Thank you all for your well wishes. In this issue's Empirical Outlook I shared a few

thoughts with regard to my vision and ideas for the future of *QEX*. Of course I cannot do anything with the magazine without your support and assistance.

Please share with me your suggestions for

ways to make *QEX* more interesting to you. I won't promise that we will make every change you suggest, but I will evaluate each suggestion for practicality, within our charter and budget. Please also submit articles about proj-

ects or concepts of interest to you. Together I am confident we can continue to keep *QEX* vibrant and interesting!

— 73, *Larry Wolfgang, WR1B, QEX Editor*
lwolfgang@arrl.org 

Upcoming Conferences

The 26th Digital Communications Conference

September 28-30, 2007, Hartford, CT

The ARRL and TAPR Digital Communications Conference is an international forum for radio amateurs to meet, publish their work, and present new ideas and techniques. Presenters and attendees will have the opportunity to exchange ideas and learn about recent hardware and software advances, theories, experimental results, and practical applications. Full information can be found at www.tapr.org/dcc.html.

Topics include, but are not limited to:

- Software defined radio (SDR)
- Digital voice
- Digital satellite communications
- Global position system
- Precise timing
- Automatic position reporting system (APRS)
- Short messaging (a mode of APRS)
- Digital signal processing (DSP)
- HF digital modes
- Internet interoperability with Amateur Radio networks
- Spread spectrum
- IEEE 802.11 and other Part 15 license-exempt systems adaptable for Amateur Radio
- Using TCP/IP networking over Amateur Radio
- Mesh and peer-to-peer wireless networking
- Emergency and Homeland Defense backup digital communications in Amateur Radio
- Updates on AX.25 and other wireless networking protocols
- Topics that advanced the Amateur Radio art.

The Conference

Friday, Saturday and Sunday: This is a must attend conference for technically inclined amateurs. Now, more than ever, amateur radio needs this great meeting of the minds to demonstrate a continued need for our current frequency allocations by pushing forward and documenting our achievements. The ARRL and TAPR Digital Communications Conference is the best way to record our accomplishments and challenge each other to do more.

This conference is for all levels of techni-

cal experience, not just for the expert. Not only is the conference technically stimulating, it is a weekend of fun for all who have more than a casual interest in any aspect of amateur digital electronics and communications.

Technical and introductory sessions are scheduled throughout the conference to introduce new technical topics for beginners and experts alike.

Friday Evening Social: Join others at the conference for a Friday evening social get together.

Saturday Evening Banquet with an invited speaker that concludes with award presentations and prize drawing. This year's speaker is well-known *Linux* advocate, Bruce Perens, K6BP.

The ever-popular *Sunday Seminar* that focuses on a topic and provides an in-depth four-hour presentation by an expert in the field. This year's seminar topic has not been confirmed at this time.

Sunday is also Tuscon Amateur Packet Radio's (TAPR) annual meeting.

Demonstration Room: Each year at the DCC a separate (and lockable) room is provided for people to bring and show off their latest projects. Tables and power will be provided. Bring your equipment and display for all to see, learn, and ask questions about. Be sure to bring a small sign and/or flyer naming and describing your project.

Hotel

Conference presentations, meetings, and seminars will be held at the Doubletree Hotel Bradley International Airport, Windsor Locks, CT.

It is highly recommended that you book your room prior to arriving. A block of rooms has been reserved at the special DCC room rate of \$79.00, single/double. This special rate is good until August 30, 2007, or until the block of rooms are all sold out. To book your room, call the hotel directly and mention the group code DCC when making reservations. Be sure to book your rooms early!

Doubletree Hotel Bradley International Airport

16 Ella Grasso Turnpike
Windsor Locks, CT 06096
Tel: (860) 627-5171

Fax: (860) 627-7029

Internet: www.doubletree.com/en/dt/hotels/index.jhtml?ctyhocn=BDLETD

Transportation: The nearest airport is Bradley International Airport (BDL). The Doubletree Hotel provides a complimentary airport shuttle service. Contact the hotel front desk for availability and scheduling.

Registration Fees

Note: Student pricing (17 years and younger) is 50% off regular registration price (meals excluded)

Pre-registration* (before September 1, 2007)

Two Day Conference — \$70.00

Friday Only Conference — \$40.00

Saturday Only Conference — \$40.00

Sunday Seminar: Sunday 8:00 AM-12:00 PM — \$25.00

Late Registration* (after September 1, 2007)

Two Day Late Registration after Sept 1 or at door — \$80.00

Friday Only Late Registration after Sept 1 or at door — \$50.00

Saturday Only Late Registration after Sept 1 or at door — \$50.00

* Conference registration includes conference proceedings, sessions, meetings.

Lunches: Friday \$15.00; Saturday \$15.00

Saturday Evening Banquet: \$35.00

Microwave Update 2007

October 18-20, 2007

Microwave Update 2007 Details

Microwave Update 2007 will be held at historic Valley Forge, near Philadelphia, Pennsylvania. Thursday sightseeing or possible surplus tour. Conference Friday and Saturday; Flea Market Friday night, Vendors on site; Banquet Saturday night; Door prizes and raffles; Hospitality room. Hosted by the Pack Rats — Mt Airy VHF Radio Club. Spouses, friends and family invited. Alternative family/spouse programs available.

\$79 early-bird registration until Sep 1 includes Conference, proceedings and banquet; \$89 from Sep 1-Oct 1; \$99 thereafter. Extra banquet Tickets \$39. Special hotel rate \$92 per night. Full info and registration at www.microwaveupdate.org.

Questions to chairpersons Philip Theis,

Jr, K3TUF, e-mail Phil@k3tuf.com or David Fleming, KB3HCL, e-mail kb3hcl@arrl.net.

2007 AMSAT-North America Space Symposium and Annual Meeting
October 26-28, 2007, Pittsburgh, PA

The Wireless Association of South Hills Amateur Radio Club announces that the 2007 AMSAT Space Symposium will be held at the Pittsburgh Airport Marriott Hotel on Friday, October 26 through Sunday, October 28, 2007.

This year, efforts are being focused on attracting local middle and high school students to the Saturday sessions of the symposium and special programs, by contacting local gifted and science teachers. As part of this, a fully operational satellite station will be available on site for demonstrations and use. More will be announced as this program develops.

The keynote speaker this year will be Mr. Sy Liebergot, a former EECOM controller responsible for the electrical and environmental systems onboard the Apollo Command Module. He was part of the team that guided Apollo 13 back to Earth following the explosion that crippled the spacecraft. For movie buffs, in the Apollo 13 movie, Sy

Liebergot was played by Clint Howard, the brother of director Ron Howard.

We are sure you will enjoy the Symposium. You can register for the Symposium online, and even make your hotel reservations and arrange for upgrades online as well! There are links on the Symposium Web page to help you find information to plan your trip to the Pittsburgh area, including links to help you arrange your travel plans, book your hotel, and enjoy your stay. See www.amsat.org/amsat-new/symposium/2007/index.php. We hope you will come for the Symposium and enjoy our beautiful area.

22nd Southwest Ohio Digital & Technical Symposium

January 12, 2008, Thesken Hall, on the Middletown Campus of Miami University, Middletown, Ohio

The 22nd annual Southwest Ohio Digital & Technical Symposium is being planned for Saturday, January 12, 2008. Admission is free. The intent of this continuing series of symposia is to provide a forum for exchanging ideas and learning about technical aspects of the hobby. Forum organizers strive to have presentations providing a good mix of the future with practical application of the present.

Call For Papers

Technical papers are solicited for presentation at the 22nd Southwest Ohio Digital & Technical Symposium and for publication in the *Proceedings*. *Proceedings* will be published on CD and presentation at the symposium is not required for publication. Papers must be received by January 1, 2008 for inclusion in the *Proceedings*. Only electronic files are accepted.

Topics of interest include almost all technical aspects of the hobby. The intent is to pique the interest of active hams to learn what is happening technically in the hobby and to encourage practical application or reapplication of the presented topic. "Back to the basics" presentations are also encouraged on topics like circuit design, test equipment construction and/or use, antenna theory and construction, etcetera.

This year's format will be slightly different, in that more emphasis will be placed on hands on interactions between presenters and attendees. There will be a limited number of formal presentations and the remainder will use a science fair/show-and-tell structure. Since this is an officially sanctioned ARRL conference, one of the formal presentations will be an ARRL forum.

We Design And Manufacture To Meet Your Requirements
*Prototype or Production Quantities
800-522-2253
This Number May Not Save Your Life...

But it could make it a lot easier! Especially when it comes to ordering non-standard connectors.

RF/MICROWAVE CONNECTORS, CABLES AND ASSEMBLIES


- Specials our specialty. Virtually any SMA, N, TNC, HN, LC, RP, BNC, SMB, or SMC delivered in 2-4 weeks.
- Cross reference library to all major manufacturers.
- Experts in supplying "hard to get" RF connectors.
- Our adapters can satisfy virtually any combination of requirements between series.
- Extensive inventory of passive RF/Microwave components including attenuators, terminations and dividers.
- No minimum order.

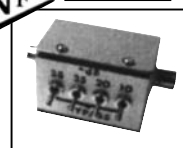
NEMAL
Cable & Connectors
for the Electronics Industry

NEMAL ELECTRONICS INTERNATIONAL, INC.
12240 N.E. 14TH AVENUE
NORTH MIAMI, FL 33161
TEL: 305-899-0900 • FAX: 305-895-8178
E-MAIL: INFO@NEMAL.COM
BRASIL: (011) 5535-2368

URL: WWW.NEMAL.COM

NATIONAL RF, INC.

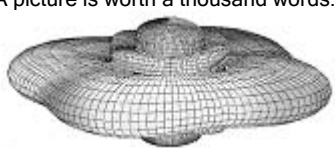


 VECTOR-FINDER Handheld VHF direction finder. Uses any FM xcvr. Audible & LED display. VF-142Q, 130-300 MHz \$239.95 VF-142QM, 130-500 MHz \$289.95	 ATTENUATOR Switchable, T-Pad Attenuator, 100 dB max - 10 dB min BNC connectors AT-100, \$89.95
 DIP METER Find the resonant frequency of tuned circuits or resonant networks—ie antennas. NRM-2, with 1 coil set, \$219.95 NRM-2D, with 3 coil sets (1.5-40 MHz), and Pelican case, \$299.95 Additional coils (ranges between 400 kHz and 70 MHz avail.), \$39.95 each	 DIAL SCALES The perfect finishing touch for your homebrew projects. 1/4-inch shaft couplings. NPD-1, 3/4 x 2 3/4 inches 7:1 drive, \$34.95 NPD-2, 5/8 x 3 3/8 inches 8:1 drive, \$44.95 NPD-3, 5/8 x 3 3/8 inches 6:1 drive, \$49.95 S/H Extra, CA add tax

NATIONAL RF, INC
7969 ENGINEER ROAD, #102
SAN DIEGO, CA 92111

858.565.1319 FAX 858.571.5909
www.NationalRF.com

A picture is worth a thousand words...



With the **ANTENNA MODEL™** wire antenna analysis program for Windows you get true 3D far field patterns that are far more informative than conventional 2D patterns or wire-frame pseudo-3D patterns.

Describe the antenna to the program in an easy-to-use spreadsheet-style format, and then with one mouse-click the program shows you the antenna pattern, front/back ratio, front/rear ratio, input impedance, efficiency, SWR, and more.

An optional **Symbols** window with formula evaluation capability can do your computations for you. A **Match Wizard** designs Gamma, T, or Hairpin matches for Yagi antennas. A **Clamp Wizard** calculates the equivalent diameter of Yagi element clamps. **Yagi Optimization** finds Yagi dimensions that satisfy performance objectives you specify. Major antenna properties can be graphed as a function of frequency.

There is **no built-in segment limit**. Your models can be as large and complicated as your system permits.

ANTENNA MODEL is only \$90US. This includes a Web site download and a permanent backup copy on CD-ROM. Visit our Web site for more information about **ANTENNA MODEL**.


Teri Software
P.O. Box 277
Lincoln, TX 78948

www.antennamodel.com
e-mail sales@antennamodel.com
phone 979-542-7952

Last year we experimented with two presentations being given remotely. We will possibly have one or two of the formal presentations done remotely again this year.

If you are interested in providing a

presentation and/or paper but desire more information, please contact Jay Slough, K4ZLE, 2554 Hamilton Rd, Lebanon, OH 45036-8849; Phone: 513-934-0235; E-mail: k4zle@arrrl.net. Look at www.arrrl.org/

[news/features/2007/01/29/1/](http://www.arrrl.org/news/features/2007/01/29/1/) for information on the 2007 symposium. Additional, more up-to-date information concerning the 2008 symposium may be found at www.swohdigi.org. 



Experience Autumn in New England at the 2007 TAPR/ARRL Digital Communications Conference


September 28-30 in Hartford, Connecticut

- Technical Sessions
- New Products and Demonstrations
- Educational Forums
- Good Food and Good Friends
- Easy Access from Bradley International Airport

See the Digital Communications Conference site on the Web at www.tapr.org/dcc/ or call TAPR at **972-671-8277** to make your reservations today.

In the next issue of

QEX

Retired RF Engineer and well-known RF technology author Cornell Drentea, KW7CD, provides insight into the design of his Star-10 transceiver. This one-of-a-kind transceiver is a very high performance, continuous coverage (from 1.8 to 30 MHz) design, which evolved from an earlier 1980s transceiver. The radio is a fully synthesized design that uses 10 Hz frequency step resolution. This multipart article promises to be a must read for anyone interested in the design of modern computer-controlled radios. You won't want to miss a word of this series! 

QEX

ARRL
225 Main Street
Newington, CT 06111-1494 USA

For one year (6 bi-monthly issues) of QEX:

In the US

- ARRL Member \$24.00
 Non-Member \$36.00

In the US by First Class mail

- ARRL Member \$37.00
 Non-Member \$49.00

Elsewhere by Surface Mail
(4-8 week delivery)

- ARRL Member \$31.00
 Non-Member \$43.00

Canada by Airmail

- ARRL Member \$40.00
 Non-Member \$52.00

Elsewhere by Airmail

- ARRL Member \$59.00
 Non-Member \$71.00

Remittance must be in US funds and checks must be drawn on a bank in the US. Prices subject to change without notice.

QEX Subscription Order Card

QEX, the Forum for Communications Experimenters is available at the rates shown at left. Maximum term is 6 issues, and because of the uncertainty of postal rates, prices are subject to change without notice.

Subscribe toll-free with your credit card **1-888-277-5289**

Renewal New Subscription

Name _____ Call _____

Address _____

City _____ State or Province _____ Postal Code _____

Payment Enclosed to ARRL

Charge:



Account # _____ Good thru _____

Signature _____ Date _____

06/01

All the information you need to design your own complete antenna system.

The ARRL

The ARRL
ANTENNA BOOK
21st Edition

ANTENNA BOOK



21st Edition

ARRL Order No. 9876

Only **\$44.95***

*shipping \$10 US/\$15.00 International

The *ultimate* reference for Amateur Radio antennas, transmission lines and propagation



Fully searchable CD-ROM included!



ARRL The national association for **AMATEUR RADIO**

SHOP DIRECT or call for a dealer near you.
ONLINE WWW.ARRL.ORG/SHOP
ORDER TOLL-FREE 888/277-5289 (US)

QEX 9/2007

Defense of Amateur Radio Spectrum is every radio amateur's business!

Over the years, ARRL has responded to challenges to Amateur Radio frequencies, at home and abroad...from Little Leos to BPL.

Who knows what the next challenge will be...

**But we do know one thing
...we MUST be prepared!**

YOU can help...

...by making your generous contribution to the 2008 Spectrum Defense Fund!

ARRL must raise more than \$304,775 this fall to fund its 2008 Spectrum Defense efforts.

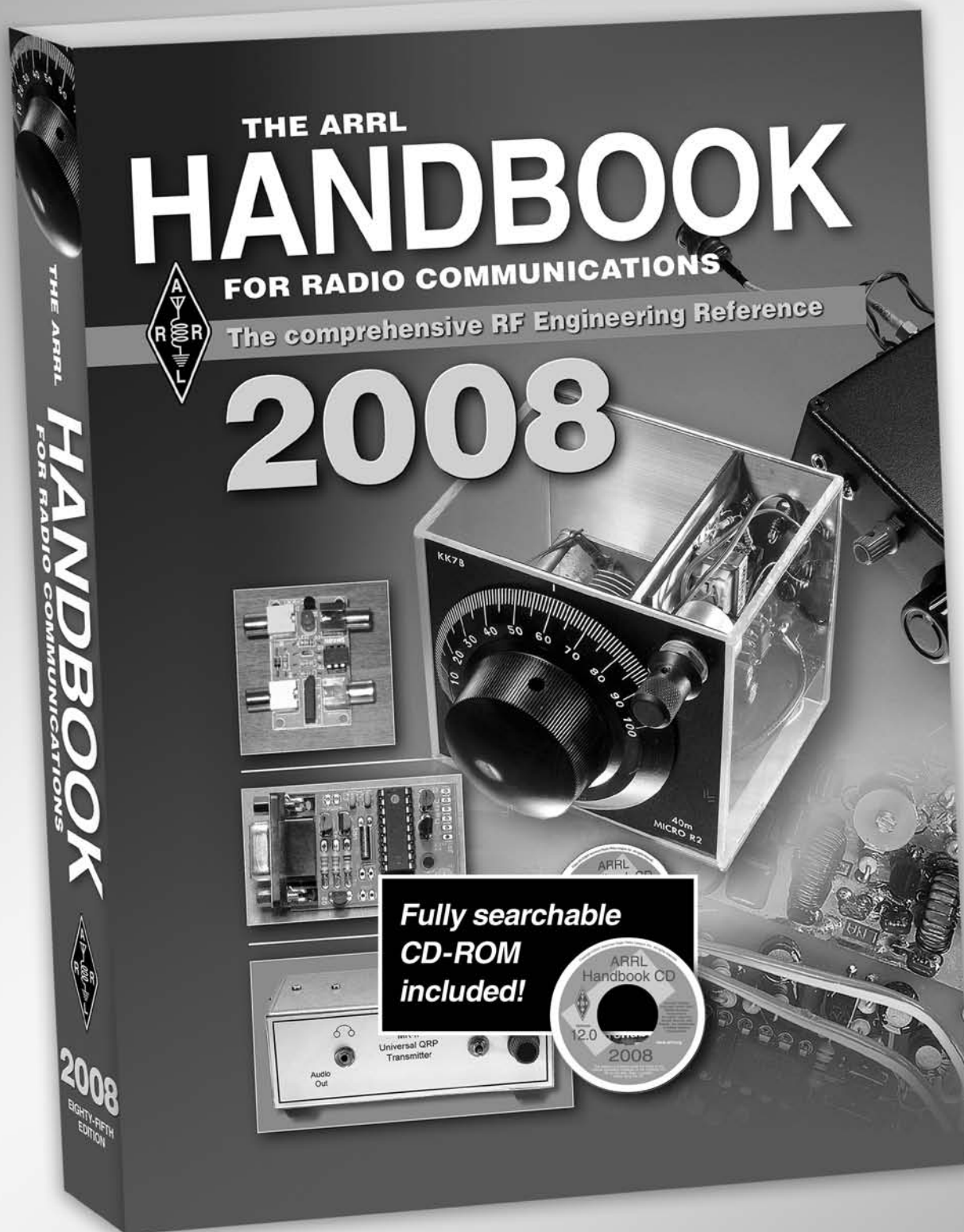
Make the largest donation you can, by mail, phone or on the web at www.arrl.org/defense

For more information, contact:

Mary M. Hobart, K1MMH
Chief Development Officer
ARRL
 225 Main Street
 Newington CT 06111-1494
 Telephone: 860-594-0397
 Email: mhobart@arrl.org



Available in October 2007



Fully searchable
CD-ROM
included!



ARRL The national association for
AMATEUR RADIO

Softcover. Includes book and CD-ROM (version 12.0)
ARRL Order No. 1018 **\$44.95** plus s&h
Hardcover. Includes book and CD-ROM (version 12.0)
ARRL Order No. 1026 **\$59.95** plus s&h

SHOP DIRECT or call for a dealer near you.
ONLINE WWW.ARRL.ORG/SHOP
ORDER TOLL-FREE 888/277-5289 (US)

QEX 9/2007

Big Winners from Array Solutions



PowerMaster Watt/VSWR Meter

- Sets the leading edge for all watt/vswr meters to follow
- Unheard of accuracy for the price
- Fast Bright reading meter
- Application software included
- Upgradeable via Internet

\$450



AIM 4170 Antenna Analyzer

- Most advanced vector impedance analyzer at a fraction of the cost
- Accurate and easy to use
- Application software included
- Lab instrument quality
- Upgradeable via Internet

\$495



OptiBeam 3 element 80 Yagi

OB3-80+

OptiBeam Antennas

German Engineering means High Performance and Reliability

Prosistel Rotators

Strongest Rotators on the Market
Prosistel PST 71 DC



AS-AYL-4

NEW 4 Direction K9AY Loop Antenna
Hear What You've Been Missing on the Low Bands

www.arrayolutions.com

Phone 972-203-2008

sales@arrayolutions.com

Fax 972-203-8811

We've got your stuff!



KENWOOD

Listen to the Future

TS-480

The Perfect Remote Base Transceiver

Straight Out of the Box!



- The perfect internet base transceiver - straight out of the box!
- Easy to operate.
- The size makes it great for base, mobile or portable operation.
- Free VoIP/Control software downloads at Kenwoodusa.com.
- Incredible RX specifications.
- No expensive sound card interface needed.

KENWOOD U.S.A. CORPORATION
Communications Sector Headquarters
3975 Johns Creek Court, Suite 300, Suwanee, GA 30024-1265
Customer Support/Distribution
P.O. Box 22745, 2201 East Dominguez St., Long Beach, CA 90801-5745
Customer Support: (310) 639-4200 Fax: (310) 537-8235

INTERNET
Kenwood News & Products
<http://www.kenwoodusa.com>
ADS# 16006



ISO 9001 Registered
Communications Equipment Division
Kenwood Corporation
ISO 9001 certification